Corrosion in CO_2 transport pipeline

Formation of corrosive phases in dense phase CO_2

Bjørn Helge Morland

Dissertation presented for the degree of

Philosophiae Doctor (Ph.D.)

Department of Chemistry

Faculty of Mathematics and Natural Sciences

UiO : University of Oslo

October 2019

Series of dissertations submitted to the
Faculty of Mathematics and Natural Sciences, University of Oslo
No. 2215

ISSN 1501-7710

Cover: Hanne Baadsgaard Utigard.
Print production: Reprosentralen, University of Oslo.

Acknowledgments

All the work presented in this thesis was carried out at the department of material and corrosion technology at the institute for Energy Technology (IFE). I am grateful to the institute and especial the department for providing research facilities and financial support to make this PhD project possible.

I would like to thank my supervisor Dr. Gaute Svenningsen for sharing his expertise with me, and for giving me the academic freedom to set up my own experiments yet challenge me when my hypothesis was out of bounds. You have given me helpful guidance and advice, and without you this thesis would not have been possible.

I am grateful to my mentor, Chief Scientist Arne Dugstad, for introducing me to field of CO_2 transport, for showing interest in my work and finding positive outcome in failed experiments. I would like to thank our department head, Rolf Nyborg, for facilitating and making the PhD-project possible.

I would also like to thank my co-supervisor, Prof. Truls Norby, for being the link to University of Oslo and making sure that everything was done by the book.

To all my colleagues at the department of Corrosion Technology who are contributing to a good and inspiring environment: It has been an honour working with you! A special thank goes to Adriana Tadesse for the invaluable help and enthusiasm in the laboratory, and to Dr. Morten Tjelta for fruitful discussions and comments on manuscripts.

The PhD work was a part of the Kjeller Dense phase CO_2 project, funded by CLIMIT research project no. 243624/E20 (KDC-II), I am thankful for the trust that was given to me to complete the project. I would also like to thank the members of the KDC-II project (Shell, Total, ArcelorMittal, OLI, and Gassco) for their knowledge and the opportunity to present my work to professionals and experts in the field of corrosion.

I would like to thank all the co-authors: Arne Dugstad, Morten Tjelta, Adriana Tadesse, Ronald D. Springer, and Andre Anderko, who have contributed to this work in different ways

Finally, a warm thank you goes to my family and friends, who has been there for me throughout the process of this PhD work. Especially, I would like to thank Cecilie for holding the fort, Christoffer and Thomas for accepting that their old dad went back to school, and for the understanding and patience when I had to work long hours.

Bjørn H. Morland
Lillestrøm, October 2019

Summary

Carbon capture and storage is suggested as one of the solutions to reduce CO_2 emissions. Material choice is an important part for the total cost of the transport system for CO_2. Although cost-considerations make carbon steel a clear material candidate for construction of the transportation system, it is important to ensure that the integrity is maintained throughout the lifetime. Corrosion and certain chemical reactions must therefore be avoided. There are many suggested specifications and recommendations for how much impurities (additional components) can be allowed in the CO_2 to be transported, but most of the impurity limits are set from a health safety and environment point of view. Due to lack of data, almost no impurity limits have been set from a material integrity point of view. This gap of knowledge makes it difficult to make a specification that will ensure safe operation.

The present work comprises investigations of corrosive situations which could occur during CO_2 transport, in particular: 1) testing of existing CO_2 specification with the impurities like H_2O, H_2S, O_2 SO_2, and NO_2 at realistic conditions to identify reactions between impurities and verification of upper limits for the mention impurities in CO_2. 2) Determination of nitric and sulfuric acid solubility in CO_2. 3) Corrosion testing with fix concentration of NO_2 or SO_2 with various water concentrations in dense phase CO_2. 4) carbon steel corrosion in water saturated with CO_2, and water dissolved in CO_2, at various at various temperature and pressure. Corrosion flow loops and autoclaves were used for this purpose and effort was made to improve the experimental setup, especially the method to introduce water to the loop.

CO_2 with various combinations and concentrations of impurities were tested in a systematic manner. It was clearly shown that many impurity combinations were basically inert, while other resulted in chemical reactions and some combinations even resulted in formation of a separate aqueous phase that contained high concentrations of sulfuric and nitric acid. This aqueous phase was highly corrosive to carbon steel. Corrosion was also observed in certain situations even if a separate aqueous phase was not observed.

CO_2 with SO_2 (75 ppmv) and O_2 (up to 220 ppmv) is not corrosive if the water concentration is less than 1600 ppmv at 100 bar and 25 °C in CO_2 streams. The same applies for CO_2 with 70 ppmv NO_2 and up to 250 ppmv H_2O. However, corrosion rates as high as 0.57 mm/y was observed for CO_2 with 70 ppmv NO_2 when the water content was increased from 250 to 670 ppmv (100 bar and 25 °C). This

principally different behaviour between CO_2 with $H_2O/SO_2/O_2$ (negligible corrosion) and CO_2 with H_2O/NO_2 (high corrosion rate) has not been fully understood, but it is a good illustration on the need to keep the water content low and that different impurity combinations behave differently.

Testing of CO_2 with multiple impurities (H_2O, H_2S, O_2 SO_2 and NO_2) under realistic pipeline transport conditions showed that nitric and sulfuric acid was formed for impurity concentrations well within existing specifications. Thus, these specifications cannot be accepted for CO_2 transportation in carbon steel pipelines. It was furthermore shown that several combinations of the impurities were non-reactive, but reactions started once CO_2 streams with H_2S and NO_2 were mixed. This finding is particularly important for a future situation with a large CO_2 transport network where streams from different sources may be mixed in a hub.

When the H_2O, H_2S, O_2 SO_2 and NO_2 impurities were present together, it resulted in several chemical reactions, and sulfuric and nitric acid formed if the impurity content was high enough. The stochiometric ratio of the consumed components showed that H_2S and NO_2 reacted and formed SO_2, NO and H_2O, while O_2 reacted with NO and formed NO_2 again. Sulfuric acid was produced through the reaction of SO_2 and H_2O with the help of NO_2. Acids were formed at 30 ppmv of H_2S, NO_2, and SO_2, while 5 and 10 ppmv gave chemical reactions but no condensation of acids.

The solubility of nitric acid and sulfuric acid in dense phase CO_2 was measured. The solubility of nitric acid (~1000 ppmv) was about 3 order of magnitude higher than the solubility of sulfuric acid (~1 ppmv). The solubility increases slightly with increasing temperature, while pressure has a much larger effect, especially between 1 and 100 bar. The results from the acid solubility in CO_2 has been implemented in the OLI thermodynamic model.

The experiments with water as the only impurity in the CO_2, showed clearly how the corrosion rate varied 3 to 4 decades depending on the water content. For very high water concentrations, were the water was present as a separate aqueous phase saturated with CO_2, the corrosion rate varied from 2 to 24 mm/y. For low water contents, where the water was fully dissolved in the CO_2 phase, the corrosion rate was less than 0.002 mm/y. It was also demonstrated how this huge difference in corrosion rate could result in various experimental artefacts. Injection of liquid water at start-up and water condensation during depressurisation can contribute significantly to the total amount corrosion. Thus, these artefacts may give erroneous corrosion rates, particularly for conditions that otherwise have low corrosivity.

Altogether, the present work has identified many important aspects of corrosion and chemical reactions for CO_2 transport. This has resulted in a better understanding of the processes that leads to corrosion. This is important information that is needed for making of a CO_2 specification which ensure the integrity of pipelines or ship. The concentration limits of the specification vary with which impurities that are present together. It has been shown that the specification must be strict, about 20 ppmv, if all the investigated impurities (H_2O, H_2S, O_2, SO_2, and NO_2) are present together at the same time. The limits can be relaxed if fewer impurities are present, but this needs to be verified experimentally for each impurity combination. Other impurities than those who have been investigated may behave differently.

Table of Contents

Abbreviations

bar	Pressure unit
CCS	Carbon capture and storage
CCUS	Carbon capture utilisation and storage
CR	Corrosion rate
CRA	Corrosion resistant alloys
EDS	Energy-dispersive X-ray spectroscopy
HSE	Health safety and environment
IC	Ion chromatography
IFE	Institute for Energy Technology
IPCC	The Intergovernmental panel on climate change
mm Hg	Pressure unit
mm/y	Corrosion rate unit: Millimeters per year
MSE	Mixed-solvent electrolyte
Mt/y	Flow unit: million tons per year
MW	Molecular weight
NETL	National Energy Technology Laboratory
NORSOK	The Norwegian shelf's competitive position
PEEK	Polyether ether ketone
ppmv	Concentration unit: Parts per million volume
ppmw	Concentration unit: Parts per million weight
RH	Relative humidity
SACROC	Scurry area canyon reef operators
SEM	Scanning electron microscopy
XRD	X-ray diffraction
µm/y	Corrosion rate unit: micrometers per year

List of publications

Paper 1 (Chapter 3) B. H. Morland and A. Dugstad, "Corrosion of carbon steel in water equilibrated with liquid and supercritical CO_2". CORROSION/2016, paper no. 7740 (Houston, TX: NACE International, 2016).

Paper 2 (Chapter 4) B. H. Morland, A. Dugstad, and G. Svenningsen, "Corrosion of carbon steel in dense phase CO_2 with water above and below the solubility limit". Energy Procedia, vol. 114, Supplement C (2017) pp. 6752-6765. https://doi.org/10.1016/j.egypro.2017.03.1807

Paper 3 (Chapter 5) B. H. Morland, M. Tjelta, A. Dugstad, and G. Svenningsen, "Corrosion in CO_2 systems with impurities creating strong acids". Accepted for publication in CORROSION journal (accepted 17th August 2019). https://doi.org/10.5006/3110

Paper 4 (Chapter 6) B. H. Morland, A. Tadesse, G. Svenningsen, R. D. Springer, and A. Anderko, "Nitric and sulfuric acid solubility in dense phase CO_2". Accepted for publication in Industrial & Engineering Chemistry Research (accepted 19th November 2019). http://dx.doi.org/10.1021/acs.iecr.9b04957.

Paper 5 (Chapter 7) B. H. Morland, T. Nordby, M. Tjelta, and G. Svenningsen, "Effect of SO_2, O_2, NO_2, and H_2O concentrations on chemical reactions and corrosion of carbon steel in dense phase CO_2". Paper accepted for publication in CORROSION journal (accepted 17th August 2019). https://doi.org/10.5006/3111

Paper 6 (Chapter 8) B. H. Morland, M. Tjelta, T. Nordby, and G. Svenningsen, "Acid reactions in hub systems consisting of separate non-reactive CO2 transport lines". Journal of Greenhouse Gas Control, vol. 87 (2019), pp. 246-255. https://doi.org/10.1016/j.ijggc.2019.05.017

Chapter 1

Introduction

1.1 Background

The carbon dioxide (CO_2) concentration in the atmosphere has increased dramatically over the last century, and much of this increase is a direct consequence of the industrial revolution followed by increased emission of flue gases [1]. The Intergovernmental Panel on Climate Change (IPCC) has identified CO_2 as a greenhouse gas which significantly contributes to global warming. There is an international agreement to reduce emission of CO_2 [2], and several initiatives are necessary to achieve this goal. Carbon dioxide capture and storage (CCS) is expected to contribute to about 20% of the total reduction of the CO_2 emission. CCS consist of a capturing plant where CO_2 from flue gasses or industrial processes is trapped, a transportation system and a permanent storage site. Carbon capture, utilisation and storage (CCUS) is basically the same except that the CO_2 is applied to something useful, like production of chemicals of commercial benefit or enhanced oil recovery. CCUS may to some extent make these large investments economically feasible. However, the demand for CO_2 is not high enough to reach the planned capture, so permanent storage is needed. Pipelines and ships are needed for transporting the CO_2 from the capturing plant to the storage site. Ships will be preferred when the distance is long and the volume is low, while pipeline would be used for large volume and shorter distance [3]. Except for very short distances, pipelines of corrosion resistant alloys (CRA) would be too costly. The transportation pipelines will therefore most likely be made of carbon steel and be designed with a long life-time. However, CO_2 can cause corrosion of carbon steel under certain conditions. Having a good understanding of the corrosion processes is therefore a key element in the integrity management of CO_2 transport pipelines.

CO_2 from natural sources has been transported in pipelines for many decades without corrosion problems [4]. Field experience has shown that corrosion is not a problem as long as the CO_2 is dried sufficiently to prevent precipitation of liquid water [4]. However, the CO_2 captured from flue gases is likely to contain additional components like oxygen, nitrogen dioxide, sulfur dioxide, and hydrogen sulfide [5,6]. These species are expected to be present at very low concentrations in the captured CO_2, and they are therefore called impurities in the present work. Even at ppm-levels, these impurities can cause corrosion, and they may introduce dust and solid formation which may lead to

operational difficulties. Previous experiments have shown that corrosive acids, like sulfuric acid and nitric acid, may form in certain CO_2 blends [7].

Little is known about how much impurities that can be accepted without risking corrosion or solids formation in a CO_2 transportation system. Even though recommendations exist [8], the impurity limits are mostly based on HSE concerns in case of accidental spill, rather than pipeline integrity problems. It is of course possible to clean the captured CO_2 to near 100% purity, but it will be costly both from an economical and energy perspective. CO_2 specifications describing the acceptable amounts of impurities in the CO_2 from a corrosion perspective is therefore needed. To achieve this, experimental data is needed to identify reactions which can occur between the impurities in the CO_2 and determined the lowest possible concentration that can be accepted for without compromising the integrity of the carbon steel pipeline.

Due to lack of experimental data, it is currently not possible to predict when chemical reactions, corrosion and solids formation could be expected in a CO_2 transportation system. The final goal would of course be to develop a tool that can be used to predict such reactions. Development of such a tool is not part of the scope of the present work, but the results should be an important contribution to such development work. Crucial for making such a tool is knowledge about reactions, interactions, and solubility of the involved species. For example, no data exists on the solubility of sulfuric and nitric acid in dense phase CO_2, which might form under certain conditions. This information is important, since precipitation of strong acids will create a highly corrosive environment (risk of corrosion of carbon steel and formation of corrosion products). But if the acid remains dissolved in the dense phase CO_2, they can probably follow the stream without affecting the transportation pipeline. Therefore, the threshold when precipitation occurs (solubility limit is exceeded) needs to be known.

1.2 Objective

The main objective of this study is to carry out experimental testing to understand corrosion and chemical reactions in CO_2 transport system. The results will be important background information for determining a safe operation window for CO_2 transport when impurities are present. SO_2, NO_2, H_2O, O_2, and H_2S are selected as impurities to study since they are expected to be present in captured CO_2 and are known to be corrosive to carbon steel individually, and they may also react and form even more corrosive species. Particular focus is therefore put on identifying chemical reactions, reaction products and formation of separate liquid phases. The effect of impurity

concentrations is also studied as part of establishing a safe operation window. If reaction products remain dissolved in the bulk CO_2 phase, they can in principle follow the CO_2 stream without causing any damage. Sulfuric acid and nitric acid, which are known to form under certain conditions, is therefore studied in detail. Data from the present work will be shared with OLI Systems, who will implement them in their Mixed-Solvent Electrolyte (MSE) model. However, the thermodynamic modelling is outside the scope of the present PhD work.

1.3 Approach

The experimental approach will be to mimic the CO_2 transport conditions in the most realistic way as possible. Impurities will be continuously injected to ensure that the initial concentration stays constant, and that the impurities are not fully consumed through corrosion or reactions in the transported CO_2 to render possible stoichiometric calculations. The impurity concentrations will be monitored using various analytical techniques, and corrosion and chemical reactions will be determined from concentration differences between injected CO_2 and exhaust CO_2. The acid solubility in CO_2 will be examined near equilibrium in a steady state condition with slow flowing CO_2 through the representative acid. The experimental equipment will consist of corrosion loops, see-through and closed autoclaves, together with advanced injection and analysing equipment.

1.4 Thesis structure

The thesis consists of six individual papers. Five papers have been published and one has been submitted for publication. An overview of work on CO_2 transport corrosion and reactions published in the literature is given in Chapter 2. The experimental setups are thoroughly described in the articles they were used (Chapter 3 through 8), and some repetition could therefore not be avoided.

Chapter 3 reports a study of corrosion of carbon steel exposed to liquid water with high CO_2 pressures. Chapter 4 reports corrosion experiments where the water was fully dissolved in the CO_2 phase (no liquid water present). Chapter 5 studied reactions that took place in CO_2 blends with impurity concentrations well within established CO_2 specifications. The solubility of nitric and sulfuric acid in dense phase CO_2 is reported in Chapter 6. Corrosion of carbon steel in dense phase CO_2 with SO_2 and NO_2 is reported in Chapter 7. Chapter 8 reports a series of experiments where multiple CO_2 blends were mixed. An overall discussion of all the results, and the literature from Chapter 2, is given in Chapter 9, with conclusions in Chapter 10 and suggestion for further work in Chapter 11.

1.5 References

[1] IPCC, "Summary for Policymakers. In: Climate Change 2007: The Physical Science Basis. Contribution of Working Group I to the Fourth Assessment Report of the Intergovernmental Panel on Climate Change", Report no. 00207829, C.U. Press, IPCC, Cambridge, UK and New York, USA.

[2] IPCC, "Summary for Policymakers. In: Climate Change 2013: The Physical Science Basis. Contribution of Working Group I to the Fifth Assessment Report of the Intergovermmental Panel on Climate Change [Stocker,T.F., D. Qin, G.-K. Plattner, M. Tignor, S.K. Allen, J. Boschung, A. Nauels, Y. Xia, V. Bex and P.M. Midgley (eds.)]. ", IPCC, Cambridge University Press, Cambridge, United Kingdom and New York, NY, USA.

[3] R. Skagestad, N. Eldrup, H. Hansen, S. Belfroid, A. Mathisen, A. Lach, H. Haugen, "Ship transport of CO_2-status and technology gaps", Report no. 2214090, Tel-Tek, 2014.

[4] IEA, "Technology roadmaps technology roadmap: Carbon capture and storage: Complete edition", Report no. 1608-019X, IEA, SourceOECD Energy.

[5] A. Oosterkamp, J. Ramsen, "State-of-the-art overview of CO_2 pipeline transport with relevance to offshore pipelines", Report no. POL-O-2007-138-A, 2008, Polytec.

[6] E. de Visser, C. Hendriks, M. Barrio, M. Mølnvik, G. de Koeijer, S. Liljemark, Y. Le Gallo, Dynamis CO_2 quality recommendations, *International Journal of Greenhouse Gas Control*, 2, (2008) p. 478.

[7] A. Dugstad, M. Halseid, B. Morland, Testing of CO_2 specifications with respect to corrosion and bulk phase reactions, *Energy Procedia*, 63, (2014) pp. 2547-2556.

[8] NETL, "CO_2 impurity design parameters", Report no. DE-FE0004001, (2013), NETL.

Chapter 2

Literature review

This chapter gives an overview of published work on corrosion and reactions relevant for dense phase CO_2 transport in carbon steel pipelines. Papers on corrosion and reactions for ship transport conditions of CO_2 were also search for, but no one was found. CCS has got increasingly more attention during the last two decades, and most papers were therefore published after 2000. Prior to this, relevant corrosion research was mainly related to oil and gas systems, which usually has much lower CO_2 partial pressures. The main focus in this review has been to summarise the present knowledge and identify knowledge gaps, with particular focus on effects of water content and impurities on corrosion of carbon steel.

2.1 Corrosion

For corrosion in CO_2 transportation systems it is important to distinguish between the two principally different situations when water is present as a separate phase and when the water is fully dissolved in the CO_2 phase. The corrosion mechanism is most likely the same, but the rates will be significantly different since the amount of water differs by many orders of magnitude. The presence of liquid water is a key factor to drive the corrosion reactions and large quantities of water will result in high corrosion rates. In contrast, water can probably be a limiting reactant by itself, and for example a small water phase (thin surface film) will result in rapid saturation of corrosion products.

2.1.1 Corrosion in a free water phase

A free water phase is not expected in CO_2 transport pipelines under normal operation, but it could occur due to accidental water ingress, equipment malfunction, carry-over from the compression stage, or other types of operational errors. This occurred in the start-up in the SACROC CO_2 injection project where wellheads and tubing was subjected to alternating water and CO_2 slugs. [1].

It is well known that carbon steel will corrode in contact with water and CO_2, and numerous data from oil and gas research show that this may result in high corrosion rates. Most of these data were acquired for a CO_2 partial pressure in the 0.1 to 10 bar range. There are many papers that discusses the mechanisms for CO_2 corrosion of carbon steel, and only a brief summary will be given here. More details can be found elsewhere [2-6]. Aqueous CO_2 is formed when dissolved in the water

phase and reacts with water to form carbonic acid (Equation 2-1). The electrochemical reactions consist of dissolution of iron (anodic, Equation 2-2) and the reduction of hydrogen, carbonic acid and bicarbonate (cathodic, Equations 2-3, 2-4, and 2-5).

$$CO_{2\,(aq)} + H_2O_{(l)} \rightarrow H_2CO_{3\,(aq)} \quad (2\text{-}1)$$

$$Fe_{(s)} \rightarrow Fe^{2+}_{(aq)} + 2e^- \quad (2\text{-}2)$$

$$2H^+_{(aq)} + 2e^- \rightarrow H_{2\,(g)} \quad (2\text{-}3)$$

$$2H_2CO_{3\,(aq)} + 2e^- \rightarrow H_{2\,(g)} + 2HCO^-_{3\,(aq)} \quad (2\text{-}4)$$

$$2HCO^-_{3\,(aq)} + 2e^- \rightarrow H_{2\,(g)} + 2CO^{2-}_{3\,(aq)} \quad (2\text{-}5)$$

$$Fe^{2+}_{(aq)} + CO^{2-}_{3\,(aq)} \rightarrow FeCO_{3\,(s)} \quad (2\text{-}6)$$

Eventually, the iron-ion and carbonate-ion will react (Equation 2-6) and precipitate. The iron carbonate corrosion product may, depending on the morphology, provide a varying degree of protection for the steel substrate. There are some publications that address corrosion in water under high CO_2 pressures. The reported corrosion rates vary significantly, and rates from 0.2 to 50 mm/y has been reported [7-15]. This wide spread of corrosion rates can in many cases be explained by the differences in experimental methods, and it emphasises the importance of comparing results under similar conditions. Zhang et al. [14] showed that the corrosion rate increased with increasing temperature (from 50 to 80 °C) under stagnant conditions. Nor et al. [16] concluded that the corrosion rate increased with increasing flow rate and with increasing temperature. The partial pressure (fugacity) of CO_2 will also influence the corrosion rate, and Seiersten et al. [7] reported increasing rates with increasing CO_2 pressure up to 40 bar, from 14 mm/y to 23 mm/y, after this point the corrosion rate started declining. However, the latter experiments were conducted at stagnant condition without replenishment of the water and the highest CO_2 pressures were therefore carried out at a higher pH. It might be different for flowing condition when corrosion products are removed from steel surface and the transport of corrosive species to the surface is enhanced. The pH will increase when corrosion products are accumulated in the water phase, which will contribute to lower corrosion rates.

2.1.2 Corrosion in CO_2 with dissolved water

Normally, the transported CO_2 should only contain small amounts of water that will be fully dissolved in the CO_2 phase, because the presence of free water gives unacceptable high corrosion rates on carbon steel. For several years the understanding has been that exposure to CO_2 with fully dissolved water leads to very low corrosion rates [12,17-24]. These rates (less than 0.010 mm/y) are so low that they are not of technological interest. However, during the last decade, significantly

higher corrosion rates in the range of 0.5 to 3 mm/y have been reported for conditions where the water nominally should be fully dissolved in the CO_2 phase [25-28]. Hua et al. [29] reported that the corrosion rate was about 0.1 mm/y with 80 bar CO_2 and 35 °C when the water content was 3400 ppmv, i.e. at the solubility limit. Furthermore, the localised (pitting) corrosion in that experiment was claimed to be as high as 0.9 mm/y. Even when the water content was reduced to 700 ppmv the pitting corrosion rate was as high as 0.2 mm/y. Similar pitting corrosion was also observed by Sim et al. [30] when they had a general corrosion of 0.03 mm/y for a large range of water contents (from 244 to 3670 ppmv water at 80 bar and 40 °C). These relatively high corrosion rates are in contrast with the previous work, which reported negligible corrosion rates as long as the water was fully dissolved in the CO_2 phase. Thus, there are conflicting results for conditions where the water is dissolved in dense phase CO_2. A summary of published corrosion values is listed in Table 2-1.

Table 2-1: Summary of reported corrosion rates for carbon steel coupons exposed to CO_2 with dissolved water.

Pressure (bar)	Temp. (°C)	Dissolved H_2O (ppmv)	Exposure time (days)	Flow/ mixing	Corrosion rate (mm/y)	Reference
63	22	610	42	No	Negligible	[19]
76	40	244	0.3	No	1.2	[25]
76	40	2440	0.3	No	2.3	[25]
76	40	4880	0.3	No	2.5	[25]
79	31	100	0.3	No	1.1	[27]
79	31	1000	0.3	No	2.5	[27]
80	50	Sat*	1	No	0.4	[26]
80	40	244-3670	7	No	0.4 - 0.6	[30]
80	35	300	2	No	0.003	[31]
80	35	700	2	No	0.005	[31]
80	35	1200	2	No	0.01	[31]
80	35	1770	2	No	0.03	[31]
80	35	3500	2	No	0.1	[31]
82	35	Sat*	5	Yes	0.026	[32]
82	35	Sat*	5	Yes	0.032	[32]
100	25	1220	18	Yes	<0.01	[33]
100	20	1220	30	No	No	[17]
100	25	488	14	Yes	No	[34]
130	40	4880	0.3	No	3.5	[25]
150	80	Sat*	28	No	0.1	[35]

*Water added in excess to ensure that the CO_2 phase was fully saturated with water.

For atmospheric corrosion, it is often referred to 60% relative humidity (RH) as a starting point of corrosion [36]. The reason is that the thickness of the adsorbed water film on the metal surface increases with increasing humidity, and at about 60% RH the surface water film has exceeded a critical thickness (in the order of 5-6 monolayers) where it has got bulk water properties [37,38]. The

conditions in a system with liquid or supercritical CO_2 are probably quite different from atmospheric conditions, but it is not unlikely that the same principles with surface absorption of water will apply. If so, the water film will at some critical thickness achieve bulk water properties, after which it can absorb CO_2 and form carbonic acid, which again may lead to corrosion reactions as explained in Chapter 2.1.1. If this link between water content in the bulk phase and mono layers of surface water applies for dense phase CO_2 conditions is not known. However, Hua et al. [31] observed an increase in general corrosion when the water content was increased from 1300 to 1800 ppmv , which equals about 40 to 54% of the solubility limits of water in CO_2.

2.2 Corrosion effects of single impurities with water

There is consensus that little or nothing happen with single impurity system without dissolved water present. Corrosion with dissolved water and other impurities are reviewed in the following chapters.

2.2.1 $O_2 – H_2O$

The published data on corrosion in CO_2 with H_2O and O_2 as impurities reports a wide spread in corrosion rates, as summarised in Table 2-2. Ayello et al. [25] reported a corrosion rate of 2.3 mm/y with 2440 ppmv water and 100 ppmw O_2 with 76 bar of CO_2 at 40 °C, and Choi et al. [26] showed in 2010 corrosion rates around 1 mm/y when 2 to 6% O_2 was present in water saturated CO_2. While in 2011, the same group [39] reported insignificant corrosion rates with 3.3 bar (equals about 2.6 mol%) O_2 and water concentrations of 650, 2000, and 3000 ppmv (80 bar and 50 °C). The latter water content is close to the saturation limit.

Table 2-2: Published corrosion data for dense phase CO_2 with O_2 and H_2O, no flow or mixing.

Pressure (bar)	Temp (°C)	H_2O (ppmv)	O_2	Exposure Time (days)	CR (mm/y)	Reference
76	40	2440	100 ppmw	0.3	2.3	[25]
80	50	sat	2 %	1	0.6	[26]
80	50	sat	4 %	1	1.1	[26]
80	50	sat	6 %	1	0.9	[26]
80	50	650	3.3 bar (2.6%)	1	<0.01	[39]
80	50	2000	3.3 bar (2.6%)	1	<0.01	[39]
80	50	3000	3.3 bar (2.6%)	1	<0.01	[39]
100	45	sat	1400 ppmv	5	0.04	[40]
100	50	sat	2000 ppmv	10	0.01	[41]
100	20	1220	200 ppmw	30	Negligible	[17]

Both Sun et al. [41] and Zeng et al. [40] reported low general corrosion rates around 0.01 and 0.05 mm/y, respectively, for corrosion tests carried out under water-saturated conditions at 100 bar and

supercritical CO_2. However, Sun et al. also reported localised attacks and suggested that it might be connected to precipitation of water. Dugstad et al. [17] found no corrosion with 1220 ppmv of water and 200 ppmw O_2 (100 bar, 20 °C). It seems like water saturated conditions increases the corrosion rates and contribute to the discrepancy.

2.2.2 $SO_2 – H_2O$

There are several papers which address corrosion in dense phase CO_2 with SO_2 and H_2O, usually compared with and without O_2. Table 2-3 summarises the data without O_2. Ayello et al. [25] studied the effect of SO_2 and H_2O, they reported a corrosion rate of 4.6 mm/y with 2440 ppmv of water and 100 ppmw of SO_2 at 76 bar and 40 °C. Choi et al. [10,39] studied corrosion in CO_2 with 650 ppmv water and in water-saturated CO_2 with 0.8 bar (about 0.7%) SO_2 at 80 bar and 50 °C. They reported a corrosion rate of 3.5 and 5.6 mm/y, respectively. The same group [42] carried out tests with 0.05% (0.04 bar) and 0.1% (0.08 bar) of SO_2, but the corrosion rate was only 0.05 and 0.03 mm/y, respectively, for the same pressure and temperature at 650 ppmv of H_2O. They also tested at 25 °C and found 0.1 mm/y at 650 ppmv of water and 0.08 bar of SO_2. Due to density increase of the CO_2 when the temperature was lowered to 25 °C, the SO_2 concentration was only 0.025% and this could indicate that it is neither the temperature nor the amount of SO_2 that decides the corrosion rate, but rather how much water is present in the CO_2. With 650 ppmv water at 25 °C, the saturation ratio of water is higher than at 50 °C due to an increase in solubility with increasing temperature. They also found localised attacks in form of pits.

Table 2-3: Published corrosion data with SO_2 and water.

Pressure (bar)	Temp (°C)	H_2O (ppmv)	SOx	Exposed (days)	Flow/ mixing	CR (mm/y)	Ref.
60	25	650	0.08 bar (0.025%)	1	No	0.1 (pits)	[42]
60	25	650	0.08 bar (0.025%)	1	Yes	0.013	[42]
75.8	40	2440	100 ppmw	0.3	No	4.6	[25]
80	50	650	0.08 bar (0.1%)	1	No	0.03	[42]
80	50	650	0.04 bar (0.05%)	1	No	0.05	[42]
80	50	Sat	0.8 bar	1	No	5.6	[26]
80	50	650	0.8 bar	1	No	3.48	[39]
95	35	Sat	500 ppm	17	Yes	0.02	[43]
95	35	Sat	500 ppm	46	Yes	0.08	[43]
100	25	488	145 ppmw	14	Yes	<0.005	[34]
100	25	488	500 ppmw	14	Yes	<0.01	[34]
100	25	1220	500 ppmw	14	Yes	0.02	[34]

Dugstad et al. [33,34] reported low general corrosion rates (<0.02 mm/y) when the water was fully dissolved in the CO_2 phase and the SO_2 concentration was below 500 ppmw (100 bar and 25 °C).

They commented that the corrosion occurred in several spots and therefore the corrosion rates could be higher at these areas. Possibly the corrosion coupon might have been hit by the liquid water when it was introduced in the system. However, these findings are supported by Patchigolla et al. [43] who found corrosion rates from 0.02 to 0.08 mm/y in a flow loop with water saturated CO_2 and 500 ppm SO_2 (unclear if this is volume or weight) at 95 bar and 35 °C.

2.2.3 $H_2S – H_2O$

There are only a few experiment with H_2S and water, Schremp and Roberson [22] reported that 1000 ppmv of water with 800 ppmv of H_2S was not corrosive for carbon steel (X-60) in 138 bar CO_2 at 3 and 22 °C. The steel also passed a sulfide cracking test (stress corrosion cracking test). El Alami et al. [35] reported corrosion rates up to 0.3 mm/y on L80 carbon steel at 150 bar and 80 °C in water saturated CO_2 with 3 mol% H_2S, and they also reported localised attacks. Wei et al. [44] found the same corrosion rate as El Alami. However, Zeng and co-workers reported corrosion rates around 0.07 mm/y with 50 and 100 ppmv H_2S at saturated water conditions [40]. This corresponds with Sun et al. [41], who published a corrosion rate of 0.05 mm/y when 2000 ppmv H_2S was present at same conditions and they reported only general corrosion. Both, Zeng and Sun, found higher corrosion rates (about 0.3 mm/y) when O_2 was introduced, and localised attacks was observed. Several years with field experience in US [45] has shown that the present of H_2S in CO_2 transport pipelines do not lead to severe corrosion and the specification allows up to 1500 ppmw of H_2S to be transported with the CO_2.

2.2.4 $NO_2 – H_2O$

Nitrogen dioxide is very interesting since it known to be strongly oxidising and together with other impurities reactions might occurs to produce other corrosive species. Dugstad et al. [33,34,46] reported that the corrosion increased when the concentration of NO_2 was increased from 200 to 500 ppmv, with a water concentration of 1220 ppmv. When the water concentration was reduced from 1220 to 488 ppmv, the corrosion rate decreased to 0.06 mm/y. The corrosion rate was also strongly affected by exposure time, which might be linked to consumption of impurities. When the impurities are partly or fully consumed through corrosion, maximum corrosion rate is achieved in the beginning of the experiment while during the rest of the exposure time the corrosion rate might be very low.

Table 2-4: Published corrosion data with the present of NO_2 and H_2O.

Pressure (bar)	Temp (°C)	H_2O (ppmv)	NOx	Exposed (days)	Flow/ mixing	CR (mm/y)	Ref.
76	40	2440	100 ppmw	0.3	No	11.6	[25]
100	25	1220	500 ppmw	10	Yes	1.6	[34]
100	25	1220	200 ppmw	10	Yes	0.7	[33,34,46]
100	25	488	200 ppmw	20	Yes	0.06	[34]
100	25	488	100 ppmw	3	Yes	0.17	[34]

2.3 Corrosion in CO_2 with multiple impurities

The limited number of papers that has been found showed that in general, the corrosion rates are strongly affected by the type of impurities, combination of impurities and concentration of impurities. Certain combinations are reported to give only negligible corrosion while other combinations may result in severe corrosion. When SO_2-H_2O and SO_2-O_2-H_2O was compared at the same conditions, a moderate increase in corrosion rates was observed when O_2 was present [10,17,29,39,47]. Xiang et al. [48-50] preformed a series of SO_2-O_2-H_2O experiments with 20000 ppmv of SO_2 and found that the corrosion rates increased with increasing water content, similar to what Hua et al. [29] reported. The corrosion rates ranged from 0.04 to 0.87 mm/y [48]. They also observed a temperature effect and an exposure time effect. The corrosion rate increased from 1.1 to 3 mm/y when the temperature was increased from 25 °C to 75 °C, while at 93 °C, the corrosion rate dropped to 1.2 mm/y [50]. The corrosion rate decreased from 1.95 to 0.75 mm/y when the exposure time was increased from 1 day to 8 days [49], and the authors related this effect of the build-up of protective surface layers. Build-up of surface layers that can provide a varying degree of protection is well known for corrosion processes, and in the oil and gas industry where free water usually is present, precipitation of iron carbonate or iron sulfide creates a protective film [2,5]. This also shows that short exposure time would present the worst-case corrosion rate while long term might give more realistic values of the corrosion. However, this would require the experimental conditions to be kept constant without consumption of the impurities due to corrosion or chemical reactions. This will be further discussed in Chapter 9.

There was not found any data that shows the effect of NO_2-O_2-H_2O combination. However, Dugstad et al. [34] observed lower corrosion (0.017 mm/y) with SO_2-NO_2-H_2O combination than with only NO_2-H_2O present (0.17 mm/y). They commented; *''Whether the lower corrosion rate is attributed to less available impurities in the short autoclave, protective corrosion product film formed on the steel surface or consumption of impurities due to impurity reactions in the bulk phase can be questioned''*.

The reported corrosion rates are surprisingly low, for the few reported multiple impurities experiment [51-56] compared to many of the reported rates with water or only two impurities present. The main reason might be related to the control of the water concentration, since all experiments were performed with water concentration at 1000 ppmv and lower, and all corrosion rates were lower than 0.1 mm/y in both static and mixing situation.

2.4 Reactions between impurities

When certain impurities are present simultaneously in the CO_2 phase they can react and form new reaction products. Several "common" impurities are regarded as oxidising agents (O_2, NO_2, and SO_2). The focus of reactions in CO_2 transport systems has mainly been directed towards carbon steel corrosion and type of corrosion products that forms on the steel surface. For example, NO_2 and SO_2 was reported to react (absorb, dissolve) with the surface water film on carbon steel [26,29,47]. It was suggested that the reactions were essentially similar as for atmospheric corrosion:

Dissolution of SO_2 in water film at the steel surface [57]:

$$SO_{2\,(g)} + H_2O_{(l)} \leftrightarrow HSO_{3\,(aq)}^{-} + H_{(aq)}^{+} \quad (2\text{-}7)$$

$$HSO_{3\,(aq)}^{-} \leftrightarrow SO_{3\,(aq)}^{2-} + H_{(aq)}^{+} \quad (2\text{-}8)$$

If oxygen is present, sulfate could form [58]:

$$SO_{3\,(aq)}^{2-} + \frac{1}{2}O_{2\,(g)} \leftrightarrow SO_{4\,(aq)}^{2-} \quad (2\text{-}9)$$

In presence of SO_2, O_2, and H_2O, the corrosion products of carbon steel would then be either ferrous sulphite ($FeSO_3$) or ferrous sulphate ($FeSO_4$) depending on the amount of oxygen present. If the excess of oxygen is high, the ferrous sulphate could be converted to ferric oxyhydroxide (FeOOH) [59].

Formation of nitric acid was reported to proceed by dissolution of NO_2 in the surface water film [60]:

$$3NO_2(g) + H_2O\,(l) \rightarrow 2HNO_3(l) + NO(g) \quad (2\text{-}10)$$

When NO_2 is present, there are numerous reaction routes, which can result in formation of nitric acid or other oxidising substances, also in the gas phase [61-64]. Graedel et al. [58] commented that nitrates are seldom found on the surface as corrosion products and the reason might be that the

nitrate salts are highly soluble and can follow the flowing media (CO_2) away from the surface, instead iron oxide is detected.

Dugstad et al. [56] reported formation of acids in dense phase CO_2 when H_2O, SO_2, H_2S, O_2, and NO_2 were present. They suggested that several chemical reactions took place in both the CO_2 phase. Paschke et al. [51] found nitric acid when NO_2 and H_2O was present, but concluded that sulfuric acid did not form when SO_2, O_2, and H_2O was present because the oxidisation of SO_2 to SO_3 with O_2 was not possible at CCS condition (4 to 50°C and 60 to 200 bar), due to the pressure and temperature. This is also in accordance with findings of Torrente-Murciano et al. [65] who found that SO_2 was not oxidised by NO_2 in the CO_2 gas phase at low pressure (5 to 15 bar), they also confirmed that NO_2 and SO_2 dissolved in water and created sulfuric and nitric acid in the water phase. This result is in contrast with Paschke et al., who found sulfuric acid when NO was added, and suggested that the lead chamber reaction took place:

$$\mathrm{NO_{2\,(g)} + SO_{2\,(g)} + H_2O_{(l)} = H_2SO_{4\,(aq)} + NO_{(g)}} \qquad (2\text{-}11)$$

There are no available data in the literature on solubility of nitric and sulfuric acid in the CO_2 phase. The solubility of these acids is important for predicting if acid producing reactions can result in precipitation of a separate phase with acids. The corrosion situation would be totally different if a second phase is formed instead of the acid remaining dissolved in the CO_2 phase. The acid solubility has been measured in air, Gimtro et al. [66] reported a vapour pressure of sulfuric acid to be 10^{-3} mm Hg (~1.3 ppmv) and 10^{-2} mm Hg (~13 ppmv) at 25 °C and 50 °C, respectively. Sproesser et al. [67] reported vapour pressures for nitric acid of 6.2 (~8200 ppmv) and 13.7 (~18300 ppmv) mm. Hg at 35 °C and 50 °C, respectively. Thus, in air the vapour pressure of nitric acid in air is about three orders of magnitude higher than for sulfuric acid. Although these vapour pressures were found at ambient pressures in air, it would not be surprising if there was a significant difference in acid solubility limits in CO_2 as well.

2.5 Expected impurity concentrations and existing CO_2 specifications

There are numerous types of capturing techniques [68] which each have different efficiencies on various types of impurities. Furthermore, there are various types of flue-gas sources which again will have different types and concentrations of impurities. In summary this means that the captured CO_2 will have a wide range of different types and concentrations of impurities. An example of expected impurity content after oxy-fuel, pre- and post-combustion capturing together with a specification from natural formation is shown in Table 2-5.

Table 2-5: The concentrations of impurities from different capturing sources and natural formation.

Compound	**Oxy-fuel [69]**	**Pre-combustion [70]**	**Post-combustion [71]**	**Natural formation Weyburn [72]**
H_2O (ppmv)	100	600	100	<20
SO_x (ppmv)	70	0	10	-
O_2 (ppmv)	100	0	150	<50
NO_x (ppmv)	100	0	20	-
H_2S/COS (ppmv)	0	<100	0	9000
CO (ppmv)	50	400	10	1000
Ar, N_2, H_2 (ppmv)	300	20000	450	<300
Hydrocarbons (vol. %)	-	0.02	-	2.3

There are many suggested specifications and recommendations in the literature for the maximum allowed impurity content in CO_2. An extensive report from the National Energy Technology Laboratory (NETL), where 55 different specification were summarised [73], showed that there is a wide spread of the number of impurities expected to be present in the CO_2 after capture. Table 2-6 shows the impurities that will be focus on in this thesis and their concentration range based on the report from NETL.

Table 2-6: Expected concentration ranges for impurities [73] transported in pipeline, CO_2 is the balance.

Compound	**Concentration (ppmv)**
H_2O	20 – 650
O_2	10 – 40000
SOx	10 – 50000*
H_2S	20 – 13000*
NOx	20 – 2500*
N_2	100 – 7000
Ar	100 – 4000
CH_4	100 – 4000
H_2	100 – 4000
CO	10 – 5000
NH_3	0 – 50
C_2H_6	0 – 1000
C_3+	0 – 1000
Glycol	0 – 0.174
Particles	0 – 1

*Often given as 100 ppmv for HSE concern.

The final recommendation made from all these reviewed specifications is summarised in Table 2-7 and compared with the Dynamis [72] recommendation which is one of the most referred to in the

literature. Due to the lack of experimental data, the both recommendations had to used HSE concern to set the limits, and for this reason they might not be the best for the integrity of the carbon steel pipeline. The NETL report pointed out that most of these concentration levels are not based experimental data but rather set by health, safety and the environmental (HSE) concerns and stressed that the experimental base for making specification was too thin and for design of transport systems more experimental results are needed in several areas. The shaded impurities in Table 2-7 are the ones investigated in this thesis. They are of most concern for corrosion of carbon steel, while the other impurities would be more interesting when it comes to flow properties inside the pipeline.

Table 2-7: Comparison of the NETL and the Dynamis recommendation.

Compound	**NETL** [73] **(ppmv)**	**Dynamis** [72] **(ppmv)**
H_2O	500	500
O_2	10	<4000
SOx	100*	100*
H_2S	100*	200*
NOx	100*	100*
N_2	4000	<4000
Ar	4000	<4000
CH_4	4000	<4000
H_2	4000	<4000
CO	35	2000
NH_3	50	-
C_2H_6	1000	-
C_3+	< 1000	-
Glycol	0.046	-
Particles	1	-

*Often given as 100 ppmv for HSE concern.

2.6 Experimental methods and equipment

Essentially all papers on corrosion in liquid and supercritical CO_2 (see chapter 2.1, 2.2, and 2.3) have used autoclaves for the experimental testing. There are many different variants of the setups, but they typically consist of; an autoclave with heating jacket, a temperature transmitter (TT), a pressure transmitter (PT), one or multiple holders for hanging corrosion coupons, and one or several valves for loading and relief, see example in Figure 2-1.

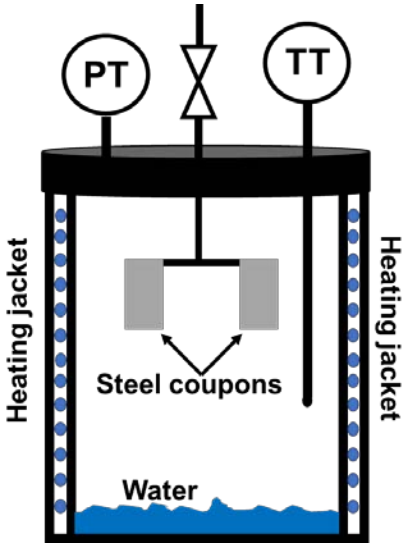

Figure 2-1: Simple sketch of a typical autoclave system with hanging coupons and injected water at the bottom. Pressure transmitter (PT) and temperature transmitter (TT) is fitted.

There are also large variations in the start-up procedures, but it usually consists of the following sequence of actions: mounting the specimens, deaerate the autoclave, injection of liquid water, deaerate, injection of impurities, and finally pressurising with CO_2. The autoclave was then kept closed throughout the experiment, and there was usually no analyses of the impurities or water content before, during, or after the experiment. The water was always added as liquid water directly in the autoclave in the beginning, either as a small amount for under-saturated experiments (water fully dissolved in the CO_2 phase) or as a large amount for water saturated experiments (water added in excess, may replenish if water is depleted from the CO_2 phase).

Information on how fast the CO_2 was loaded into the autoclave or how fast the depressurisation process was at the end of the experiment was not reported in any of the papers. Apparently, all papers assumed that the liquid water dissolved rapidly into the CO_2 bulk phase, but it was not possible to find any experiments that actually had measured the dissolution rate. Slow dissolution of liquid water was indirectly reported in a paper from Thodla and Ayello [25,27], they used electrochemical impedance spectroscopy (EIS) to study the corrosion in pressurised CO_2. One droplet of water, equal 100 ppmw if dissolved in the bulk CO_2 phase, was still present after 6 hours in the CO_2 at 76 bar.

Several experiments were conducted with a relatively short exposure time [9,26,31,39,74], even as short as 6 hours [25,27]. For a closed autoclave system with on-going corrosion processes, it is reasonable to keep the test time short to prevent that the impurities will be fully consumed. On the other hand, it is well known that many corrosion processes need longer time (weeks) to reach a

steady rate, and thus the relevance of the very short experiments could be questioned. Hua and colleagues [29] concluded that the amount of corrosion compared with the amount of consumed impurities was negligible for their experiments with low corrosion rates.

2.7 Summary

The present literature study has identified that the amount - and state - of water is extremely important for carbon steel corrosion in dense phase CO_2 systems. The corrosion rate is several decades higher when carbon steel is exposed to a free water phase (20 to 50 mm/y) compared to exposure to CO_2 with fully dissolved water (0.001 to 0.1 mm/y). Experiments with corrosion coupons exposed to water-saturated CO_2, usually reports higher corrosion rates (0.1 to 1.5 mm/y) than similar experiments with exposure to undersaturated CO_2. Collier et al. reported a high degree of scatter in the corrosion data and concluded that there are several limitations in the experimental method. They found essential the same corrosion rate, about 0.02 mm/y, in pure and water-saturated CO_2.[32] Although the corrosion rates probably would increase when the water content approaches saturation, it is not clear if the this increase should be just slightly or several decades since the amount water dissolved in the CO_2 phase is small. However, essentially all water-saturated experiments have applied an excess of water in the autoclave, which increases the chances of accidental spilling of liquid water to the corrosion coupons – especially during pressurising and depressurisation. Furthermore, for a fully water saturated CO_2 phase, small temperature and pressure fluctuations may cause intermittent periods with water condensation. In almost every corrosion experiment with water dissolved in the CO_2 phase, the water was injected in liquid state before the system was pressurised with CO_2. It was therefore, implicitly, assumed that the dissolution rate of liquid water in dense phase CO_2 is fast, but experiments that measured the dissolution rate were not found. Thus, there are some uncertainties around these experiments, especially those with very short exposure time.

The review identified several components that is expected to be present at low concentrations in the captured CO_2 (often referred to as impurities). Of most interest with respect to corrosion are SO_2, NO_2, H_2S, H_2O, and O_2. The presence of impurities had very varying effects on corrosion and chemical reactions, depending both on the combination and concentration of impurities. According to the literature, certain impurity combinations are non-reactive while other may result in chemical reactions and corrosion. For example, H_2S and O_2 will alone not cause corrosion. However, the results with H_2S and O_2 (present individually and together) are somewhat contradictive, which could

most likely be connected to the presence of excess/liquid water rather than the impurities itself. For example it was reported it was reported up to 1 mm/y with O_2 and water-saturated condition [26], while others [40,41] reported 0.01 to 0.04 mm/y. The review also identified that SO_2 and NO_2 may result in corrosion either by direct reactions or due to formation of acids, especially if present together with water and O_2.[51,55] Both, Dugstad et al.[55] and Paschke et al.[51], suggested that the lead chamber reaction might occur and NO_2 could be the catalysing part to form sulfuric acid.

Several corrosion reactions have been proposed in CO_2 with dissolved water, and the general opinion is that the thin water film on the steel surface could attract impurities like SO_2 and NO_2 to create acids.[75] Thus, the main understanding has been that these reactions occur on the steel substrate and typically corrosion products would be $FeCO_3$, $FeSO_3$, $FeSO_4$, and FeOOH. A normal operation situation for CO_2 transport will occur with water fully dissolved (and much lower than the solubility limit) in the CO_2, and it might be that there is not enough water to produce a water film thick enough to allows these surface reactions to proceed. In a fully water-saturated condition, the water surface film may be thicker, which possibly could let such reactions occur without too much hinderance. There is however indication that some reaction is occurring in the CO_2 phase creating aggressive species that could attack carbon steel. [51,55]

Some papers reported that sulfuric and nitric acid could form from reaction of certain impurities. These acids are very corrosive to carbon steel, and it is therefore important to know if these acids will precipitate or dissolve in the CO_2 phase. The literature search did not find any solubility data for sulfuric and nitric acid in dense phase CO_2. However, ambient pressure experiments showed several decades difference in solubility between nitric acid and sulfuric acid in air, the latter had the lowest value.

2.8 References

[1] L. E. J. Newton, R. A. McClay, "Corrosion and Operational Problems, CO_2 Project, Sacroc Unit", SPE Permian Basin Oil and Gas Recovery Conference (SPE: Society of Petroleum Engineers, 1977).

[2] S. Nesic, Key issues related to modelling of internal corrosion of oil and gas pipelines – A review, *Corrosion Science*, 49, 12 (2007) pp. 4308-4338.

[3] S. Nesic, "A Critical review of CO_2 corrosion modelling in the oil and gas industry", 10th Middle East Corrosion Conference 7-10 March 2004 (2004).

[4] S. Nesic, J. Postlethwaite, S. Olsen, An electrochemical model for prediction of corrosion of mild steel in aqueous carbon dioxide solutions, *CORROSION*, 52, 4 (1996) pp. 280 - 294.

[5] A. Dugstad, "Fundamental aspects of CO_2 metal loss corrosion - Part 1: Mechanism", CORROSION/2006 (Houston, TX: NACE International, 2006).

[6] A. Dugstad, "Fundamental aspects of CO_2 metal loss corrosion, Part I: Mechanism revisited", CORROSION/2015 (Houston, TX: NACE International, 2015).

[7] M. Seiersten, "Materials Selection for Separation, Transportation and Disposal of CO_2", CORROSION/2001, paper no. 01042 (Houston, TX: NACE International, 2001).

[8] S. M. Hesjevik, S. Olsen, M. Seiersten, "Corrosion at high CO_2 pressure", CORROSION/2003, paper no. 03345 (Houston, TX: NACE International, 2003).

[9] Y. Choi, S. Nesic, "Corrosion behaviour of carbon steel in supercritical CO_2 – water environments", CORROSION/2009, paper no. 09256 (Houston,TX: NACE International, 2009).

[10] Y.-S. Choi, S. Nesic, D. Young, Effect of Impurities on the Corrosion Behavior of CO_2 Transmission Pipeline Steel in Supercritical CO_2–Water Environments, *Environmental Science & Technology*, 44, 23 (2010) pp. 9233-9238.

[11] Y.-S. Choi, S. Nešić, Determining the corrosive potential of CO_2 transport pipeline in high pCO_2–water environments, *International Journal of Greenhouse Gas Control*, 5, 4 (2011) pp. 788-797.

[12] A. Dugstad, B. Morland, S. Clausen, Corrosion of transport pipelines for CO_2 - Effect of water ingress, *Energy Procedia*, 4, (2011) pp. 3063-3070.

[13] Y. Zhang, K. Gao, G. Schmitt, "Inhibition of Steel Corrosion Under Aqueous Supercritical CO_2 Conditions", CORROSION/2011, paper no. 11379 (Houston, TX: NACE International, 2011).

[14] Y. Zhang, X. Pang, S. Qu, X. Li, K. Gao, The relationship between fracture toughness of CO_2 corrosion scale and corrosion rate of X65 pipeline steel under supercritical CO_2 condition, *International Journal of Greenhouse Gas Control*, 5, 6 (2011) pp. 1643-1650.

[15] Y. Zhang, X. Pang, S. Qu, X. Li, K. Gao, Discussion of the CO_2 corrosion mechanism between low partial pressure and supercritical condition, *Corrosion Science*, 59, (2012) pp. 186-197.

[16] A. M. Nor, M. F. Suhor, M. F. Mohamed, M. Singer, S. Nesic, "Corrosion Of Carbon Steel In High CO_2 Containing Environments - The Effect Of High Flow Rate", CORROSION/2012, paper no. 1683 (Houston, TX: NACE International, 2012).

[17] A. Dugstad, S. Clausen, B. Morland, "Transport of dense phase CO_2 In C-steel pipelines - When is corrosion an issue?", CORROSION/2011 (Houston, TX: NACE International, 2011).

[18] T. E. Gill, "Canyon Reef Carriers, Inc. CO_2 Pipeline: Description and 12 years of operation", ASME Energy-Source Technol. Conf, Pipeline Eng. Symp. (1985).

[19] B. P. McGrail, H. T. Schaef, V. A. Glezakou, L. X. Dang, A. T. Owen, Water reactivity in the liquid and supercritical CO_2 phase: Has half the story been neglected?, *Energy Procedia*, 1, 1 (2009) pp. 3415-3419.

[20] L. E. Newton, "SACROC CO_2 Project – Corrosion problems and solutions", CORROSION/84, paper no. 67 (Houston, TX: NACE International, 1984).

[21] W. A. Propp, T. E. Carleson, C. M. Wai, P. R. Taylor, K. W. Daehling, S. Huang, M. Abdel-Latif, "Corrosion in supercritical fluids", Report no. DE96014006, US Department of Energy, Washington, DC.

[22] F. Schremp, G. Roberson, Effect of Supercritical CO_2 on Materials of Construction, in: Meeting of Society of Petroleum Engineers of AIME in Las Vegas, Nevada, (1973).

[23] F. W. Schremp, G. R. Roberson, Effect of supercritical carbon dioxide on construction materials, *Society of Petroleum Engineers Journal*, 15, (1975) pp. 227-233.

[24] J. M. West, "Design and operation of a supercritical CO_2 pipeline-compression system Sacroc unit, Scurry County, Texas", SPE Permian Basin Oil Recovery Conference, paper no. 4804 (Society of Petroleum Engineers, 1974).

[25] F. Ayello, K. Evans, R. Thodla, N. Sridhar, "Effect of impurities on corrosion of steel in supercritical CO_2", CORROSION/2010, paper no. 10193 (Houston, TX: NACE International, 2010).

[26] Y.-S. Choi, S. Nesic, "Effect of impurities on the corrosion behavior of carbon steel in supercritical CO_2 - water environments", CORROSION/2010, paper no. 10196 (Houston, TX: NACE International, 2010).

[27] R. Thodla, A. Francois, N. Sridhar, "Materials Performance In Supercritical CO_2 Environments", CORROSION/2009, paper no. 09255 (Houston, TX: NACE International, 2009).

[28] S. Sim, I. S. Cole, F. Bocher, P. Corrigan, R. P. Gamage, N. Ukwattage, N. Birbilis, Investigating the effect of salt and acid impurities in supercritical CO_2 as relevant to the corrosion of carbon capture and storage pipelines, *International Journal of Greenhouse Gas Control*, 17, (2013) pp. 534-541.

[29] Y. Hua, R. Barker, A. Neville, The influence of SO_2 on the tolerable water content to avoid pipeline corrosion during the transportation of supercritical CO_2, *International Journal of Greenhouse Gas Control*, 37, (2015) pp. 412-423.

[30] S. Sim, F. Bocher, I. S. Cole, X. B. Chen, N. Birbilis, Investigating the Effect of Water Content in Supercritical CO_2 as Relevant to the Corrosion of Carbon Capture and Storage Pipelines, *CORROSION*, 70, 2 (2014) pp. 185-195.

[31] Y. Hua, R. Barker, A. Neville, Effect of temperature on the critical water content for general and localised corrosion of X65 carbon steel in the transport of supercritical CO_2, *International Journal of Greenhouse Gas Control*, 31, (2014) pp. 48-60.

[32] J. Collier, S. Papavinasam, J. Li, C. Shi, P. Liu, J.-P. Gravel, "Effect of impurities on the corrosion performance of steels in supercritical carbon dioxide: Optimization of experimental procedure", CORROSION/2013 (Houston, TX: NACE International, 2013).

[33] A. Dugstad, M. Halseid, B. Morland, S. Clausen, "Dense phase CO_2 transport – When is corrosion a threat", Northern Area Western Conference/2011 (Houston, TX: NACE International, 2011).

[34] A. Dugstad, M. Halseid, B. Morland, A. O. Sivertsen, "Corrosion in dense phase CO_2 with small amounts of SO_2, NO_2 and water", Eurocorr 2012, paper no. 1603 (2012).

[35] H. El Alami, C. Augustin, B. Orlans, J.-J. Servier, "Carbon capture and storage projects: material integrity for CO_2 injection and storage", Eurocorr 2011, paper no. 4741 (2011).

[36] S. L. Pohlman, *Atmospheric corrosion*, in: ASM Handbook (Metals Park, OH: ASM International, 1987) pp. 80-83.

[37] C. Leygraf, *P. Marcus, J. Oudar (Eds.), Corrosion Mechanisms in Theory and Practice*, (New York, 1995).

[38] Y. Ben-Da, S. Meilink, G. W. Warren, P. Wynblatt, Water adsorption and surface conductivity measurements on alumina substrates, *Components, Hybrids, and Manufacturing Technology, IEEE Transactions on*, 10, 2 (1987) pp. 247-251.

[39] Y.-S. Choi, S. Nesic, "Effect of water content on the corrosion behavior of carbon steel in supercritical CO_2 phase with impurities", CORROSION/2011, paper no. 11377 (Houston, TX: NACE International, 2011).

[40] Y. Zeng, H. Arafin, C. Shi, R. Zavadil, "Influence of impurity hydrogen sulfide on the corrosion performance of pipeline steels in supercritical carbon dioxide stream", CORROSION/2016, paper no. 7223 (Houston, TX: NACE International, 2016).

[41] J. Sun, C. Sun, G. Zhang, X. Li, W. Zhao, T. Jiang, H. Liu, X. Cheng, Y. Wang, Effect of O_2 and H_2S impurities on the corrosion behavior of X65 steel in water-saturated supercritical CO_2 system, *Corrosion Science*, 107, Supplement C (2016) pp. 31-40.

[42] F. Farelas, Y. S. Choi, S. Nesic, "Effects of CO_2 phase change, SO_2 content and flow on the corrosion of CO_2 transmission pipeline steel", CORROSION/2012, paper no. 1322 (Houston, TX: NACE International, 2012).

[43] K. Patchigolla, J. E. Oakey, E. J. Anthony, Understanding dense phase CO_2 corrosion problems, *Energy Procedia*, 63, (2014) pp. 2493-2499.

[44] L. Wei, X. Pang, K. Gao, Effect of small amount of H_2S on the corrosion behavior of carbon steel in the dynamic supercritical CO_2 environments, *Corrosion Science*, 103, Supplement C (2016) pp. 132-144.

[45] IPCC, "IPCC special report on carbon dioxide capture and storage. Prepared by Working Group III of the Intergovernmental Panel on Climate Change", 2005, C.U. Press, Intergovernmental Panel on Climate Change, Cambridge and New York.

[46] A. Dugstad, M. Halseid, B. Morland, "Corrosion in dense phase CO_2 pipelines – State of the art", Eurocorr 2011, paper no. 4954 (2011).

[47] Y. Xiang, Z. Wang, C. Xu, C. Zhou, Z. Li, W. Ni, Impact of SO_2 concentration on the corrosion rate of X70 steel and iron in water-saturated supercritical CO_2 mixed with SO_2, *The Journal of Supercritical Fluids*, 58, 2 (2011) pp. 286-294.

[48] Y. Xiang, Z. Wang, X. Yang, Z. Li, W. Ni, The upper limit of moisture content for supercritical CO_2 pipeline transport, *The Journal of Supercritical Fluids*, 67, (2012) pp. 14-21.

[49] Y. Xiang, Z. Wang, Z. Li, W. D. Ni, Effect of exposure time on the corrosion rates of X70 steel in supercritical $CO_2/SO_2/O_2/H_2O$ environments, *CORROSION*, 69, 3 (2012) pp. 251-258.

[50] Y. Xiang, Z. Wang, Z. Li, W. D. Ni, Effect of temperature on corrosion behaviour of X70 steel in high pressure $CO_2/SO_2/O_2/H_2O$ environments, *Corrosion Engineering, Science and Technology*, 48, 2 (2013) pp. 121-129.

[51] B. Paschke, A. Kather, Corrosion of pipeline and compressor materials due to impurities in separated CO_2 from fossil-fuelled power plants, *Energy Procedia*, 23, (2012) pp. 207-215.

[52] O. Yevtushenko, R. Bäßler, I. Carrillo-Salgado, "Corrosion stability of piping steels in a circulating supercritical impure CO_2 environment", CORROSION/2013, paper no. 2372 (Houston, TX: NACE International, 2013).

[53] O. Yevtushenko, R. ler, "Water impact on corrosion resistance of pipeline steels in circulating supercritical CO_2 with SO_2- and NO_2- impurities", CORROSION/2014, paper no. 3838 (Houston, TX: NACE International, 2014).

[54] H. Rütters, "COORAL – CO_2 purity for capture and storage", 7th CO2GeoNet Open Forum (2012).

[55] A. Dugstad, M. Halseid, B. Morland, "Experimental techniques used for corrosion testing in dense phase CO_2 with flue gas impurities", CORROSION/2014, paper no. 4383 (Houston, TX: NACE International, 2014).

[56] A. Dugstad, M. Halseid, B. Morland, Testing of CO_2 specifications with respect to corrosion and bulk phase reactions, *Energy Procedia*, 63, (2014) pp. 2547-2556.

[57] W. L. Jolly, W. L. Jolly, *Modern inorganic chemistry*, (McGraw-Hill New York, 1991).

[58] T. Graedel, M. Mandich, C. Weschler, Kinetic model studies of atmospheric droplet chemistry: 2. Homogeneous transition metal chemistry in raindrops, *Journal of Geophysical Research: Atmospheres*, 91, D4 (1986) pp. 5205-5221.

[59] I. Allam, J. Arlow, H. Saricimen, Initial stages of atmospheric corrosion of steel in the Arabian Gulf, *Corrosion Science*, 32, 4 (1991) pp. 417-432.

[60] C. H. Nelli, G. T. Rochelle, Nitrogen dioxide reaction with alkaline solids, *Industrial & engineering chemistry research*, 35, 4 (1996) pp. 999-1005.

[61] J. Wang, B. E. Koel, IRAS studies of NO_2, N_2O_3, and N_2O_4 adsorbed on Au (111) surfaces and reactions with coadsorbed H_2O, *The Journal of Physical Chemistry A*, 102, 44 (1998) pp. 8573-8579.

[62] S. Oesch, The effect of SO_2, NO_2, NO and O_3 on the corrosion of unalloyed carbon steel and weathering steel—the results of laboratory exposures, *Corrosion Science*, 38, 8 (1996) pp. 1357-1368.

[63] M. Pradhan, N. Suchak, P. Walse, J. Joshi, Multicomponent gas absorption with multiple reactions: modelling and simulation of NOx absorption in nitric acid manufacture, *Chemical engineering science*, 52, 24 (1997) pp. 4569-4591.

[64] B. Finlayson-Pitts, L. Wingen, A. Sumner, D. Syomin, K. Ramazan, The heterogeneous hydrolysis of NO_2 in laboratory systems and in outdoor and indoor atmospheres: An integrated mechanism, *Physical Chemistry Chemical Physics*, 5, 2 (2003) pp. 223-242.

[65] L. Torrente-Murciano, V. White, F. Petrocelli, D. Chadwick, Study of individual reactions of the sour compression process for the purification of oxyfuel-derived CO_2, *International Journal of Greenhouse Gas Control*, 5, Supplement 1, (2011) pp. S224-S230.

[66] J. I. Gmitro, T. Vermeulen, Vapor-liquid equilibria for aqueous sulfuric acid, *AIChE Journal*, 10, 5 (1964) pp. 740-746.

[67] W. C. Sproesser, G. B. J. Taylor, Vapor pressures of aqueous solutions of nitric acid, *Journal of the American Chemical Society*, 43, 8 (1921) pp. 1782-1787.

[68] M. Mohitpour, A. Jenkins, G. Nahas, A generalised overview of requirements for the design, construction, and operation of new pipelines for CO_2 sequestration, *The Journal of Pipeline Integrity*, 7, 4 (2008) pp. 237-252.

[69] A. Kather, S. Kownatzki, Assessment of the different parameters affecting the CO_2 purity from coal fired oxyfuel process, *International Journal of Greenhouse Gas Control*, 5, (2011) pp. S204-S209.

[70] A. Kather, B. Paschke, S. Kownatzki, "CO_2-Reinheit für Abscheidung und Lagerung", Report no. FKZ 0327790E, Hamburg University of Technology.

[71] R. T. J. Porter, M. Fairweather, M. Pourkashanian, R. M. Woolley, The range and level of impurities in CO_2 streams from different carbon capture sources, *International Journal of Greenhouse Gas Control*, 36, (2015) pp. 161-174.

[72] E. de Visser, C. Hendriks, M. Barrio, M. Mølnvik, G. de Koeijer, S. Liljemark, Y. Le Gallo, Dynamis CO_2 quality recommendations, *International Journal of Greenhouse Gas Control*, 2, (2008) p. 478.

[73] NETL, "CO_2 impurity design parameters", Report no. DE-FE0004001, (2013), NETL.

[74] F. Farelas, Y. S. Choi, S. Nesic, Corrosion behavior of API 5L X65 carbon steel under supercritical and liquid carbon dioxide phases in the presence of water and sulfur dioxide, *CORROSION*, 69, 3 (2012) pp. 243-250.

[75] C. Sun, J. Sun, S. Liu, Y. Wang, Effect of water content on the corrosion behavior of X65 pipeline steel in supercritical CO_2-H_2O-O_2-H_2S-SO_2 environment as relevant to CCS application, *Corrosion Science*, 137, (2018) pp. 151-162.

Chapter 4

Corrosion of carbon steel in dense phase CO_2 with water above and below the solubility limit

Bjørn H. Morland, Arne Dugstad and Gaute Svenningsen

Published in *Energy Procedia*, **vol. 114**, Supplement C (2017) pp. 6752-6765.
https://doi.org/10.1016/j.egypro.2017.03.1807

Available online at www.sciencedirect.com

ScienceDirect

Energy Procedia 114 (2017) 6752 – 6765

Energy Procedia

13th International Conference on Greenhouse Gas Control Technologies, GHGT-13, 14-18 November 2016, Lausanne, Switzerland

Corrosion of carbon steel in dense phase CO_2 with water above and below the solubility limit

Bjørn H. Morland[a,b], Arne Dugstad[a], Gaute Svenningsen[a]

[a]*Institute for Energy Technology, PO Box 40, NO-2027 Kjeller, Norway*
[b]*University of Oslo, POBox 1072 Blindern, NO-0316 Oslo, Norway*

Abstract

Few experimental studies have addressed corrosion under dense phase CO_2 transport conditions and very different corrosion rates (CR) are reported for apparently the same concentration of impurities (i.e. water) in the CO_2 stream. The differences reflect short-comings in the experimental methodology and demonstration the need for a commonly agreed test approach.

An experimental set up allowing accurate control of the water concentration was developed and used in the present work, which provides a more realistic condition mimicking the situation in the operating pipelines. Five corrosion experiments were conducted at 95 bar to determine the corrosion rate of carbon steel in CO_2 with various concentration of dissolved water. The water concentration was increased stepwise from 100 ppmv to the solubility limit and the limit was also exceeded in one of the experiment. The temperature was varied between 8 °C and 35 °C.

The general corrosion rates determined by weight loss were around 1.0 µm/y and no localised attacks were observed as long as the water content was below the solubility limit or exceeding the solubility limit with 10 percent for 400 hours. The results indicate that the corrosion rate of carbon steel will be negligible in the CO_2-water system as long as the water is kept below the solubility limit. The presence of other impurities than water will change the condition for precipitation of corrosive aqueous phases.

Peer-review under responsibility of the organizing committee of GHGT-13.

Keywords: CCS; dense phase CO_2; corrosion; dissolved water; carbon steel; saturation degree; entrained water

Peer-review under responsibility of the organizing committee of GHGT-13.
doi:10.1016/j.egypro.2017.03.1807

1. Introduction

The CO_2 concentration in the atmosphere has increased dramatically over the last century, and much of this increase is a direct consequence of human activities. Being a greenhouse gas, CO_2 significantly contributes to global warming, and there is an international agreement to reduce emission of CO_2 [1]. One method of reducing the CO_2 release is carbon dioxide capture and storage (CCS).

In CSS, the site of storage could be quite far from the site of capture, thus transport of the captured CO_2 will be necessary. CO_2 can be transported by ships, pipelines or a combination of both. However, for large volume and short to medium distances, pipeline transport is usually the most cost effective means of transportation. For a number of countries, including Norway, the preferred storage locations will be offshore, necessitating offshore pipelines between the capture and the storage facilities. USA has routinely transported CO_2 in land based pipelines for over 30 years, giving rise to the assumption that CO_2 transport in CCS will not involve corrosion challenges, and that research on this topic is of less importance [2, 3]. Although valuable data can be acquired from the existing CO_2 transport pipelines, CCS pipelines will deal with different challenges since the captured CO_2 may contain other components (impurities), including water, at varying concentrations. Limited amount of water will be present after the capture process, but water may also enter the CCS pipelines in response to accidents or operational errors. Water flooding might increase the corrosion rate considerably, and reduce the lifetime of the pipeline [4].

It is very important to distinguish between water present as a separate aqueous phase and water dissolved in the CO_2. It is well known that a free water phase under the high CO_2 pressures expected in CCS pipelines will result in unacceptably high corrosion rates, which can range from 0.2 to 40 mm/y depending on pressure, temperature and flow rate [4-13].

Most of the published CO_2 transport specifications have a recommended maximum water concentration between 20 and 650 ppmv [14]. In a pure water-CO_2 system, this water range is far below the solubility limit indicated in Figure 1 and the water will therefore not precipitate as a separate phase in the given temperature range. When the water concentration is below the solubility limit, most labs find the corrosion rate to be insignificant for pure CO_2-H_2O systems [4, 8, 15-21] (Table 1). However, some researchers have reported higher corrosion rates, even above 3 mm/y in lab experiments [22-24] for the same content of dissolved water. There have also been reported localised attacks up to 1.4 mm/y [25, 26]. In summary the effect of water on the corrosion rate is an important parameter, but it is not consensus on how it affects the corrosion of carbon steel.

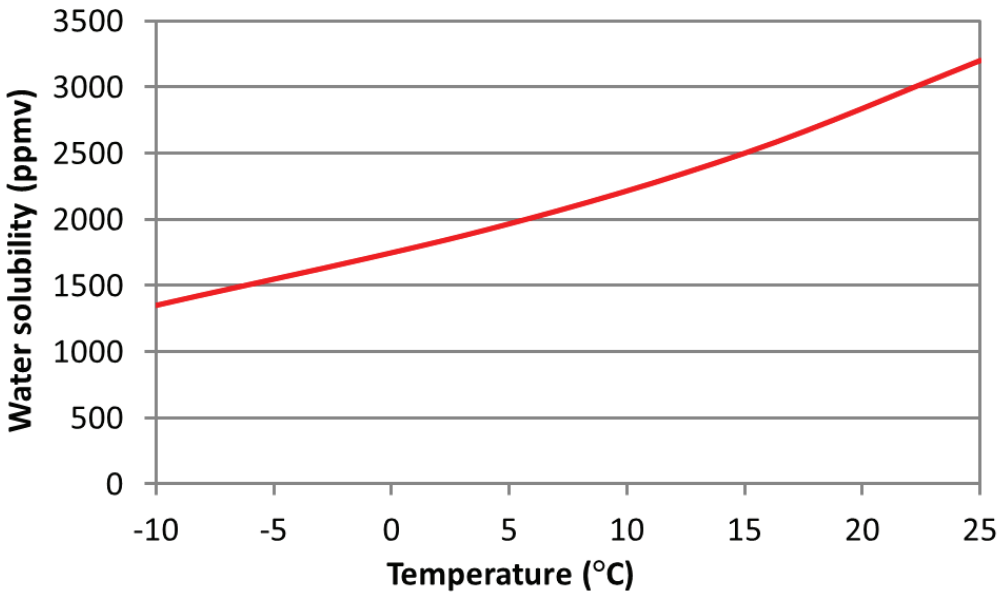

Figure 1. Solubility of water in pure CO_2 as a function of temperature at a pressure of 100 bar [3].

Table 1. Summary of lab experiments with dissolved water in CO_2 at stagnant condition.

H_2O (ppmv)	Pressure (bar)	Temp (°C)	Exposed days	CR (mm/y)	Ref.
100	79	31	0.25	1.1	[24]
240	80	40	7	0.08	[27]
244	76	40	0.25	1.2	[22]
300	80	35	2	0.003	[25]
490	80	40	7	0.07	[27]
610	63	22	42	No	[16]
700	80	35	2	0.004	[25]
730	80	40	7	0.06	[27]
980	80	40	7	0.08	[27]
998	63	22	21	Slight	[16]
1000	79	31	0.25	2.5	[24]
1220	100	20	30	No	[4]
1200	80	35	2	0.01	[25]
1200	80	40	7	0.07	[27]
1770	80	35	2	0.03	[25]
2440	76	40	0.25	2.3	[22]
2650	80	50	2	0.014	[25]
2800	80	35	2	0.07	[25]
3670	80	40	7	0.08	[27]
4880	76	40	0.25	2.5	[22]
4880	130	40	0.25	3.5	[22]
Sat	80	35	0.6	0.11	[25]
Sat	80	35	1	0.11	[25]
Sat	80	35	2	0.10	[25]
Sat	80	40	7	0.11	[27]
Sat	80	40	7	0.17	[27]
Sat	80	40	7	0.11	[27]
Sat	80	50	0.6	0.09	[25]
Sat	80	50	1	0.03	[25]
Sat	80	50	2	0.02	[25]
Sat	80	50	1	0.4	[23]
Sat	150	80	28	0.1	[28]

Most of the published papers discussing corrosion in dense phase CO_2 with dissolved water are based on stagnant autoclave experiments where water is injection before the addition of CO_2. Very few paper actually analyses of the water content in the CO_2 during the experiment. Thus it is possible that the water was unevenly distributed inside the test equipment or that part of the water was consumed. The present work was carried out in an advanced loop

system with good control of the water content. The loop system has four important advantages: accurate control of water dosing and continuous replenishment of CO_2 and water, measurement of the actual water level in the CO_2 phase, no uncontrolled water droplet formation, and no overdosing in the beginning of the experiment.

The results presented in this paper were produced in a recent master thesis at IFE and the University of Oslo [29].

2. Experimental

2.1. Loop/reaction chamber

The experiments were carried out in a high pressure loop built in Hastelloy C276, a highly corrosion resistant material. The loop is designed for a pressure up to 500 bar and is placed inside a ventilated cabinet for HSE reasons (see Figure 2). A cooling unit and heating clamps controlled the loop temperature in the range 0 °C to 60 °C. The loop volume was 2.15 L. There was an inlet for CO_2 pre-mixed with water and an outlet for CO_2 that was routed to the analyser where the water concentration was measured.

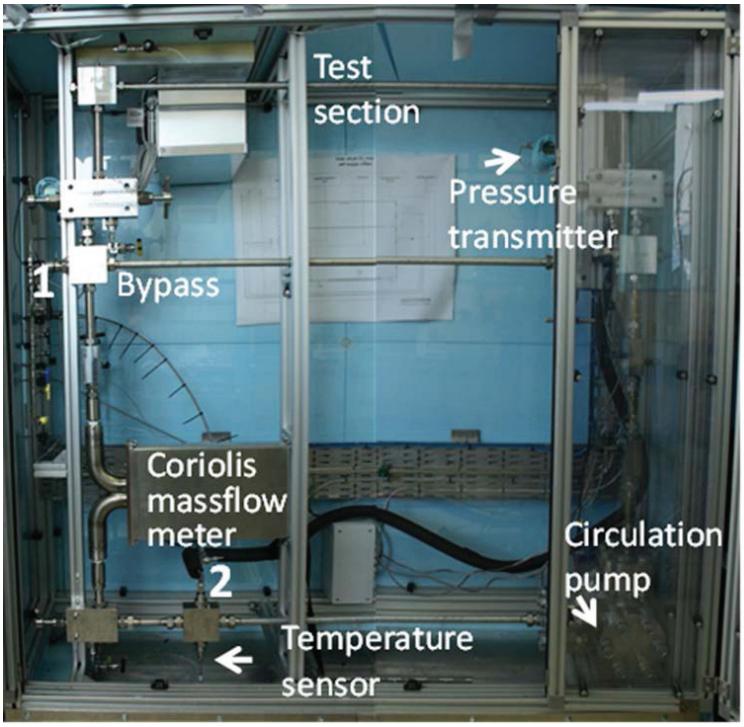

Figure 2. The high pressure CO_2 impurity loop. The test section is on the top where the carbon steel sample can be placed. Bypass of the test section is in the middle, temperature sensor, two pressure transmitters, and a coriolis massflow meter are placed as indicated on the figure. The inlet for the CO_2 with pre-mixed levels of water is indicated with "1", and the outlet from where CO_2 can be sent to the analyser for the determination of water concentration in CO_2 is indicated with "2".

The carbon steel test coupon was placed in the test section before the loop was flushed with CO_2 to make sure that no oxygen was present. A booster pump was then used to fill the loop, with dry CO_2 until the pressure reached 95 bar. The test section which was closed before the feeding of wet CO_2, was by-passed until the required water level was reached. The circulation pump was adjusted to give a flow velocity of 0.4 m/s.

2.2. Water dosing unit

Accurate water dosing was acquired by adjusting the flow ratio of dry CO_2 and water saturated CO_2 using mass flow meters (see Figure 3). The water saturated CO_2 was produced by letting dense phase CO_2 flow slowly through a tank with liquid water (wetting chamber). The saturation concentration of water in CO_2 is temperature dependent (Figure 1), so the temperature of the wetting chamber will affect the amount of water in the wet CO_2. The temperature was fixed at 20 °C in the present study. Since the system was continuously dosed, the wet CO_2 was possibly not in complete equilibrium, but this was compensated for by adjusting the mixing ratios of dry and wet CO_2. The dosing unit could deliver water concentration range from 10 ppmv to about 2500 ppmv at 20 °C, depending on the flow rate. Higher flow gives less time to saturate the CO_2.

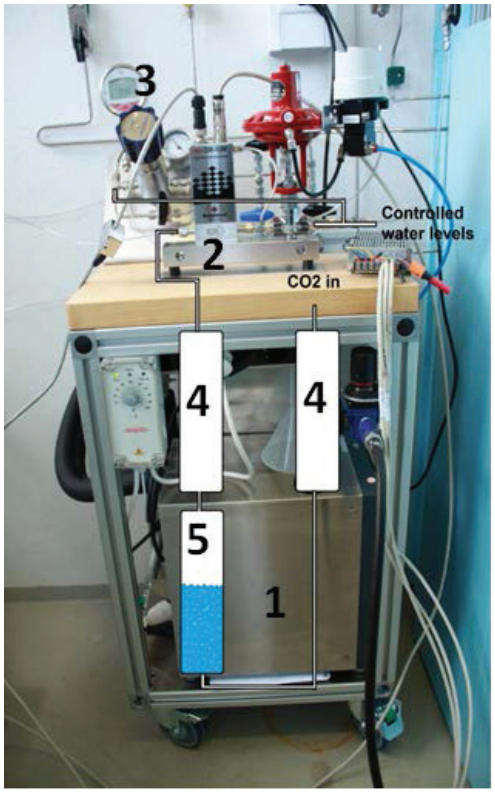

Figure 3. The water dosing unit consists of a thermostatic bath from Huber (1), a mini-coriolis mass flow controller from Bronkhorst (2), a liquid pressure regulator (3), CO_2 expansion tanks (4), and a humidifier tank from Swagelok (5). The dense phase CO_2 enters the first expansion tank before it gets wetted in the humidifier, then the CO_2 enters the second expansion tank so water droplets can fall out. All tanks are temperature controlled. The wetted CO_2 is then dosed in by the mass flow controller and mixed with 95 bars of dry CO_2 from the liquid pressure regulator before it enters the CO_2 loop.

2.3. Analysing module

There are several techniques for measuring water concentration in gases, but the high pressure makes it difficult to measure the water content of the dense phase CO_2 directly. Therefore the pressure was reduced from 95 bar to 2 bar in the venting line, after which the CO_2 entered the analysing module as a gas phase. This module consist of various instruments for measuring impurity concentrations, but only the water analyser (a tunable diode laser) and the oxygen analyser (a zirconia sensor) were used in the present work. The gas flow to the analysers was controlled by a mass flow controller to ensure a stabile gas flow rate.

2.4. Corrosion rate

The corrosion rate was determined from weight loss after the corrosion products sticking to the steel surface were removed in an inhibited HCl solution.

Since one mole of iron consumes one mole of water when the steel corrodes the corrosion rate can also be calculated from the water consumption rate according to equation 1. The sensitivity is about 0.5 mm/y during continuously dosing of CO_2 and water. A higher sensitivity can be achieved by closing both the dosing and venting system for a certain period of time, allowing the water in the closed system to be consumed by corrosion and then measure the decrease in water concentration.

$$CR = \frac{C_{H2O} \cdot V_{CO2} \cdot \rho_{CO2} \cdot MW_{Fe}}{A_{Fe} \cdot \rho_{Fe} \cdot MW_{CO2} \cdot 100} \quad (1)$$

where, CR is the corrosion rate (mm/y), C_{H2O} is the consumed water (ppmv/y), V_{CO2} is the volume of dense phase CO_2 in the loop (L), ρ_{CO2} is the density of CO_2 (g/cm^3), MW_{CO2} is the molar mass of CO_2 (g/mol), A_{Fe} is the area of the carbon steel sample (cm^2), ρ_{Fe} is the density of iron (g/cm^3), MW_{Fe} is the molar mass of iron (g/mol),

2.5. Materials

The corrosion coupons were cut from carbon steel foils. The chemical composition of the steel which is denoted S355J2 (a type of mild steel equivalent to St52-3N) is shown in Table 2. Shavings from the same material were packed in a mesh cylinder and placed in the test section to increase the exposed steel surface area.

Table 2. The chemical composition (wt. %) of the carbon steel grade S355J2.

	C	Mn	Si	P	S	Cu	Fe
S355J2	≤0.2	≤1.6	≤0.55	≤0.030	≤0.030	≤0.55	Balance

The coupons were first washed in acetone and then in isopropanol, wiped with a lint free tissue and ground by hand with a 600 grit abrasive paper.

High purity (5.0) CO_2 from a bottle with riser was used in this work.

3. Results

One blank test (without corrosion coupons) and five corrosion experiments were performed. Test conditions and results are summarised in Table 3.

Table 3. Test conditions and corrosion rate for the experiments performed in the loop at pressure of 95 bar with the flow rate of 0.4 m/s.

Experiment	Temperature, (°C)	Water conc. (ppmv)	Exposure (h)	Sample surface area (cm^2)	Corrosion rate (µm/y)
Exp1 (blank)	25	150 – 2360*	362	N/A	N/A
Exp2	25	570 – 2380*	422	1246	0.8
Exp3	27 → 12**	2300	189	1252	1.4
Exp4	8 ↕ 14**	2300	551	1254	1.0
Exp5	35	2500	334	233	N/A
Exp6	25	100	890	251	0.2

* Ramping of concentration to five different water levels.

** Temperature ramping, constant water levels.

3.1. Ramping water concentration

The blank test (Exp1) was performed in order to fine tune the water dosing system and to see how the system reacted when dry CO_2 was injected (referred to as a dry-up period) in the loop that was full of moist CO_2. As the water concentration in Exp1 never reached the solubility limit, no pool of precipitated water is expected in the loop. Injection of dry CO_2 will therefore decrease the measured water concentration according to a first-order system if there is not too much adsorption and desorption of water on the loop walls [29]. The dry up rate which is shown in Figure 6 (green line) was used for comparison with dry up lines in experiments where the solubility limit of water was exceeded and where the shift in the dry up curve depended on the amounts of precipitated water.

Exp2 (Figure 4) was carried out in the same manner as the blank test, but with carbon steel coupons present. The corrosion rate was so low that it could not be detected from water consumption (equation 1) when water was continuously replenished. Therefore, the system was closed for three different periods of time (grey area in Figure 4, CO_2 routed directly to the analyser) to measure the decrease of the water concentration. These closed periods did not give a significant decrease of the water concentration, indicating again that the corrosion rate is very low. The average corrosion rate measured by weight loss after the exposure was 0.8 µm/y.

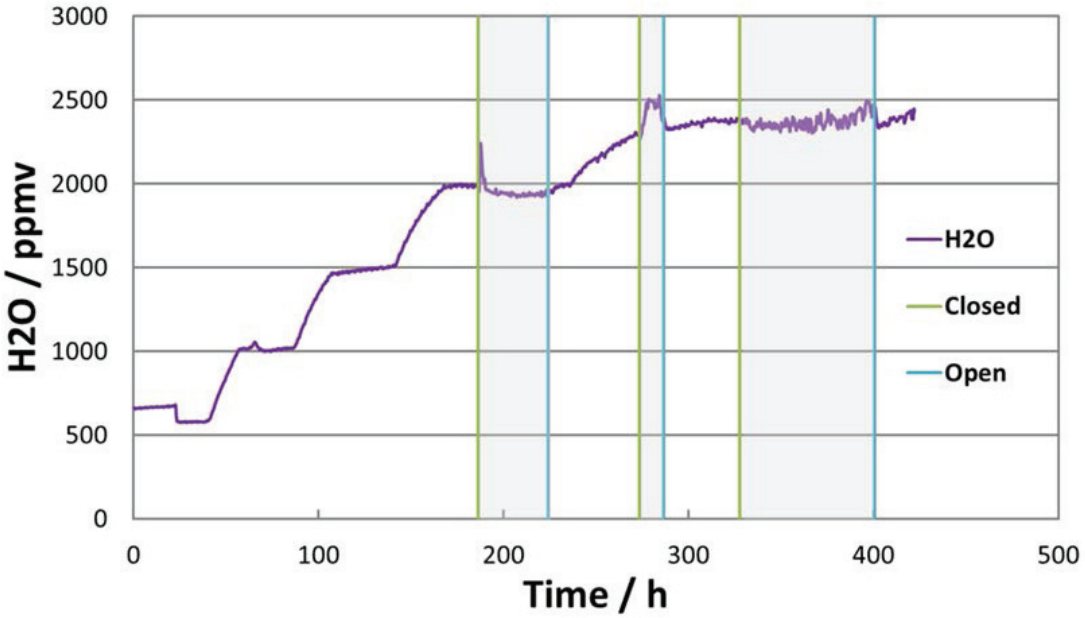

Figure 4. The measured water level of the exhaust gas (purple line) of Exp2 plotted as a function of time. The grey area indicates closed loop with no dosing, the CO_2 would then bypass the loop and go directly to the analyser. Exp2 was performed at 25°C, 95 bar and 0.4 m/s flow velocity.

3.2. Ramping temperature

To prevent liquid water precipitation and entrainment of droplets in the dosing lines, the dosing unit was not used to feed fully water saturated CO_2. To reach and exceed the water solubility limit the loop system was therefore cooled a few degrees (see Figure 1) in Exp3 and Exp 4. In Exp3 (Figure 5) the temperature was decreased stepwise from 27 °C to 12 °C. The injected CO_2 contained 2300 ppmv water, and the solubility limit was reached when the temperature became 15°C. This can be seen as a reduction in the dissolved water concentration at lower temperatures, i.e. water precipitation takes place (see also Exp4, Figure 6).

The saw tooth shape of both the temperature and the water concentration curves is due to the defrosting of the cooler. In an attempt of getting rid of these, the defrosting program of the cooler system was stopped when the temperature reached 16 °C. This worked fine until the cooler was blocked with ice at around 130 hours, leading to an increase in temperature, as shown in Figure 5.

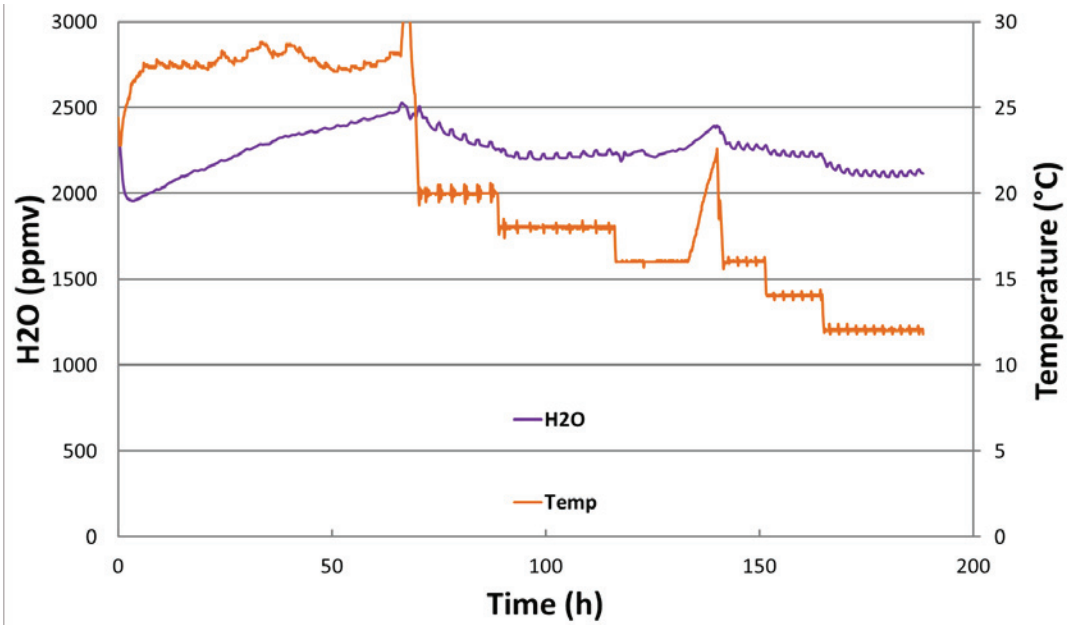

Figure 5 . The Exp3 experiment was performed at the temperature 25°C, 95 bars of pressure, and with a flow of 0.4 m/s. The measured water level of the exhaust gas (purple line) and the temperature (orange line) are plotted as a function of time.

The mutually correlation between the water and temperature curves is clearly observed in Figure 6, Exp4. Since the measured water concentration is lower than the actual dosing rate (about 10 percent), precipitation of water inside the loop system is occuring. This is also supported by the increase of water concentration seen when the temperature was increased to 25 °C. The water concentration should increase to 2300 ppmv which is the dosing rate, but instead it increased to 2800 ppmv. The CO_2 in the loop system is now dissolving the previously precipitated water.

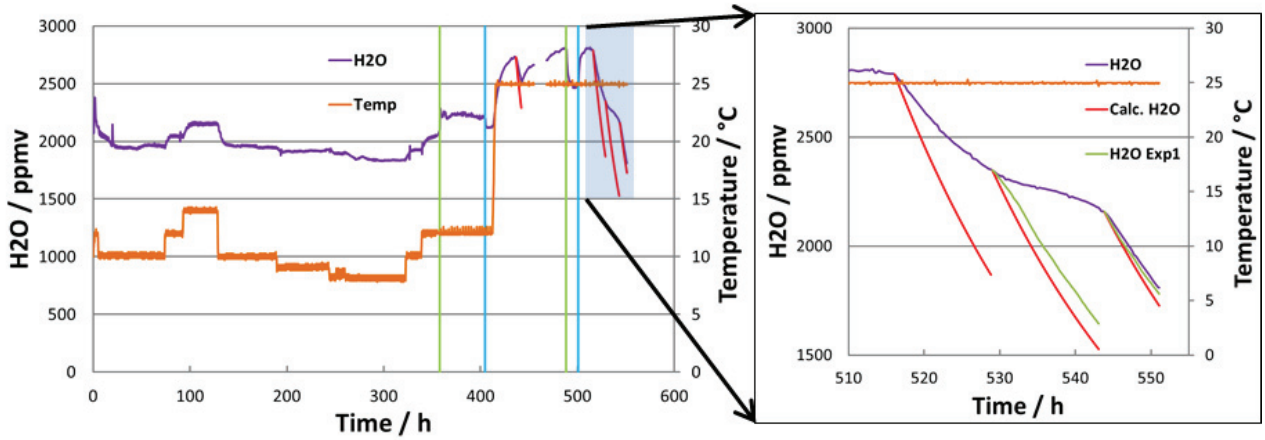

Figure 6. The measured water level of the exhaust gas (purple line) and the temperature (orange line) plotted as a function of time in Exp4. The loop system was closed between the green and the blue line. The right graph shows the dry-up period at an enlarged scale.

When dry CO_2 was injected after 515 hours (see enlarged Figure 6), the measured water concentration did not follow the calculated diluting rate (red line) or the previously measured dry-up period from Exp1 (green line). Instead it forms a plateau, and when all of the precipitated water was dissolved all lines aligned to form the same trend. The corrosion rate in Exp3 was found to be 1.0 µm/y and in Exp4 1.4 µm/y by weight loss (shown in Table 3).

3.3. Steady temperature and water concentration

In Exp5 the carbon steel coupon was exposed to super critical CO_2 with about 2500 ppmv water, as shown in Figure 7 below. This is as the highest water content the wetting system could deliver. There are some periods in the beginning and in the end which has a lower content of water. In the beginning the system needed some time to achieve the right level and in the end of the experiment, the humidifier in the dosing unit ran out of water. Four closed loop periods (between the green and blue lines) was carried out to control and adjust the water level to about 2500 ppmv of water. After the third close period (230 - 255 hours) the water concentration decreased with about 100 ppmv in the loop. If this decrease in water concentration was caused by corrosion alone, it would correspond to a corrosion rate of 59 µm/y (calculated with equation 1).

The weight loss was too low to give a conclusive corrosion rate for Exp5.

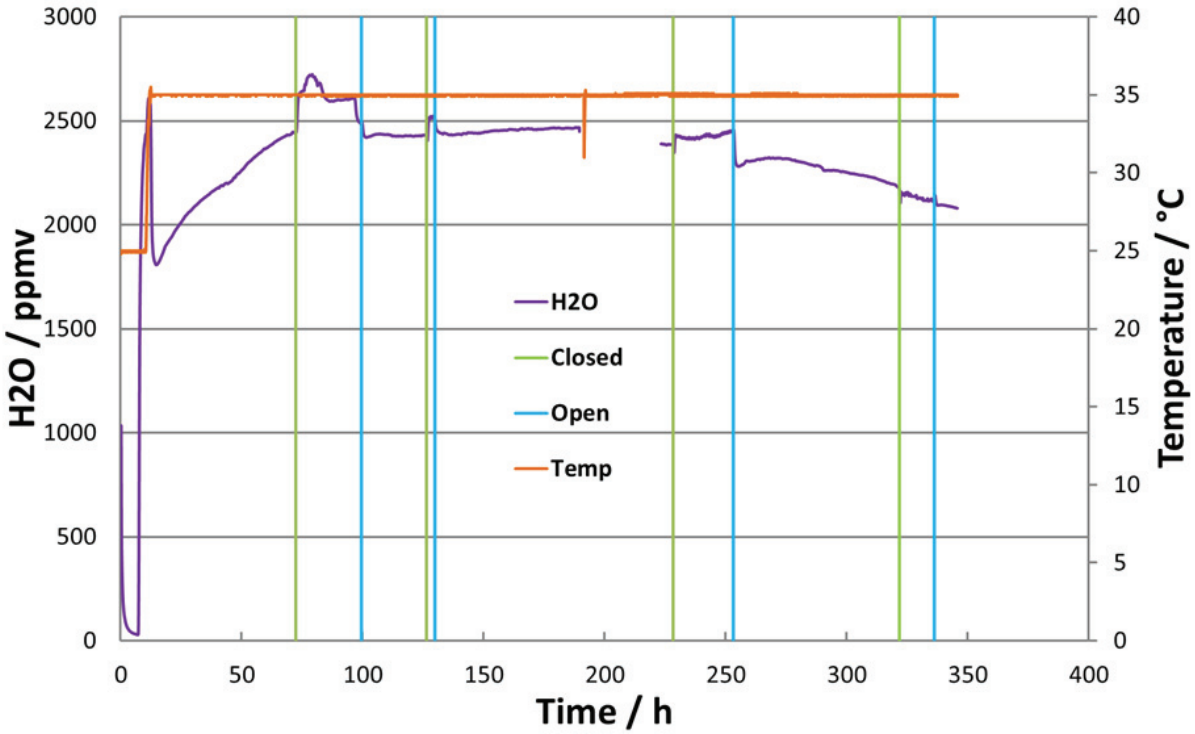

Figure 7. Exp5 was performed at the temperature 35°C, 95 bar pressure, and a flow of 0.4 m/s. The measured water content of the exhaust gas (purple line) and the temperature (orange line) are plotted as a function of time.

Figure 8 shows Exp6, a long term experiment which started with about 130 ppmv and ended with about 100 ppmv of water in the CO_2. Corrosion rate determined by weight loss was found to be 0.2 µm/y.

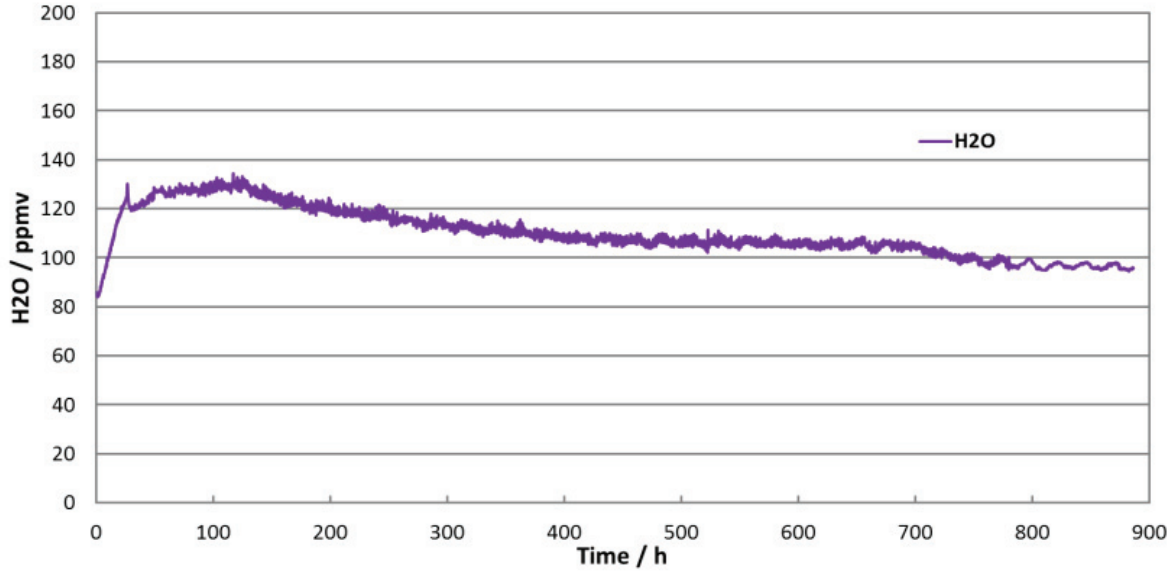

Figure 8. Exp6, water concentration plotted as a function of time. The pressure was 96 bar and temperature at 25 °C.

3.4. Corrosion coupons

A small amount of corrosion products were found on all coupons (see Figure 9). There was more products on the specimens surfaces exposed in Exp3 and Exp4, than Exp2 and Exp5. This is expected since the corrosion rate of Exp3 and Exp4 was somewhat higher. Exp6 had most products on the surface, which cannot be explained from the corrosion rate alone. EDS investigation documented that the surface products contained a lot of sulphur, which was contamination from another experiment that was carried out with H_2S and SO_2.

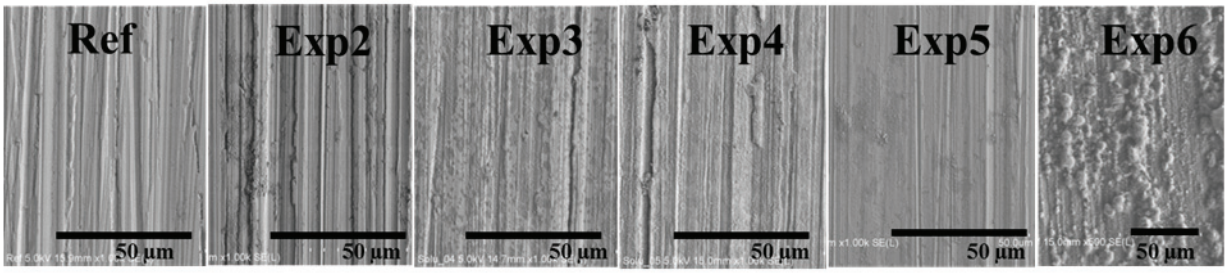

Figure 9. SEM of carbon steel coupons from all the experiments and a reference sample which has not been exposed. All picture expect Exp6, has been magnified 1000 times. Exp6 is magnified 500 times.

The EDS analysis (Figure 11a) of the other coupons indicated iron carbonate on the surface. The thickness of the corrosion products was calculated by film weight to be around 100 nm thick if evenly distributed on the coupons. The similar was found by using a Monte-Carlo simulation (CASION[30]) compared to the EDS analysis (see Figure 10), assuming that all the substrate was iron carbonate [29]. The program can simulate a large amount of electron trajectories in a solid and intend to represent the actual interaction conditions in SEM. Iron carbonate was used as the substrate, and penetration depth at different acceleration voltages was studied. When the iron carbonate atomic ratio; $FeCO_3$, 1:1:3 is moved towards an increasing level of iron in the EDS analysis, we can assume that the accelerating voltage is so high that it goes through the iron carbonate layer and into the carbon steel matrix underneath.

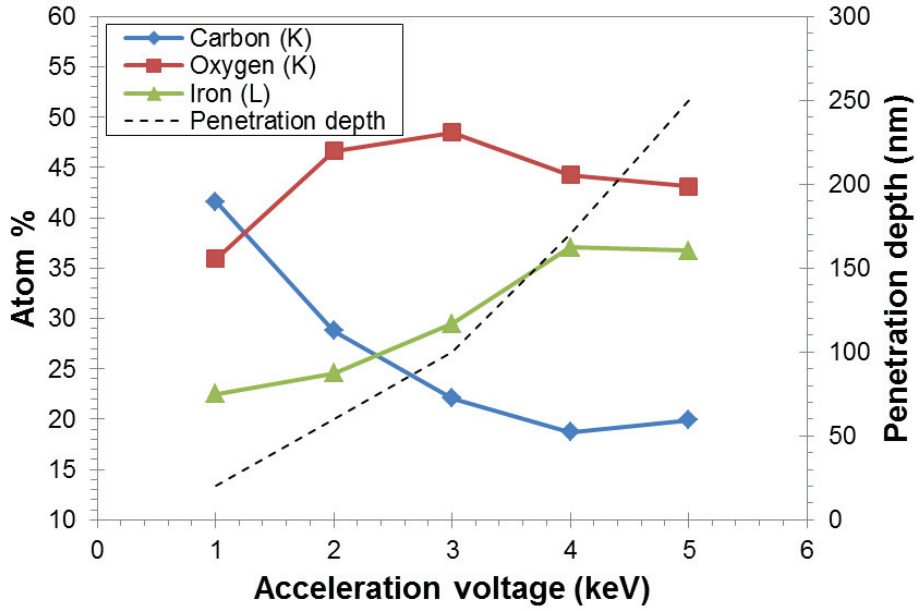

Figure 10. The measured element concentration (atomic per cent) and the simulated penetration depth versus acceleration voltage of the electron beam [29].

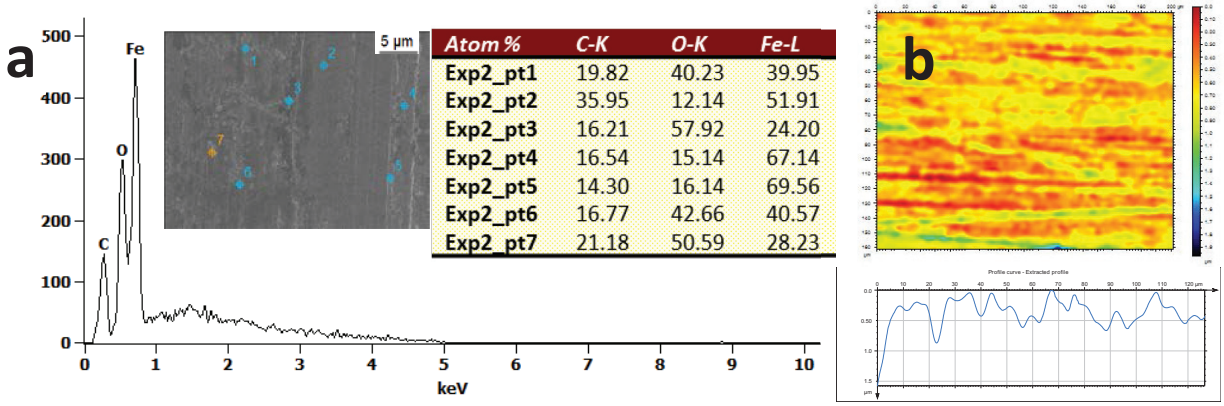

Figure 11. (a) An EDS analysis of Exp2. (b) A profile picture with extracted profile curve taken of Exp5.

The corrosion products were removed with inhibited HCl solution and a visual inspection show no localised attacks on the surface. The profilometer scan (Figure 11b) of the surface also verified this.

4. Summary and discussion

The present work has shown that a free water phase is essential for corrosion in dense phase CO_2. In the absence of free water the corrosion rate was less than 1 µm/y which is not regarded as a threat for the pipeline integrity. But it increased slightly (1.4 µm/y) when small amounts of water precipitated. It should be noted that the measured corrosion rates were (Table 3) close to the practical detection limit and the relative error might be high.

When free water is present, it is likely that the corrosion rate depends on the amount of liquid water that is present. The corrosion rate in Exp4 would therefore be higher if the injection rate of wet CO_2 had been higher (more liquid water would have precipitated in the loop). The presence of a bulk water phase will definitely increase the corrosion rate. It has been claimed that for more than three monolayers of water on the surface the properties

approach those of bulk water [31]. In atmospheric condition this happens around 60 to 80 percent of relative humidity (in air) [32]. Dense phase CO_2 with water is of course very different from air, but if it is assumed that the same principle applies, a few monolayers of water would form between 2000 and 2500 ppmv at 25 ^{0}C and 100 bar. This can explain the presence of the tiny amount of corrosion products that were found on the exposed steel surfaces. The average thickness of the corrosion product layer was about 100 nm. A much thicker iron carbonate film is usually required [33] to give good corrosion protection (passivation) in oil and gas pipelines. Therefore it is possible that the corrosion process was limited by water supply in the present experiments rather than a protective corrosion product film on the surface.

There are thousands of papers that report very high CO_2 driven corrosion rates (0.1 to 50 mm/y) when free water phase is present. Water did clearly precipitate in Exp3 and Exp4, but the resulting corrosion rate was still low (<< 0.1 mm/y), and more importantly it was much lower than what would be expected if all available free water was consumed by corrosion. Consumption of all free water would give an average corrosion rate of about 0.4 mm/y according to equation 1. How the free water phase is distributed in the CO_2 stream in the loop is not documented. It is possible that the precipitated water never reached the carbon steel coupons, but was adsorbed on the wall or was trapped in dead legs and crevices. The amount of precipitated water was calculated to be about five gram in Exp4.

An increasing flow rate can increase the corrosion rate by enhancing the transport of corrosive species toward, or remove protective product from, the surface. The flow rate and flow pattern also affect how water is entrained in oil phases[34] and it is assumed that free water can be entrained in a CO_2 in a similar way. It should be noted that the density difference between water and liquid CO_2 is less than between water and oil. The free water does not need to be lifted up by the flowing CO_2 if the water precipitates directly as droplets in the CO_2 bulk phase. So it could be likely that some, if not all, of the precipitated water is entrained and over saturation (super saturation) is need to get water on the carbon steel surface. No published data was found addressing entrainment of water in dense phase CO_2.

A wide range of corrosion rates in dense phase CO_2 has been reported in the open literature, from no corrosion [4, 8, 15-21] to 3.5 mm/y [22-24], depending on the water content, pressure, and temperature. The large spread in reported corrosion rates for apparently the same experimental conditions indicates the technical difficulties of such corrosion experiments and the importance of having full control of the water distribution in the system. The experimental setup used in the present work is the first of its kind allowing water injection to be droplet free since the water saturation is taking place outside the loop. In previous published work with dense phase CO_2 the water was typically injected as a liquid. When corrosion rates of 0.01 mm/y and higher were reported, the exposed samples had often droplet shaped attacks on the surface. This could indicate that the sample either had been hit by water droplets or that water had condensed on the surface during the experiment [29]. In the latter case, the situation changes and CO_2 corrosion in water (free water phase) will occur. It is well known in the literature that this type of corrosion will have high corrosion rates, even up to 40 mm/y until the water becomes saturated with corrosion products [4].

The corrosion process will continue until the water is consumed, leaving droplet-shaped corrosion product clusters with localised attacks underneath [29]. In such cases the transport of water to the surface is limiting the corrosion rate. As shown in Figure 9, the coupons exposed in Exp3 and Exp4 had most corrosion product on their surfaces. They also were exposed to higher degree of saturation, even though both Exp2 and Exp5 were exposed to a higher concentration level of ppmv (2300 and 2500 versus about 2000 ppmv). The duration of Exp3 was shorter than both Exp2 and Exp5, but still more visible corrosion products. It seems like the degree of saturation is the key factor here, which control the deposition on and the hydration of the surface. Further supporting this hypothesis is the observation made in Exp5, where the temperature was the highest, but the corrosion rate was below detection limit and low amounts of products were present on the surface. Normally in free water/CO_2 system, the corrosion rate increases with temperature [35]. The degree of saturation in Exp5 is among the lowest only Exp6 was lower, and this is probably the reason for the low corrosion rate. Unfortunately, no good conclusion can be drawn from Exp6, except for the low overall corrosion rate (0.2 µm/y), since it was contaminated with impurities from other experiments. It can of course be argued if the difference in corrosion rate is significant between the experiments, but the amount of products is clear. It should be noted that the average corrosion rate is discussed here, thus, some periods of the experiments can have higher or lower rates.

In a CO_2 transport situation, where cooling or heating of the CO_2 in the pipeline comes from the outside, the water would precipitate on the carbon steel walls if saturation limits are exceeded. So as long as the water

concentration in the CO_2 is lower than the solubility limit of the coldest spot in the pipeline, it would be safe from a corrosion point of view.

These observations would only be valid for CO_2/H_2O systems, if other impurities are introduced the conditions could change.

5. Conclusion

The corrosion rate of carbon steel in dense phase CO_2 was < 1 µm/y as long as the water is dissolved. By increasing the water content slightly above the solubility limit, the average corrosion rate increased to 1-1.4 µm/y. No localised corrosion was observed on the carbon steel coupons. For all cases a thin non homogeneous layer of $FeCO_3$ corrosion products was identified by SEM/EDS.

It seems like the degree of water saturation in CO_2, or formation rate of free water phase is the determining factor for corrosion and formation of protective corrosion products on the surface, and not the dissolved water concentration.

The results obtained in the present study indicate that corrosion will not threaten the integrity of CO_2 transport pipelines as long as the water is kept below the solubility limit. However, water control and water analysis will be an important part of a CCS pipeline integrity system and operating procedures.

References

[1] IPCC, Summary for Policymakers. In: Climate Change 2013: The Physical Science Basis. Contribution of Working Group I to the Fifth Assessment Report of the Intergovermmental Panel on Climate Change [Stocker,T.F., D. Qin, G.-K. Plattner, M. Tignor, S.K. Allen, J. Boschung, A. Nauels, Y. Xia, V. Bex and P.M. Midgley (eds.)]. , in, IPCC, Cambridge University Press, Cambridge, United Kingdom and New York, NY, USA., 2013.
[2] CCP, CO2 capture project, CO2 transport, in, Web page, 2013.
[3] E.D. Visser, C. Hendriks, M. Barrio, M.J. Mølnvik, G.d. Koeijer, S. Liljemark, Y.L. Gallo, Dynamis CO2 quality recommendations, International Journal of Greenhouse Gas Control 2(2008) 478.
[4] A. Dugstad, B. Morland, S. Clausen, Corrosion of transport pipelines for CO2 - Effect of water ingress, Energy Procedia, 4 (2011) 3063-3070.
[5] Y.-S. Choi, S. Nesic, Effect of impurities on the corrosion behavior of carbon steel in supercritical CO2 - water environments, in: CORROSION/2010, NACE International, 2010.
[6] Y. Choi, S. Nesic, Corrosion behaviour of carbon steel in supercritical CO2 – water environments, in: CORROSION/2009, NACE International, 2009.
[7] Y.-S. Choi, S. Nešić, Determining the corrosive potential of CO2 transport pipeline in high pCO2–water environments, International Journal of Greenhouse Gas Control, 5 (2011) 788-797.
[8] A. Dugstad, S. Clausen, B. Morland, Transport of dense phase CO2 In C-steel pipelines - When is corrosion an issue?, in: CORROSION/2011, NACE International, 2011.
[9] M. Seiersten, Materials Selection for Separation, Transportation and Disposal of CO2, in: CORROSION/2001, NACE International, 2001.
[10] M. Seiersten, Corrosion in CO2 pipelines, in, 2003.
[11] Y. Zhang, K. Gao, G. Schmitt, Inhibition of Steel Corrosion Under Aqueous Supercritical CO2 Conditions, in: CORROSION/2011, NACE International, 2011.
[12] Y. Zhang, X. Pang, S. Qu, X. Li, K. Gao, The relationship between fracture toughness of CO2 corrosion scale and corrosion rate of X65 pipeline steel under supercritical CO2 condition, International Journal of Greenhouse Gas Control, 5 (2011) 1643-1650.
[13] Y. Zhang, X. Pang, S. Qu, X. Li, K. Gao, Discussion of the CO2 corrosion mechanism between low partial pressure and supercritical condition, Corrosion Science, 59 (2012) 186-197.
[14] NETL, CO2 impurity design parameters, in, 2013.
[15] T.E. Gill, Canyon Reef Carriers, Inc. CO2 Pipeline: Description and 12 years of operation, in: ASME Energy-Source Technol. Conf, Pipeline Eng. Symp., 1985, pp. 59.
[16] B.P. McGrail, H.T. Schaef, V.A. Glezakou, L.X. Dang, A.T. Owen, Water reactivity in the liquid and supercritical CO2 phase: Has half the story been neglected?, Energy Procedia, 1 (2009) 3415-3419.

[17] L.E. Newton, SACROC CO2 Project – Corrosion problems and solutions, in: CORROSION/84, NACE International, 1984.
[18] W.A. Propp, T.E. Carleson, C.M. Wai, P.R. Taylor, K.W. Daehling, S. Huang, M. Abdel-Latif, Corrosion in supercritical fluids, in, US Department of Energy, Washington, DC, 1996.
[19] F. Schremp, G. Roberson, Effect of Supercritical co 2 on Materials of Construction, in: Meeting of Society of Petroleum Engineers of AIME in Las Vegas, Nevada, 1973.
[20] F.W. Schremp, G.R. Roberson, Effect of supercritical carbon dioxide on construction materials, Society of Petroleum Engineers Journal, 15 (1975) 227-233.
[21] J.M. West, Design and operation of a supercritical CO2 pipeline-compression system sacroc unit, Scurry County, Texas, in: SPE Permian Basin Oil Recovery Conference, Society of Petroleum Engineers, Midland, TX, 1974.
[22] F. Ayello, K. Evans, R. Thodla, N. Sridhar, Effect of impurities on corrosion of steel in supercritical CO2, in: CORROSION/2010, NACE International, Houston, TX, 2010.
[23] Y.-S. Choi, S. Nesic, D. Young, Effect of Impurities on the Corrosion Behavior of CO2 Transmission Pipeline Steel in Supercritical CO2−Water Environments, Environmental Science & Technology, 44 (2010) 9233-9238.
[24] R. Thodla, A. Francois, N. Sridhar, Materials Performance In Supercritical CO2 Environments, in: CORROSION/2009, NACE International, 2009.
[25] Y. Hua, R. Barker, A. Neville, Effect of temperature on the critical water content for general and localised corrosion of X65 carbon steel in the transport of supercritical CO2, International Journal of Greenhouse Gas Control, 31 (2014) 48-60.
[26] S. Sim, I.S. Cole, F. Bocher, P. Corrigan, R.P. Gamage, N. Ukwattage, N. Birbilis, Investigating the effect of salt and acid impurities in supercritical CO2 as relevant to the corrosion of carbon capture and storage pipelines, International Journal of Greenhouse Gas Control, 17 (2013) 534-541.
[27] S. Sim, F. Bocher, I.S. Cole, X.B. Chen, N. Birbilis, Investigating the Effect of Water Content in Supercritical CO2 as Relevant to the Corrosion of Carbon Capture and Storage Pipelines, Corrosion, 70 (2014) 185-195.
[28] H. El Alami, C. Augustin, B. Orlans, J.-J. Servier, Carbon capture and storage projects: material integrity for CO2 injection and storage, in: Eurocorr 2011, Stockholm, Sweeden, 2011.
[29] B.H. Morland, Corrosion in CO2 transport pipeline: The effect of dissolved and free water in dense phase CO2, in: Chemistry, University of Oslo, DUO, 2015, pp. 145.
[30] P. Hovington, D. Drouin, R. Gauvin, CASINO: A new monte carlo code in C language for electron beam interaction —part I: Description of the program, Scanning, 19 (1997) 1-14.
[31] Y. Ben-Da, S. Meilink, G.W. Warren, P. Wynblatt, Water adsorption and surface conductivity measurements on alumina substrates, Components, Hybrids, and Manufacturing Technology, IEEE Transactions on, 10 (1987) 247-251.
[32] C. Leygraf, P. Marcus, J. Oudar (Eds.), Corrosion Mechanisms in Theory and Practice, New York, 1995.
[33] S. Nesic, Key issues related to modelling of internal corrosion of oil and gas pipelines – A review, Corrosion Science, 49 (2007) 4308-4338.
[34] M. Wicks, J.P. Fraser, Entrainment of Water by Flowing Oil, Materials Performance, 14 (1975) 9-12.
[35] B.H. Morland, A. Dugstad, Corrosion of carbon steel in water equilibrated with liquid and supercritical CO2, in: CORROSION/2016, NACE International, Vancouver, BC, 2016.

Chapter 8

Acid reactions in hub systems consisting of separate non-reactive CO_2 transport lines

Bjørn H. Morland, Morten Tjelta, Truls Nordby and Gaute Svenningsen

Published in *Journal of Greenhouse Gas Control* **vol. 87** (2019), pp. 246-255.
https://doi.org/10.1016/j.ijggc.2019.05.017

International Journal of Greenhouse Gas Control 87 (2019) 246–255

Contents lists available at ScienceDirect

International Journal of Greenhouse Gas Control

journal homepage: www.elsevier.com/locate/ijggc

Acid reactions in hub systems consisting of separate non-reactive CO_2 transport lines

Bjørn H. Morland[a,b,*], Morten Tjelta[a], Truls Norby[b], Gaute Svenningsen[a]

[a] Institute for Energy Technology, PO box 40, NO-2027, Kjeller, Norway
[b] University of Oslo, Department of Chemistry, FERMiO, Gaustadalléen 21, NO-0349, Oslo, Norway

ARTICLE INFO

Keywords:
CCUS
CO_2
Transport
CO_2 hub
Impurities
Specification test
H_2SO_4
HNO_3

ABSTRACT

Corrosion in carbon steel pipelines is a major threat for safe CO_2 transport, and there have been several projects studying the corrosivity of impurities which could be found in captured CO_2. Often only two or three of these impurities have been present while performing the experiments. Although these experiments have delivered valuable knowledge, there are still questions of what happens when impurities are present together. Furthermore, several transport pipelines may deliver CO_2 to a main pipeline through a hub system for storage or utilization, and while these streams may be safe individually, the blend in the main pipeline could create components that are hazardous for carbon steel.

The present study used a novel experimental setup to realistically simulate a CO_2 hub. Three individual "pipelines" were joined inside a glass tube in a transparent autoclave. The three "pipelines" were connected to three different reservoir pumps, simulating different capturing sources with dissimilar types of impurities. This gave a mix of low (ppmv) levels of oxygen (O_2), sulphur dioxide (SO_2), hydrogen sulphide (H_2S), nitrogen dioxide (NO_2), and water (H_2O). Three different experiments were performed with concentrations ranging from 5 to 35 ppmv of the impurities and a total pressure of 100 bar at 25 °C. All impurities were measured before and after the streams were mixed in the autoclave.

The experiments revealed that reactions between certain species occured even at concentrations as low as 5 ppmv, but the reaction products were not considered detrimental in terms of corrosion. If the impurity concentrations were increased to about 35 ppmv, acids and solids were produced, and the situation became unacceptable for carbon steel.

1. Introduction

Carbon capture and storage is needed to meet the goal set by the International Energy Agency (IEA) (Energy Technology Perspectives, 2010) and the Intergovernmental Panel on Climate Change (IPCC) (IPCC, 2019). This will involve CO_2 capture, transportation, and permanent storage, and it is essential that the cost of the overall processes is kept as low as practically possible. Carbon steel is the only material that is economically feasible for long transport pipelines. However, the captured CO_2 may contain small amounts of additional components (called impurities in the present paper), which may be corrosive to carbon steel or cause operational problems. A quality specification for the CO_2 to be transported is therefore crucial to ensure the integrity of the pipeline. Several CO_2 specifications have been suggested, but most of them have not been tested in realistic experiments. Consequently, the validity of these specifications is unclear. Some impurities (i.e. NO_2 and SO_2) have concentration limits based on health, safety, and environmental reasons, while possible chemical and corrosion reactions have not been considered. Reaction between many of these impurities is likely to occur (Dugstad et al., 2014), but the practical consequences have not been investigated in detail. Table 1 shows the large range of impurity limits that have been suggested in various literature sources (IEAGHG, 2019; NETL, 2013; Mohitpour et al., 2012).

Previous work from our research group (Dugstad et al., 2014; Dugstad and Morland, 2016; Halseid et al., 2014) has shown that strong acids and elemental sulphur may form in CO_2 blends that are within established quality specifications (NETL, 2013; de Visser et al., 2008). The COORAL-project did also find traces of sulfuric acid and elemental sulphur in both gas and supercritical CO_2 experiments (Ruhl and Kranzmann, 2013; Yevtushenko et al., 2013; Yevtushenko et al., 2014). If these impurities react in the capture process they can most likely be removed before they enter the transportation system. However, it has

* Corresponding author at: Institute for Energy Technology, PO box 40, NO-2027, Kjeller, Norway.
E-mail address: bjornhm@ife.no (B.H. Morland).

https://doi.org/10.1016/j.ijggc.2019.05.017
Received 29 August 2018; Received in revised form 4 April 2019; Accepted 14 May 2019
1750-5836/

Table 1
Expected impurities and concentration ranges from a review of 55 specifications (NETL, 2013), CO_2 is the balance.

Compound	Concentration (ppmv)
H_2O	20 – 650
O_2	10 – 40000
SOx	10 – 50,000*
H_2S	20 – 13,000*
NOx	20 – 2500*

* Often given as 100 ppmv for HSE concern.

been suggested that future transport projects will consist of multiple capturing sites which deliver CO_2 to a hub system with a main transport line, either as pipeline or by ships. One example of this is the full-scale CCS demonstration projects in Norway (OED, 2016), where the captured CO_2 will come from three different capturing sites: a concrete factory, an ammonia plant, and a waste fuelled energy recovery plant. It is likely that these three CO_2 sources will have different impurity contents that may be unreactive within each individual stream, but reactions could occur at a later stage when the streams are mixed in the transportation network.

The aim of this study was to identify chemical reactions that are likely to occur in a realistic mix of impurities in CO_2 and/or verify if there is a safe operation window for transporting impure CO_2 in pipelines without creating a corrosive environment for the pipeline material. The impurities in Table 1 were split up in three different transport streams so the impurities could not react before the reaction chamber. In so, they represent three induvial safe CO_2 stream without chemical reaction and corrosion. Mixing in a hub system was simulated by injecting these streams in an autoclave (reaction chamber). The present work applied a novel transparent autoclave that was built in-house. Reactions between impurities were studied visually and with high performance gas analysers.

2. Materials and methods

The experimental setup consisted of three parts; the reaction chamber (transparent autoclave) with camera, an impurity injection system, and the analysing module.

2.1. The reaction chamber

A transparent autoclave (Fig. 1) was used as reaction chamber to allow in-situ visual observation of the experiment. The autoclave body was made of 316 stainless steel, and it had a volume of 330 ml with a maximum working pressure of 200 bar. The transparent windows consisted of soda lime glass (exposed to the CO_2 phase) and polycarbonate plates (exposed to air) which acted as pressure support for the lime glass. A magnetic stirrer was placed in the bottom of the autoclave to promote mixing of the CO_2 streams.

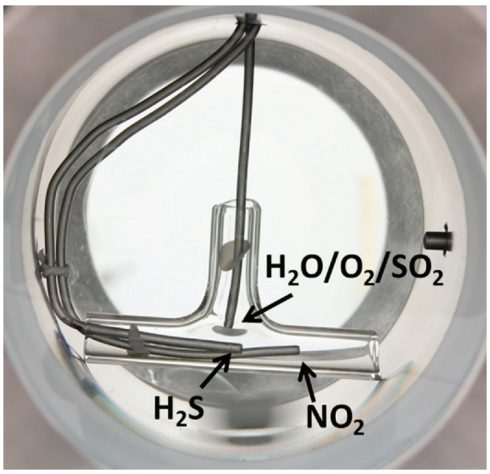

Fig. 2. Glass tee tube (simulated CO_2 hub) with three individual injection lines. The glass tee was located inside the autoclave.

A T-shaped glass tube was placed inside the autoclave to simulate a CO_2 hub where three different streams were mixed. The first injection line delivered CO_2 with small levels (see Tables 3–5) of O_2, SO_2, and H_2O. The second stream contained CO_2 with H_2S and the third stream contained CO_2 with NO_2. Fig. 2 shows the hub with the inlet tubes marked.

A camera was used to take still-images inside the autoclave, and a LED-lamp was used to achieve constant light conditions. Typically, one still image was taken every 10 min. The images were used to create videos showing the experimental development.

The temperature (25 °C) and the pressure (100 bara) were kept stable during all experiments.

2.2. Impurity injection system

The impurities were injected as pre-mixed solutions of CO_2 and the respective impurities. Three high precision piston pumps (266 ml volume) from Teledyne was used for this purpose. All pumps were held at a pressure slightly more than 100 bar. In addition, pure CO_2 (sometimes with H_2O) from a booster pump was also injected to the autoclave. The latter stream was controlled by a liquid pressure regulator that ensured a constant pressure of 100 bar. All four streams were injected at the same rates (about 25% each), but if one of the piston pumps was stopped, the pure CO_2 flow would increase correspondingly to maintain the pressure and the same total flow. The piston pumps needed to be filled with four times higher concentration since each pump represent one fourth of the flow. Thus, the concentration at the tip of the injection tubes and inside the glass tee was higher since the stream had not yet

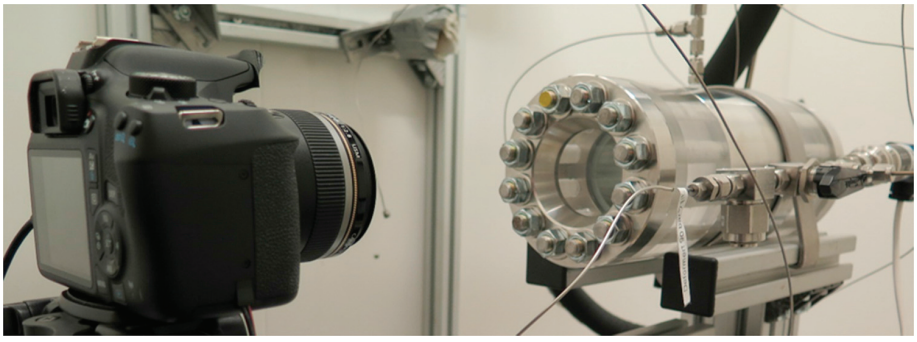

Fig. 1. Transparent autoclave with camera and injection tubing.

been mixed (diluted) with the other streams. With the applied settings the piston pumps lasted about 24 h before they had to be refilled.

The exhaust CO_2 was taken to a heated vaporizing regulator (to prevent hydrate formation and precipitation of impurities) where the pressure was reduced from 100 to 1 bar before the gas was sent to the analysing module. A mass flow controller from Bronkhorst was placed at the low-pressure side to regulate the exhaust flow rate. Normally this flow was about 0.85 g/min during the experiment.

The water content in the "pure" CO_2 stream could be adjusted at any concentration from nominally bottle dry to saturation by mixing dry CO_2 and CO_2 saturated with water at 25 °C at a desired ratio using a mini Cori-flow controller from Bronkhorst. Therefore, no liquid water was injected into the reaction chamber in these experiments, only water fully dissolved in CO_2.

2.3. Analysing module

The analysing module consisted of two multicomponent laser-based analysing systems (Emerson CT5400 and ap2e ProCeas) and one oxide-based analyser (Michell XZR400) that were set in series to analyse the same gas. The system was configured in such a manner that either the exhaust CO_2 from the autoclave, or one of the individual CO_2 streams could be sent directly to the analyser module. Thus, the consumption of impurities could be detected as a measured difference in inlet and outlet concentrations. The CT5400 is a Quantum Cascade Laser (QCL) that could continuously analyse SO_2, NO, NO_2, N_2O, CO, and COS. The ProCeas is an Optical Feedback Cavity Enhanced Absorption Spectroscopy (OFCEAS) that uses infrared laser to continuously measure H_2O, H_2S, and O_2. None of the analysers could handle a pressure of 100 bar so the pressure was reduced to about 1 bar prior to the analysis. The O_2 content was analysed with a XZR400 from Michell in the first two experiments (Hub01 and Hub02), while the laser based ProCeas was used for the last experiment (Hub3). The XZR400 has a zirconium oxide sensor with metallic sealed reference. The sensor could not be exposed to corrosive or flammable gases, so the sampling gas had to be scrubbed through a scavenger which removed SO_2, NO_2, and H_2S. The instrument was therefore located as the last analyser in the gas analysis line. It was sometimes observed that right after a new impurity injection was started, the O_2 signal was too low during a transient period, before it came back to the expected level. The exact reason for this not understood, but it could be related to remnants of impurities in the analysis system.

The accuracy of the analysers was about 1 percent of the full scale, which amount to about ± 1 ppmv for SO_2, NO_2, H_2S. While H_2O and O_2 had an accuracy of ± 3 ppmv. Since the measurements was performed at ambient pressure, ppm volume equals ppm mole at 25 °C and 1 bara. The analysers report concentrations in ppmv, therefore ppmv was used in this paper. When analysing the impurities from a 100 bar experiment it is important to remember that the reported ppmv are equal to ppm mole and the volume in ppmv is not related to the volume of the liquid CO_2 or the autoclave.

The heated vaporizing regulator could in theory trigger some additional reactions or precipitation since phase transition occurred at somewhat elevated temperature (45 °C). The solubility limits for acid and solids would also change in this environment due to the pressure transient through the regulator. This might give some deviation between the measured concentration at 1 bar and the real concentration at 100 bar.

Replacing the autoclave volume of liquid once took about 6.5 h with the applied settings, and about 18 h was needed to reach a stable impurity level (3 times volume replacement would give about 95% of the correct value). The sampling line from the autoclave to the analysers was made of 1/16″ tubing, which gave a lag time of about 8 min.

2.4. Chemicals

Gas qualities used to make pre-mixed solutions of CO_2 are listed in Table 2.

Table 2
Gas qualities of impurities used in the experiments.

Gas type	Purity (%)
CO_2	99.999
NO_2	99.0
SO_2	99.9
H_2S	99.8
O_2	99.999

2.5. Start-up procedure

After the glass tee tube was mounted and the autoclave was closed, the system was first purged with low pressure CO_2 (3 bar for one hour) and then high-pressure CO_2 (100 bar), to remove air and moisture from the autoclave. Previous experience has shown that moisture absorbs on the internal surfaces during installation. After the low-pressure purging process, the water concentration was typically around 50 ppmv. To reduce the concentration to an acceptable level of 10 ppmv, about five days with dry CO_2 at a flow rate of 0.85 g/min was required.

The impurity concentration of the stock solutions in the piston pumps was determined by running them one by one directly to the heated vaporizing regulator and then to analysing module. The injection rate of the piston pumps was fine-tuned to reach the target impurity level.

The sequence for impurity injection varied slightly from experiment to experiment. In the first experiment injection of all impurities was started at the same time, but in the other two experiments the injection

Table 3
Concentration of injected impurities in Hub01.

Compound	Concentration in stock solutions (ppmv)	Theoretical concentration in autoclave (ppmv)
H_2O	500[#]	~100
SO_2	40	5
O_2	110	12
NO_2	23	5
H_2S	22	5.5

[#] H_2S was contaminated with H_2O, giving a total content of about 500 ppmv.

Table 4
Concentration of injected impurities in Hub02.

Compound	Concentration in stock solutions (ppmv)	Theoretical concentration in autoclave (ppmv)
H_2O	initially 220-270	35
SO_2	40	12
O_2	110	31
NO_2	60	10
H_2S	88	10

Table 5
Concentration of injected impurities in Hub03.

Compound	Concentration in stock solutions (ppmv)	Theoretical concentration in autoclave (ppmv)
H_2O	120	120
SO_2	370	38
O_2	890	95
NO_2	200	26
H_2S	300	41

was started consecutively one by one. For the latter case the order was somewhat different from experiment to experiment, but it was typically started by first injecting SO_2 and O_2 (first stream). Once the concentrations in the autoclave had stabilized, indicated by stable measurements of the exhaust gas, injection of the next impurity stream was started (often this was NO_2). After the values had stabilized, injection of the last impurity stream with H_2S was started. The order of impurity injection varied in order to detect any reactions that might occur with only two or three streams.

3. Results

Three experiments were conducted with three different concentration levels (5, 10 and 35 ppmv) of the key impurities. The concentration levels were given as what the concentration would be when mixed in the autoclave if no reactions occurred. The concentrations in the stock solutions were higher. These data are listed in the tables (Tables 3–5).

3.1. Hub01 (5 ppmv)

This experiment was carried out with stock solutions in the 22–110 ppmv range. The target concentration inside the hub was 5 ppmv for SO_2, NO_2, and H_2S (see Table 3). The H_2S stock solution was unfortunately contaminated with water, resulting in much higher water levels than what was initially intended.

The experiment was divided in two injection periods, the first was at 0–46 h (Fig. 3) and the second was at 116–164 h (Fig. 4). At 0 h all impurities (all four streams) were injected at the same time (Fig. 3). If no reactions occurred, then the concentrations should stabilize at the values given in Table 3 after some time (about 18 h). This was not the case, based on the analysis results, suggesting that one or more reactions were occurring.

The water content, mainly originating from the H_2S stock solution, increased as expected, but the rest of the impurities did not reach their target levels. H_2S was not detected at all. NO_2 was almost zero (about 0.2 ppmv) until the H_2S injection was stopped at 26 h, after which NO_2 increased up to the target value. SO_2 was measured at higher concentrations than the target level and O_2 was much lower than the target level. SO_2 and O_2 impurities were injected from the same piston pump in a ratio of 1:3. NO was detected even if it was not injected. At 26 h the H_2S injection was stopped and the system changed considerably, with a trend of all other impurities slowly changing towards the target (i.e. inlet) levels. The H_2S injection was started again at 41 h, resulting in mostly the same situation as when H_2S was injected for the first time. One difference, however, was that the oxygen content was lower and continued to decrease towards zero. At 46 h, injection of all impurities was stopped, and only pure CO_2 was injected.

The second injection period started at 116 h (Fig. 4). This time the impurity injections were not started at the same time. Injection of SO_2/O_2 was started first and when they stabilized, the H_2S injection was started (136 h). To reduce the stabilization time for H_2S, it was injected at a higher rate for the first three hours, and then reduced to the correct set-point. At 143 h the NO_2 injection was started, and the system changed character: SO_2 and NO increased while H_2S and O_2 decreased. NO_2 was not detected and at 154 h O_2 and H_2S reached the lower detection limit. At 163 h, injection of all impurities was stopped.

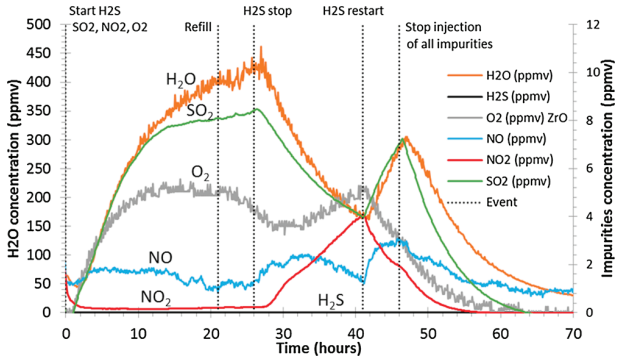

Fig. 3. Exhaust gas analysis of Hub01, first injection period (0–46 h).

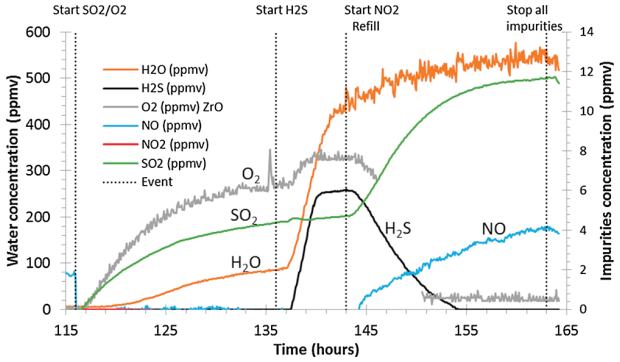

Fig. 4. Exhaust gas analysis of Hub01, second injection period (115–165 h).

Still-pictures were taken repeatedly during the experiment (Fig. 5). Some colour changes inside the chamber were observed, but no separate liquid phases or solids could be identified.

3.2. Hub02 (10 ppmv)

The target values for this experiment were 10 ppmv for SO_2, NO_2, and H_2S. Table 4 shows the concentration injected (stock solutions) and the expected (theoretical) concentration after mixing, presuming that no reactions took place. The water content was initially high (about 250 ppmv) in this experiment, due to remnants of water in the impurity injection lines from a previous experiment.

The experiment was started with injection of SO_2/O_2 (0 h), and O_2 and SO_2 increased in the following period, see Fig. 6. At 12 h the injection rate of SO_2 /O_2 was temporarily increased (to reach the target faster), which caused an increase in the SO_2 /O_2 content. At the same time (12 h) injection of H_2S was also started, and H_2S was detected shortly after. Injection of NO_2 was started at 19 h, and this caused an increase of the SO_2 content to a stable plateau of about 20 ppmv while the H_2S content decreased to zero. The O_2 content increased intermittently before it decreased rapidly and after some time stabilised around 8 ppmv. This is not an expected behaviour and the reason for it is not quite understood. It could be caused by reactions in the wet scavenger compartment. In a test experiment (not shown) we confirmed that reactions involving oxygen can take place here. The oxygen in this and the previous experiment was measured with a zirconia sensor. This type of sensor is sensitive to flammable and corrosive gases, therefore the gas needed to be scrubbed before analysis. NO was detected after the NO_2 injection was started, and it increased slowly until the abrupt drop of O_2, after which it slowly decreased toward zero. NO_2 was detected after the abrupt O_2 drop, and it increased slowly with time.

At 84 h the NO_2 injection was stopped and at 108 h the experiment stopped due to a failure of the analyser. Before this occurred, the concentration of the remaining injected impurities moved towards their target injection values.

Still pictures (Fig. 7) taken during the experiment show colour change inside the chamber and in the lower right end of the glass tube there is some colour change at 62 h (Fig. 8).

3.3. Hub03 (35 ppmv)

For the last experiment the target concentration for SO_2, NO_2, and H_2S was increased to about 35 ppmv. There was some water

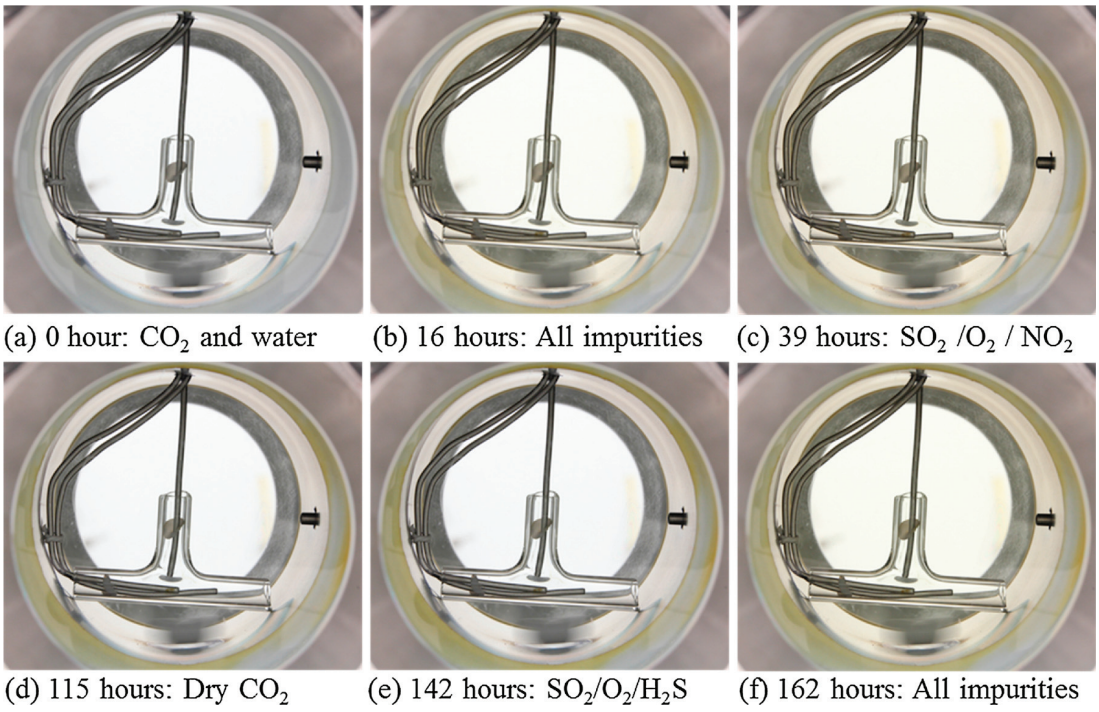

Fig. 5. Still pictures taken during the first and second injection periods in Hub01.

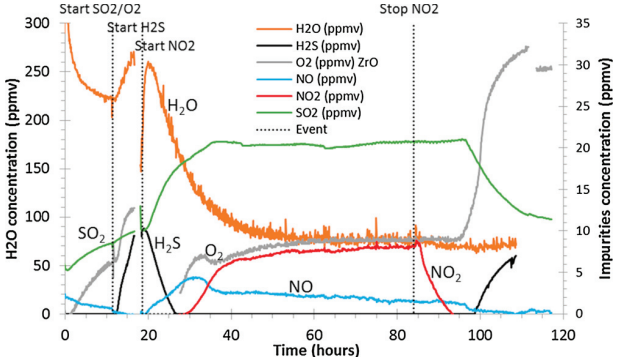

Fig. 6. Analysis of exhaust gas from Hub02.

contamination in the injection system, resulting in a water content of about 120 ppmv. Table 5 sums up the stock and expected solution concentrations.

SO_2 and O_2 was injected first, see Fig. 9, and after about 20 h the injection of NO_2 was started. This led to a decrease in the O_2 concentration. To verify that this decrease was real, the SO_2/O_2 stock solution was routed directly to the analyser (shown as discontinuous lines in Fig. 9 between 41–45 h), and it proved that the oxygen consumption was real. H_2S was introduced to the system at 51 h, and an immediate change in impurity concentrations was observed. The water concentration increased together with SO_2. At the same time, O_2 decreased rapidly while, NO_2 decreased slowly. H_2S was not detected until 10 h after the NO_2 injection was stopped at 101 h. The system then slowly reverted back to the original target values. When H_2S was stopped at 134 h the system was not affected, except for the decrease in water because contaminant water was injected together with H_2S. Finally, injection of O_2/SO_2 was stopped after 145 h.

Still-pictures (Fig. 10) acquired during the experiment showed that both, colour change, and precipitation of liquids and solids occurred inside the autoclave. The glass tee went from clear to yellow, then some solids and later liquids formed, and in the end the glass tube turned opaque. The first sign of precipitation occurred at 52 h (Fig. 9) about 1 h after the H_2S injection started, observed as blackening of the bottom glass tee (Fig. 10). At 53 h the first sign of dew occurred on the centre

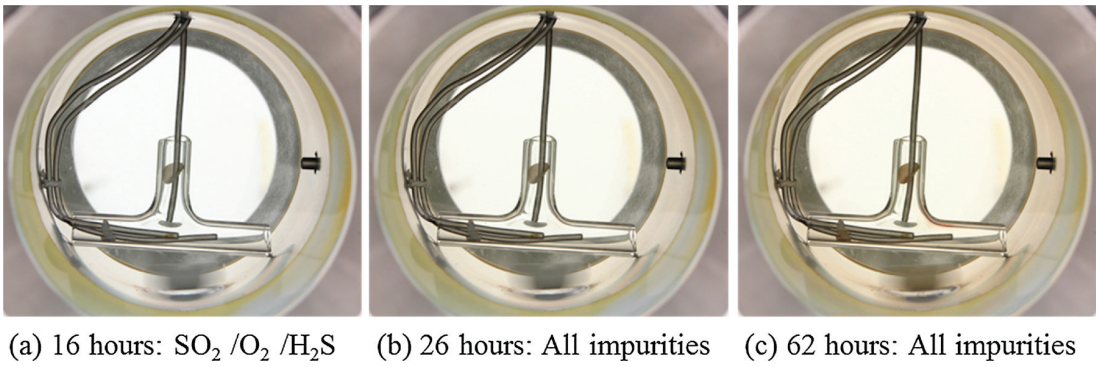

Fig. 7. Still pictures taken during the injection period in Hub02.

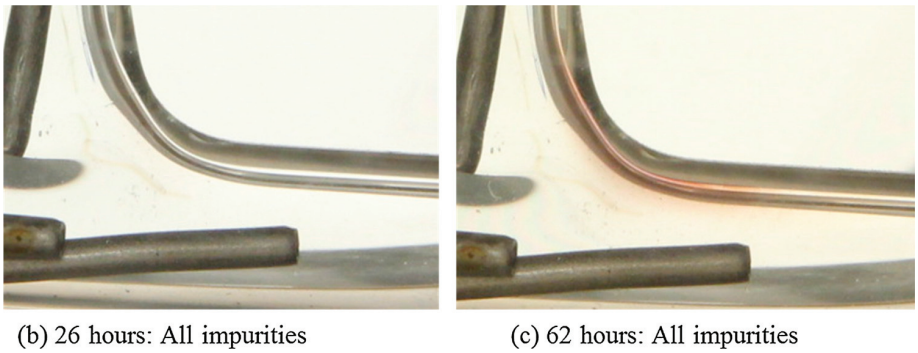

Fig. 8. Enlargement of still pictures in Fig. 7, showing slight colour change of glass tube wall.

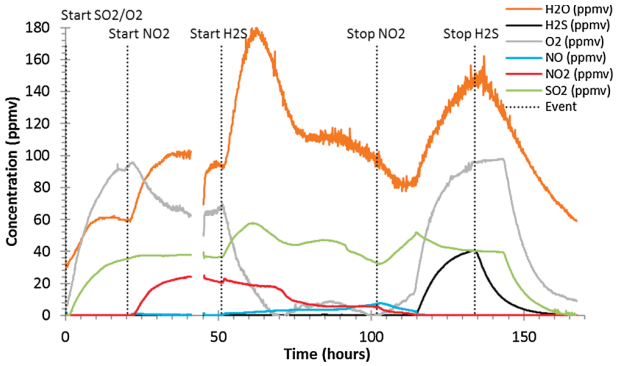

Fig. 9. Analysis of exhaust gas from Hub03.

tube in the glass tee, and both the black deposits and the dew were clearly visible at 62 h (picture c in Fig. 10). At 65 h the first sign of droplet formation became visible, and after this the liquid accumulated fast. The view became impervious after NO_2 was stopped. The liquid inside the autoclave was analysed using ion chromatography after the experiment. Both SO_4^{2-} and NO_3^- were detected, which most likely originated from sulfuric acid and nitric acid formed during the experiment. The molar ratio was about 10:1 of SO_4^{2-} (sulfuric acid) to and NO_3^- (nitric acid). At about 68 h the NO_2 pump was refilled with a more dilute stock solution with a theoretical concentration of 20 ppmv NO_2. This could explain some of the decrease occurring at this time.

4. Discussion

In summary, the present test campaign has demonstrated that chemical reactions occur for certain blends of impurities. However, not all blends caused reactions and not all reaction products formed corrosive species. When corrosive species did form, the amount increased with increasing impurity content.

4.1. Fully dissolved reaction products

The first experiment (Hub01) clearly showed (Fig. 3) that several reactions occurred when all impurities were introduced simultaneously,

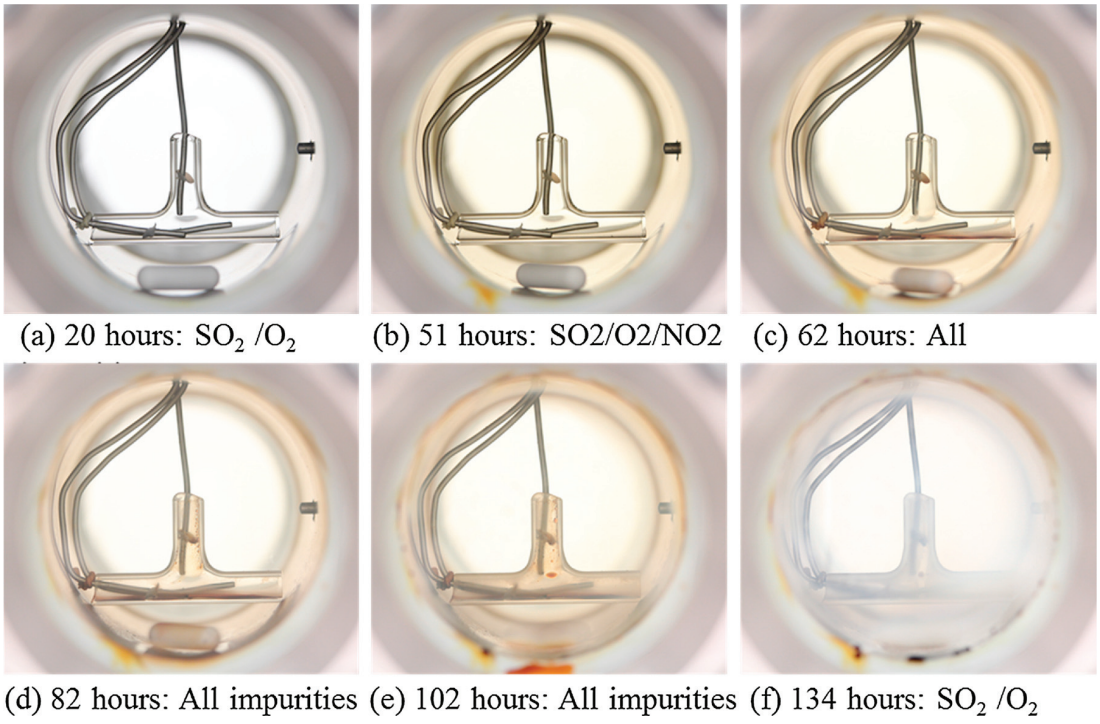

Fig. 10. Still pictures taken during the injection period in Hub03.

since none of the impurities reached their target concentrations. However, because all impurities were introduced at the same time it was difficult to identify possible individual reactions. The impurities were therefore added sequentially for the rest of the work.

In the second injection period of Hub01 there were no reactions until NO_2 was introduced, demonstrating that a mixture with H_2S, H_2O, SO_2, and O_2 was stable under these conditions. This contrasts with observations in other systems, where reaction of H_2S and O_2 have been reported (Craig, 2002; Song et al., 2010; Song et al., 2011; Song et al., 2012). When the NO_2 injection was started the second time (143 h in Fig. 4), indication of reactions became clear. The H_2S content decreased at the same amount as SO_2 increased. Another interesting observation was that the O_2 content was reduced and after some time fully consumed. The new species NO was detected, while the NO_2 level was at the detection limit. These trends were also observed in the other experiments, except that O_2 did not completely disappear in Hub02 and Hub03, and the measured NO_2 concentration was then higher. There was not much difference if NO_2 was injected before H_2S or vice versa, both had to be present simultaneously for reactions to occur.

A more detailed study of the measured and theoretical impurity content is shown in Figs. 11 and 12. The theoretical concentration is the calculated concentration if no reactions occurred (injection and dilution). With exception of Hub03, where liquid acid precipitated, the SO_2 analysis was close to the sum of SO_2 and H_2S that was injected, clearly proving that all H_2S was converted to SO_2 in the presence of NO_2. It can also be observed that NO_2 was present in the exhaust feed only if O_2 also was present. Furthermore, if no liquid acids were formed, the sum of NO and NO_2 was always the same as the injected NO_2 level.

It was demonstrated multiple times that H_2S, O_2 and SO_2 can coexist (at least up to about 35 ppmv) together with water without reactions taking place, suggesting that NO_2 is a very important reactant under these conditions. These observations lead to the proposal of the following reaction:

$$H_2S + NO_2 + O_2 \rightarrow SO_2 + H_2O + NO \quad (1)$$

H_2S, NO_2 and O_2 react to produce SO_2, H_2O and NO. This is very clear in the second period of Hub01. It should be stressed that this is assumed to be the overall reaction, not including possible intermediate reactions. However, there are several indications that reaction 1 is not occurring under all conditions. For example, in Hub02 after the NO_2 injection was stopped, the SO_2 level continues to remain high for many hours (green and blue lines in Fig. 11b) until NO/NO_2 has been removed from the system, after which the other impurities go back to their injection levels. This could indicate that H_2S does not react directly with O_2, but rather with NO_2. If H_2S and O_2 could react directly, the SO_2 level should have remained high also after NO_2 had been removed from the system. Apparently even low concentrations (ppb) of NO_2 is enough to oxidise H_2S. It is therefore suggested that the following reactions can occur either in parallel with, or instead of, reaction 1:

$$H_2S + 3NO_2 \rightarrow SO_2 + H_2O + 3NO \quad (2)$$

$$NO + \frac{1}{2}O_2 \rightarrow NO_2 \quad (3)$$

Thus, it is suggested that NO_2 is acting as an oxidation agent for H_2S to form NO, SO_2 and H_2O, while O_2 reacts with NO to form NO_2 that again can react with H_2S. Clear indication of this is shown in Fig. 11b, where the SO_2 level (green line) continues to remain high until NO/NO_2 is completely removed from the system, after which H_2S and SO_2 returns to their injection levels. If NO_2 was not needed to oxidize H_2S, the SO_2 should have followed the dashed blue line, which would represent dilution of already reacted H_2S. Further support for this is the fact that NO_2 is only detected if also O_2 is present in the exhaust gas. Since the SO_2 content follows the injection levels of the reactants to an almost perfect fit of the theoretical values (Figs. 11 and 12), it must mean that the reactions (1) - (3) are fast compared to the residence time (approximately18 h).

However, there is some discrepancy for the oxygen analysis. Apparently, more O_2 is consumed than what can be accounted for with reactions (1) - (3). Some of this is most likely related to analytical challenges (see Section 2.3), but it could also be related to production of certain species that were not analysed for. When NO_2 was introduced to the system there were always observed some irregularity with the oxygen analysis. This could indicate that some form of reaction between O_2 and NO/NO_2 is taking place and producing some unidentified species.

4.2. Precipitated reaction products

Even though most of the reactants and products could be accounted for in the experimental campaign (see the previous paragraph), additional precipitated products were visually observed in Hub02 and Hub03. In Hub02 there was just a slight blackening of the glass tee, and the small amount of product that formed was not enough to be analysed. However, in Hub03 (Fig. 9) there was clear formation of liquid products (Fig. 10) and ion chromatograph analysis showed that these contained SO_4^{2-} and NO_3^-. Most likely this was sulfuric acid (H_2SO_4) and nitric acid (HNO_3), as also observed in previous work (Dugstad et al., 2014; Yevtushenko et al., 2014), but it could in principle also be H_2SO_3 or HNO_2 acids that were further oxidised by air during sampling or by the aqueous eluent in the IC column during analysis. However, H_2SO_3 cannot exist in solution (Sülzle et al., 1988) and HNO_2 cannot exist in gas phase (Kameoka and Pigford, 1977). Thus, the observed

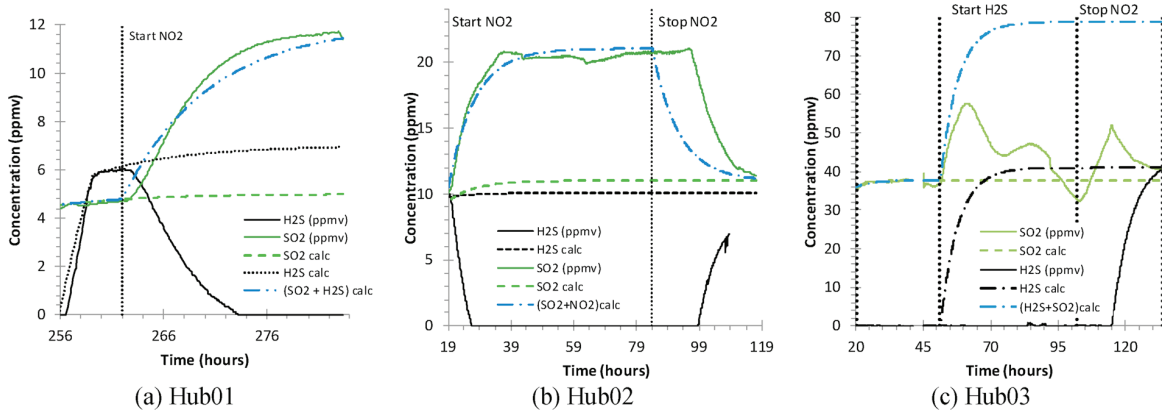

Fig. 11. Analyzed SO_2 (solid green lines) and analyzed H_2S (solid black lines) compared with the theoretical compositions (dashed lines) and the sum of the theoretical compositions (dashed blue lines).

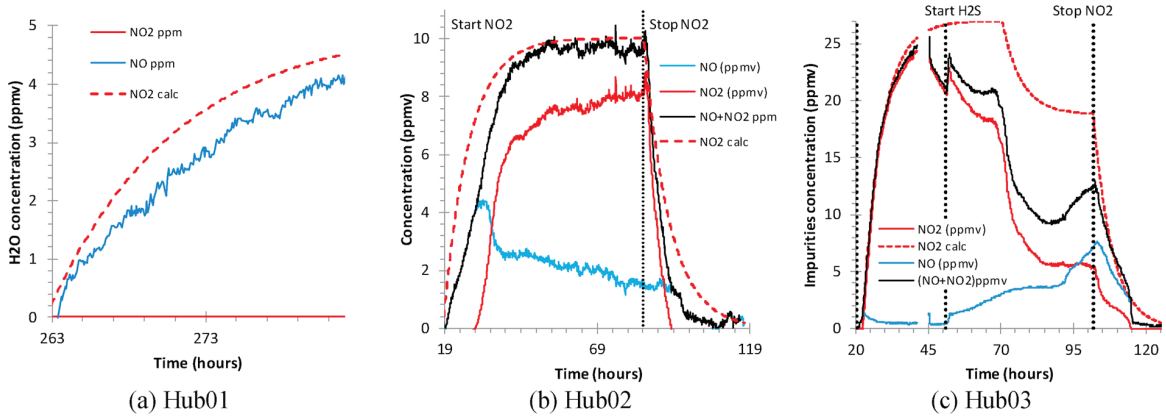

Fig. 12. Comparison of analyzed NO_2 (red solid line) and NO (blue solid line) compared to the theoretical NO_2 concentration (red dashed lines) if no reactions occurred. The black line is the sum of NO_2 and NO.

precipitate in the Hub03 is probably H_2SO_4 and HNO_3. The first sign of "dew" occurred shortly after the injection of H_2S started (53 h in Fig. 9). Interestingly, the first sign of larger brown droplets was just after both SO_2 and H_2O started to decline. In addition, the SO_2 concentration never reached the sum of SO_2 and H_2S injected (which was 79 ppmv, see Fig. 11c). Instead it peaked at 57 ppmv, meaning that after 60 h, reaction 1 or 2 were not the only reactions in this experiment. When both SO_2 and H_2O started to decrease (62 h in Fig. 9), the amount of produced liquid precipitation visually increased in the reaction chamber. By using the fact that both SO_2 and H_2O decreased significantly, and NO_2 also decreased slightly while NO increased slowly, the following reaction is suggested:

$$SO_2 + H_2O + NO_2 \rightarrow NO + H_2SO_4 \quad (4)$$

In-house data, which will be included in a later publication, have shown that the solubility of sulfuric acid in dense phase CO_2 may be as low as 1 ppmv suggesting that the "dew" and the first liquid observed on the glass tee was H_2SO_4 that had precipitated since the solubility limit was exceeded. The formation of nitric acid could be through many different routes, such as:

$$3NO_2 + H_2O \rightarrow 2HNO_3 + NO \quad (5)$$

However, Eq. (5) is not favourable based on standard Gibbs energy, with a positive value of 15.3 kJ/mol for gas phase reaction and 9.4 kJ/mol for liquid phase reaction (data in dense phase CO_2 are not available). Instead it is proposed that NO_2 reacts to nitrous and nitric acid in an aqueous solution. Since sulfuric acid is highly hygroscopic, it will absorb water from the CO_2 phase and thus provide the aqueous solution needed for the disproportionation of NO_2. The reactions would then be:

$$2NO_2 + H_2O \rightarrow HNO_3 + HNO_2 \quad (6)$$

$$3HNO_2 \rightarrow HNO_3 + 2NO + H_2O \quad (7)$$

As shown previously, NO can be re-oxidized by O_2 to NO_2, therefore the overall reaction suggested by our data, would be:

$$2HNO_2 + O_2 \rightarrow 2HNO_3 \quad (8)$$

The ratio of 10:1 between sulfuric acid and nitric acid could reflect the amount of water available through absorption for reaction 6, but in-house data (to be published) show that the solubility of HNO_3 in dense phase CO_2 is 3 orders of magnitude higher than H_2SO_4. Thus, the nitric acid could be dissolved in the CO_2 and transported out of the autoclave. In fact, HNO_3 was frequently detected inside the heated vaporizing regulator on the exhaust line. Consequently, the ratio between those acids cannot be used as measure of the production ratio of these acids.

4.3. Estimation of produced species

The difference between the theoretical concentration and the measured concentration can be used to predict how much of the acids or other compounds that were produced in Hub03 (Fig. 13). Since the concentrations are ppm volume at 1 bar and 25 °C which are equal to ppm mole, the concentration can be used directly to determine the amount of the produced species. From 20–50 h there is a drop in the oxygen content that is not fully understood, but it is assumed to be an analytical artefact since the SO_2 and NO_2 content followed the theoretical curves for non-reactive conditions. There are not any other reactions occurring before the injection of H_2S started.

Certain species like the strong acids (H_2SO_4, HNO_3), H_2 and some nitrogen oxides were not analyzed with the gas analyzer in the present work. An accounting (element balance) for all species that were injected and analyzed in the exhaust CO_2 (Fig. 13) was therefore carried out to try to give a rough estimate of the amount of produced components (the precipitated liquids/solids). Formation of H_2SO_4, would need the consumption of 2 x H, 1 x S, and 4 x O, likewise, HNO_3 formation will consume 1 x H, 1 x N and 3 x O. Consumed elements is basically the difference between the injected (theoretical) and the measured concentration. The elements available to produce acids can be found in Fig. 13. For example, at 75 h the difference between injected O_2 and measured O_2 was 90 ppmv (equal to 180 ppmv "O-consumed"). The difference between injected H_2S and measured H_2S was 40 ppmv, which gives 80 ppmv "H-consumed" and 40 ppmv "S-consumed". As for SO_2, there was no consumption but instead about 6 ppmv was produced. This gives negative numbers of –6 ppmv sulphur and -12 ppmv of oxygen.

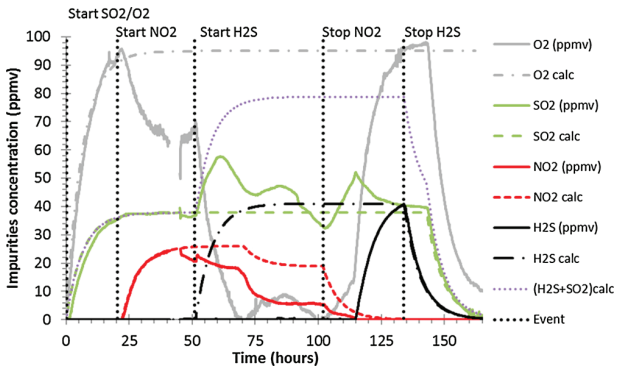

Fig. 13. The difference between theoretical (dashed lines) and measured (solid lines) impurities for Hub03.

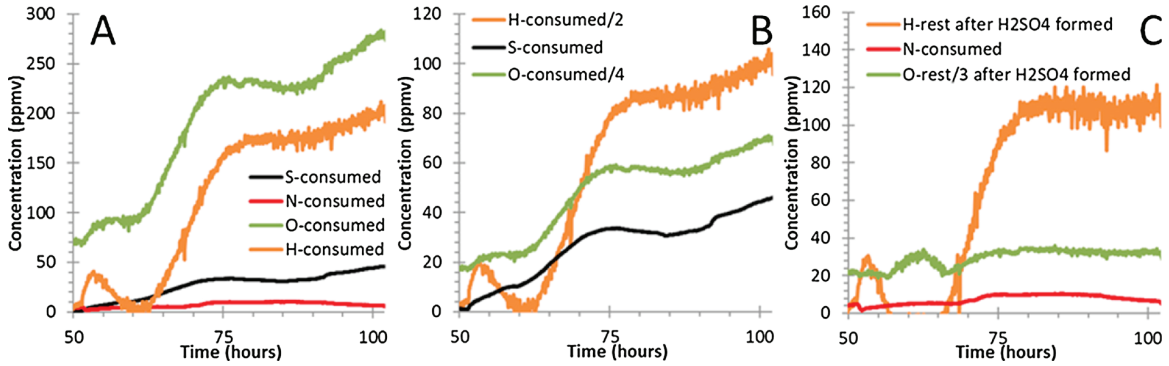

Fig. 14. Calculation of the amount of possible produced acids during Hub03. The diagram to the left (A) shows the balance of all elements involved. The diagram in the middle (B) shows the matching of sulfuric acid. The diagram to the right (C) shows matching of HNO_3 after sulfuric acid is produced (in B).

The elemental balance for of all injected and analyzed species are summarized in Fig. 14a. The calculations showed that formation of both acids was limited by the excess of N and S, most of the time (i.e. H and O excess concentrations were larger than the equivalent excess N and S content). Fig. 14b shows the balance for production of H_2SO_4 and the lower line was the limiting reactant. Fig. 14c shows the balance for production of HNO_3 after H_2SO_4 was produced first (b) and again the lowest line would be the limiting reactant. These calculations show that hydrogen was the limiting reactant in the period between 55 and 65 h, partly preventing formation of H_2SO_4 and HNO_3. The reason for the low amount of hydrogen was the production/emission of H_2O in this period (55–65 h in Fig. 9). Still there was a consumption of sulphur, and this could indicate the formation of elemental sulphur. Precipitates were observed in the bottom of the glass tee in Fig. 10 after 62 h. In Fig. 14 it was assumed that sulfuric acid was produced first and that nitric acid was produced from the excess compounds (after sulfuric acid). For simplicity it is assumed that these assumptions are valid throughout the whole set of calculations.

The estimated product produced during the experiment between 50 and 100 h is shown in Fig. 15. There is some excess oxygen after the formation of the strong acids and elemental sulphur. There could be several reasons for this excess. First, the water contaminated impurity injection system would represent some uncertainty regarding the water feed. Analytical deviations could also contribute to less accurate calculations, especially regarding O_2, which decreased when the NO_2 injection was started at 20 h (Fig. 9) in Hub03. The shown O_2 analysis was carried out using a high-performance laser analyser, while at the same time also a zirconia-based oxygen analyser was connected (results not shown for Hub03). The zirconia-based sensor can be damaged by NO_2 and H_2S, so the gas was always routed through a scavenger first, before the gas entered the zirconia analyser (this analyser is the last instrument in low pressure the analysis line). The zirconia-analyser however, did not detect the decrease of 30 ppmv oxygen during 25–50 h in Hub03, in fact the oxygen moved towards the target value. This could indicate that some unknown process that consumed O_2 occurred during this period and that this reaction was reversed in contact with the scavenger.

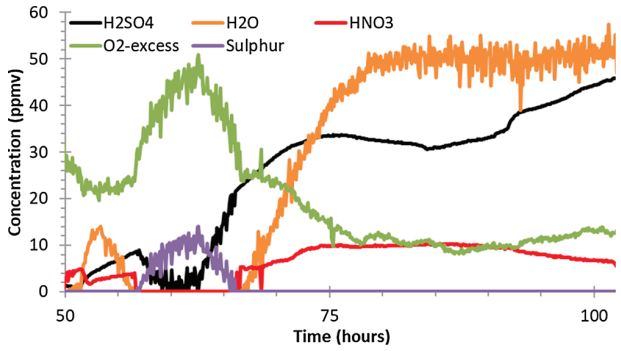

Fig. 15. Estimate of the amount of produced species.

The analyses of the precipitate after the experiment showed that sulfuric and nitric acid were formed, but exact quantification was not possible. The calculations show that sulfuric and nitric acid were produced at a maximum average concentration of 44 and 11 ppmv, respectively. The solubility limit of sulfuric acid was therefore exceeded according to in-house data, meaning that sulfuric acid would precipitate and form a liquid phase, which was indeed observed. Nitric acid, on the other hand, was always present well below its solubility limit in pure CO_2, meaning that most of it was transported away with the vented CO_2. However, HNO_3 was also present in the liquid precipitates, indicating that the reaction took place in the newly formed liquid phase.

4.4. CO_2 transport specification

The results presented in the present paper clearly show that, when present in more than 35 ppmv, these impurities do create corrosive reaction products (strong acids) which is not acceptable for carbon steel pipelines. Even though no corrosion coupons were exposed in the present work, it is well known that HNO_3 and H_2SO_4 are corrosive for carbon steel. Thus, a CO_2 specification should not allow for these impurities to be present at values as high as 35 ppmv. According to the present results, an acceptable impurity level should be somewhere between 10 and 35 ppmv if H_2S, NO_2, SO_2, and O_2 are present. Another approach could be to completely remove one of the reactants. Removal of NO_2 is probably the best solution, but it should be noted that the present results indicate that even small amounts of NO_2 could start reactions. The only reaction that actually removes NO_2 from the CO_2 bulk phase is the production of HNO_3. In the production of sulfuric acid, NO_2 acts somewhat like a catalyst and is not part of the overall reaction in Eq. (4). Thus, just slight NO_2 could trigger formation of H_2SO_4 which may cause severe corrosion. Interestingly, the major acid formation started when H_2O and SO_2 reached about 180 and 60 ppmv, respectively. This could indicate that there is a threshold level above which production of acid starts. Hub01 and Hub02 had much higher H_2O concentrations, but the SO_2 content was $\leq$ 20ppmv and no acids were observed. This could indicate that the acceptable SO_2 level is somewhere between 20 and 60 ppmv. Since H_2S may react to form SO_2, it would probably be best to use the sum of $H_2S + SO_2$ as the limiting level for these impurities.

Reactions occurred also in the experiments with 5 and 10 ppmv, but since the reaction products remained fully dissolved in the CO_2 phase they are probably not corrosive for the carbon steel pipeline. If they precipitate later in the pipeline, e.g. at other temperatures or pressures,

corrosive phases could form and be a threat to the pipeline. Further work should be carried out to study the corrosiveness of the products of the reactions at 5 and 10 ppmv.

5. Conclusion

When separate CO_2 streams with water, O_2, SO_2, H_2S, and NO_2 were mixed to simulate a CO_2 transportation hub system, reactions were observed. The types of products that formed were concentration dependent, and no corrosive species were observed for the lowest impurity concentrations (5 and 10 ppmv). A separate liquid phase containing H_2SO_4 and HNO_3 formed when the impurity concentration was 35 ppmv of SO_2, NO_2, H_2S, and 95 ppmv O_2. An impurity concentration of 10 ppmv and lower resulted in reactions, but the products were not corrosive and did not form a separate liquid phase and are therefore not considered a threat for carbon steel. Thus, a safe operation limit for these impurities will be somewhere between 10 and 35 ppmv of SO_2, NO_2, and H_2S.

Acknowledgements

The present work was carried out as part of the Kjeller Dense Phase CO_2 Corrosion II project (KDC-II). The authors would like to thank CLIMIT (Norwegian Research Council, project no. 243624/E20), Shell, Total, ArcelorMittal, OLI, and Gassco for financial and technical support.

Appendix A. Supplementary data

Supplementary data associated with this article can be found, in the online version, at https://doi.org/10.1016/j.ijggc.2019.05.017.

References

Craig, B., 2002. Corrosion poduct analysis - A road map to corrosion in oil and gas production. Mater. Perform. (August), 56–58.
de Visser, E., Hendriks, C., Barrio, M., Mølnvik, M., de Koeijer, G., Liljemark, S., Le Gallo, Y., 2008. Dynamis CO2 quality recommendations. Int. J. Greenh. Gas Control. 2, 478.
Dugstad, A., Morland, B.H., 2016. Formation of Corrosive Phases in Dense Phase CO_2. Eurocorr, pp. 2016.
Dugstad, A., Halseid, M., Morland, B., 2014. Testing of CO_2 specifications with respect to corrosion and bulk phase reactions. Energy Procedia 63, 2547–2556.
Energy Technology Perspectives, 2010. Scenarios & Strategies to 2050. IEA.
Halseid, M., Dugstad, A., Morland, B., 2014. Corrosion and bulk phase reactions in CO_2 transport pipelines with impurities: review of recent published studies. Energy Procedia 63, 2557–2569.
IEAGHG, 2019. Effects of Impurities On Geological Storage of CO_2. IEAGHG, IEAGHG.
IPCC, 2019. Summary for policymakers. In: Stocker, T.F., Qin, D., Plattner, G.-K., Tignor, M., Allen, S.K., Boschung, J., Nauels, A., Xia, Y., Bex, V., Midgley, P.M. (Eds.), Climate Change 2013: The Physical Science Basis. Contribution of Working Group I to the Fifth Assessment Report of the Intergovermmental Panel on Climate Change. IPCC, Cambridge University Press, Cambridge, United Kingdom and New York, NY, USA.
Kameoka, Y., Pigford, R.L., 1977. Absorption of nitrogen dioxide into water, sulfuric acid, sodium hydroxide, and alkaline sodium sulfite aqueous solutions. Ind. Eng. Chem. Fundam. 16 (1), 163–169.
Mohitpour, M., Seevam, P., Botros, K., Rothwell, B., Ennis, C., 2012. Pipeline Transportation of Carbon Dioxide Containing Impurities. ASME Press.
NETL, 2013. CO_2 Impurity Design Parameters. Report no. DE-FE0004001. NETL.
OED, 2016. Feasibility Study for Full-scale CCS in Norway. Ministry of Petroleum and Energy. http://www.gassnova.no/en/Documents/Feasibilitystudy_fullscale_CCS_Norway_2016.pdf.
Ruhl, A.S., Kranzmann, A., 2013. Investigation of corrosive effects of sulphur dioxide, oxygen and water vapour on pipeline steels. Int. J. Greenh. Gas Control. 13, 9–16.
Song, Y., Palencsar, A., Svenningsen, G., Kvarekvål, J., 2010. Effect of oxygen and temperature on aqueous sour corrosion systems. EuroCorr 2010.
Song, Y., Palencsar, A., Svenningsen, G., Kvarekvål, J., Hemmingsen, T., 2011. Effect of O_2 and Temperature on Sour Corrosion. CORROSION/2011, paper no. 11077. NACE International, Houston, TX.
Song, Y., Palencsar, A., Svenningsen, G., Kvarekvål, J., Hemmingsen, T., 2012. Effect of O_2 and temperature on sour corrosion. Corrosion 68 (7), 662–671.
Sülzle, D., Verhoeven, M., Terlouw, J.K., Schwarz, H., 1988. Generation and characterization of sulfurous acid (H_2SO_3) and of its radical cation as stable species in the gas phase. Angew. Chemie Int. Ed. English 27 (11), 1533–1534.
Yevtushenko, O., Bäßler, R., Carrillo-Salgado, I., 2013. Corrosion Stability of Piping Steels in a Circulating Supercritical Impure CO_2 Environment. CORROSION/2013, paper no. 2372. Houston, TX: NACE International.
Yevtushenko, O., Bettge, D., Bohraus, S., Bäßler, R., Pfennig, A., Kranzmann, A., 2014. Corrosion behavior of steels for CO_2 injection. Process. Saf. Environ. Prot. 92 (1), 108–118.

Chapter 9

Discussion

9.1 The effect of water condition and experimental artefacts

The setup used in most of the experiments reported in the literature have serious short comings and an important part of the present PhD has been the development of an improved test approach. The main improvement was pre-dissolving the water in the CO_2 before entering the test system and introduction of continuous replenishment of impurities (including water) during the experiments [1]. The system also included analysers that monitored the impurity concentration before, during, and after the experiments. In addition, a transparent autoclave that allowed visual observations inside the autoclave during experiments was designed [2-5].

The literature review (Chapter 2) showed how important it is to distinguish between three different corrosion situations; corrosion coupons submerged in a free water phase in equilibrium with a CO_2 phase, corrosion coupons hanging in a water-saturated CO_2 phase, and corrosion coupons hanging in a CO_2 phase under-saturated with respect to water. The corrosion mechanism is probably the same, for the three conditions, but the corrosion rates are significantly different. The amount of water is a key component for the reactions, and the presence of a separate water phase will favour high corrosion rates. It is crucial to keep control of how much water that is present and especially if it is above or below the solubility limit. The phase properties of the system can easily change when the temperature or pressure is altered and controlling the water saturation of CO_2 is not straightforward for corrosion experiments. The differences between free water, under-saturated, and water-saturated conditions, and the consequences of the conditions are discussed in the following chapters.

9.1.1 Effect of water on corrosion in systems with dense phase CO_2

The experiments with a free water phase (Chapter 3) showed clearly that the corrosion rate of carbon steel exposed to a bulk water phase in equilibrium with dense phase CO_2 is very high. Rates in the range of 10 - 20 mm/y were measured in the present work, but 5 - 50 mm/y have also been reported, depending on pH, flow, pressure and temperature. Even with a corrosion allowance of several mm, a pipeline would last for less than a year if exposed to such conditions. The parallel experiments in chapter 3, which exposed carbon steel to liquid water, had corrosion rates with a

standard deviation of about 30 %, indicating that the results were relatively reproducible and well within the same order of magnitude. Although there are some spread in the reported corrosion rates in liquid water with CO_2, it is clear that the rates are too high to be acceptable from a pipeline integrity point of view. Thus, it can be concluded that liquid water must be avoided in CO_2 transportation systems of carbon steel, even for shorter periods.

However, when it comes to water that is fully dissolved in the CO_2 phase, there has been a large spread in the corrosion rates reported during the last decade, even for apparently similar conditions (chapter 2.1.2). Corrosion rates ranging over three orders of magnitude, from 0.003 to 2.5 mm/y, have been reported for water concentrations far below the solubility limit. Many of these reported rates are in complete contradiction with the present experimental results (Chapter 4), for which the corrosion rate was about 1 µm/y, even when the water concentration was close to the solubility limit. The discrepancy is very important for operation of CO_2 transport pipelines and will be discussed further in the next chapters.

In the literature review, it was observed that the corrosion experiments in dense phase CO_2 have been carried out using autoclaves or flow loops, and with many different approaches to reach the target conditions. Also, how the test systems were taken back to the ambient conditions after the experiments were finished varied and were often poorly described. Thus, it is most likely that the large difference in reported corrosion rates is caused by the different experimental approaches, rather than a fundamental different corrosion rate or corrosion mechanism. If the goal of one experiment is to investigate under-saturated water conditions, then it is important to be sure that the water is in fact fully dissolved in the CO_2 phase and that water precipitation does not occur on the corrosion coupons. One important difference in the way the present experiments and the experiments reported in the literature were carried out is how the water was introduced to the test chamber (autoclave). Many papers report that water was injected by weight or volume into the autoclave, meaning that the water was introduced as liquid water before the autoclave was filled with CO_2. Thus, water was present in the liquid state until it had completely dissolved in the CO_2 phase. The autoclave systems were usually closed during the whole experiment, and the concentration of the water during or after experiments was rarely measured. Ayello and Thodla [6-8] ran a series of experiments which has been frequently refereed in the literature, and they concluded that: "*A very small amount of water (~100ppm) in supercritical CO_2 is sufficient for the formation of a second phase containing water. In consequence, the corrosion rate of carbon steel in the presence of a small quantity of water as a second phase in supercritical CO_2 is very high (1-2mm/year)*". This

conclusion is in contradiction to the present work. It is not likely that an amount of water which is about 50 times lower than the solubility limit for the system, would form a second phase (liquid phase), at least not at equilibrium. All the injected water would dissolve if given enough time. However, the water was added as a droplet onto their corrosion coupon, and electrochemical measurements were used for monitoring the corrosion rates for 5 to 6 hours. They observed that the corrosion rate decreased during the experiments with both 100 and 1000 ppmw of added water, which probably was caused by the accumulation of alkaline corrosion products in the water droplet due to corrosion and loss of water to the CO_2. The experiments are therefore not representative for a situation with 100 or 1000 ppmw of under-saturated water, but for a transient period with liquid water dissolving in an under-saturated CO_2 phase. This could for example occur in a pipeline after accidental ingress of small amounts of water.

The method used in the present work was to dissolve the water in CO_2 first, and then inject the "moist" CO_2 into the autoclave. In this way no *liquid* water was introduced into the system, and the results were consequently not affected by the time required for the water to dissolve. The corrosion coupons were present from the start, the water concentration in the CO_2 inside the autoclave was always less than 5 ppmv in the beginning of each experiment (lowest practical achievable water content), and the water content was then gradually increased to the target by injection of "moist" CO_2. The water concentration was measured before, during, and after each experiment with an accuracy of 10 ppmv. Furthermore, all experiments were ended by 20 hours injection of dry CO_2 to get the water concentration below 20 ppmv before depressurization. This procedure prevented water precipitation during depressurisation. The water solubility is known to be reduced with pressure reduction, and particularly with phase change (CO_2 going from liquid/super critical to gas phase). Information about depressurisation procedures and possible water precipitation/condensation was usually not included in the reviewed corrosion papers. It is likely that this type of experimental artefact may have contributed, partly or fully, to the high corrosion rates that have been reported.

9.1.2 Experimental pitfalls with liquid water injection

When liquid water is introduced into an autoclave with corrosion coupons, different scenarios can be foreseen: (1) Micro droplets of water may accidentally hit the corrosion coupons during loading or depressurization of CO_2, resulting in artificially higher corrosion rates. (2) The time for water to dissolve in the bulk CO_2 phase has not been experimentally investigated. However, some experiments indicated that this process could take many hours [6,9] In-house data (to be published

[1]) showed that it took up to 20 hours for a droplet of water to fully dissolve in 0.3 dm² CO_2 at 25°C and 100 bar. The dissolution time will probably be affected by droplet size, temperature and convection, but anyway the consequence will be higher corrosion rates on the coupons exposed to water droplets, and lower corrosion rates on the coupons without droplets, since the expected water concentration in the CO_2 phase was never reached or reached later than expected. (3) During depressurization the solubility limits for certain impurities can be exceeded, and especially water precipitation may occur since the solubility limit is reduced with reducing pressure, as shown in Figure 9-1. The data is calculated by OLI studio version 9.6.3.[10-12]

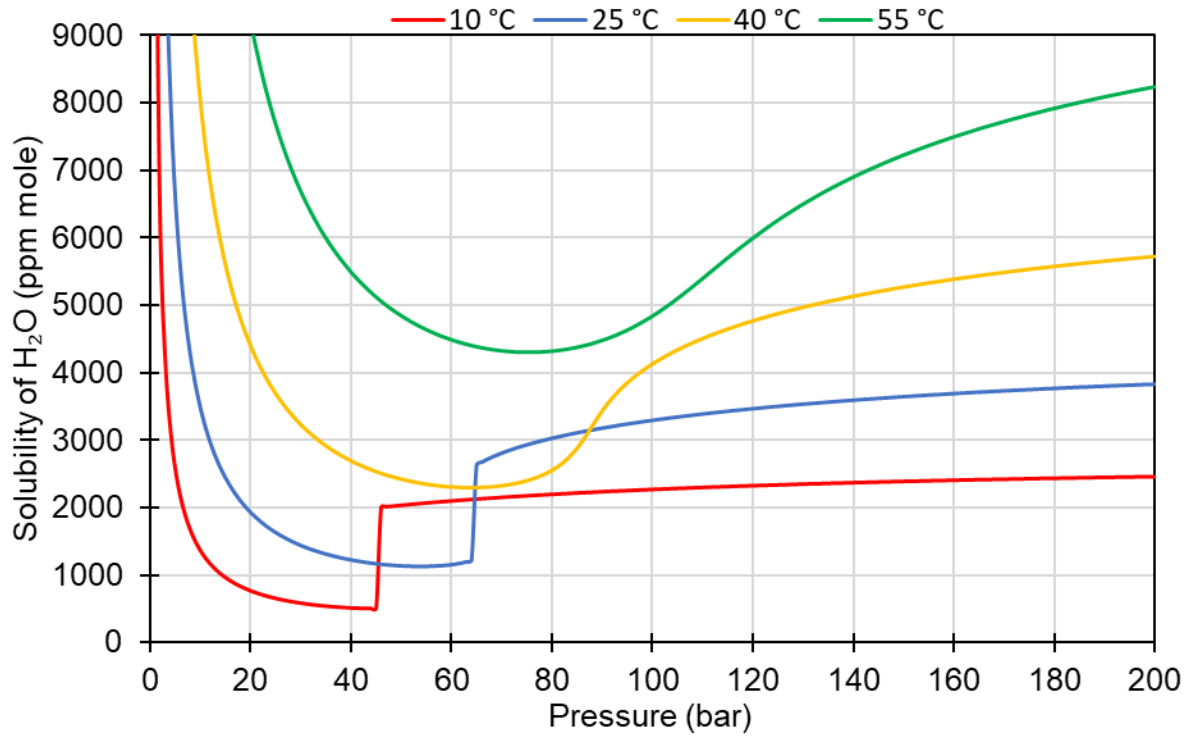

Figure 9-1: Water solubility in CO_2 (calculated with OLI studio, OLI systems).

The Joule-Thomson effect will lower the temperature during depressurization, which in turn lowers the solubility limit (see different temperature lines in Figure 9-1). All dense phase CO_2 experiments have to go through depressurization to collect the exposed coupons, two examples of depressurizations are shown in Figure 9-2.[1] The fast depressurization took 19 minutes for which the temperature decrease inside the autoclave was 25 °C, while the slow depressurization took 308 minutes and had a temperature decrease of only 3 °C. The main temperature drop occurs when the system goes from one phase (liquid) to two phases (liquid-gas) and the temperature starts increasing when all liquid phase is vaporized and only the gas phase is left.

[1] To be presented at the CORROSION/2020 conference.

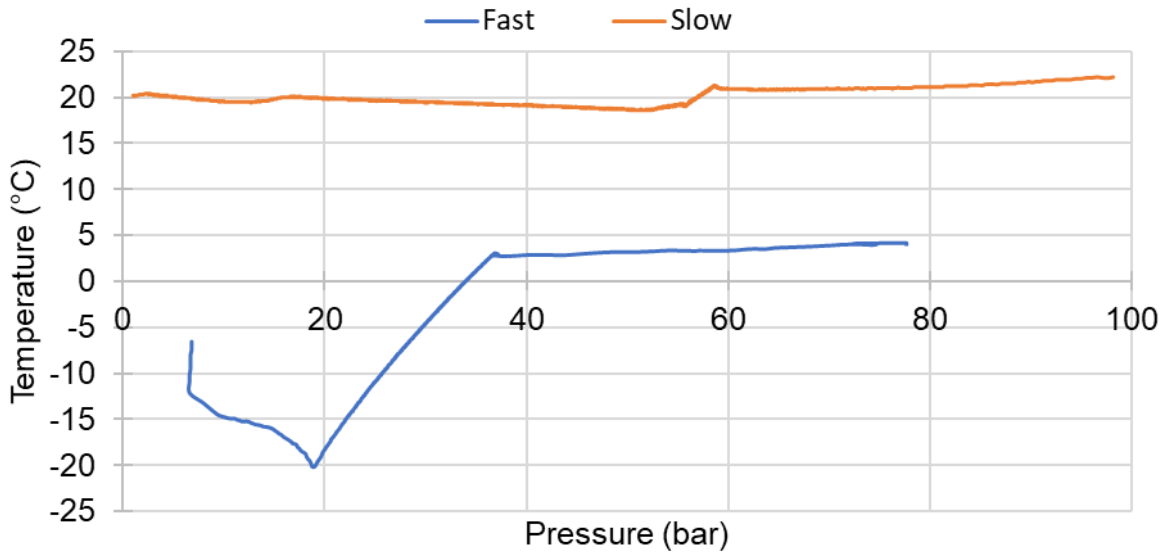

Figure 9-2: Pressure vs temperature during fast (19 minutes) and slow (308 minutes) depressurization.

In sum these two effects (decrease of temperature and pressure) will increase the risk of liquid water precipitation, which obviously will enhance the corrosion since there will still be a significant amount of CO_2 present in the system. Scenario 1 and 3 will not only enhance the corrosion, but also increase the risk of localized attacks since micro droplet hitting the steel surface may sustain corrosion until completely consumed, thus leaving a pit behind. There is also a risk of oxygen corrosion (flash rust) if the wet coupons are exposed to air when the autoclave is opened after the experiment is finished. Present experiments with pre-dissolved water (Chapter 4) did not show any indications of localized attacks, even when the solubility limit was exceeded due to cooling of the system. Care was taken to make sure that no liquid water was present during loading or depressurisation. The exposed coupons were immediately submerged in isopropanol when the autoclave was opened as a precaution for avoiding corrosion by moist air and oxygen. Figure 9-3 shows coupons which have been exposed to essentially similar conditions, but the outcome is very different.

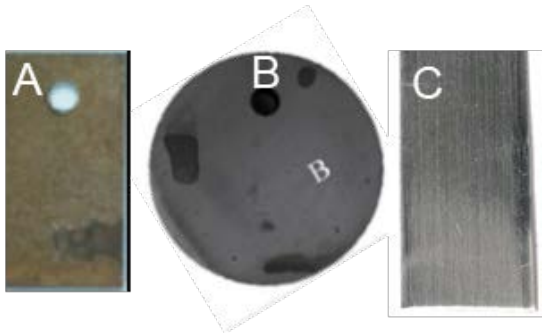

Figure 9-3: Images of exposed corrosion coupons. Coupon A has been exposed to 1220 ppmv H_2O with 80 bar of CO_2 at 40 °C [13], coupon B has been exposed to 3400 ppmv H_2O with 80 bar CO_2 at 35 °C [14], and coupon C has been exposed to 2500 ppmv H_2O with 100 bar CO_2 at 35°C [1].

Sim et al. [13] exposed carbon steel coupons for seven days to supercritical CO_2 with 1220 ppmv H_2O at a pressure of 80 bar at 40 °C. The experiment was carried out in a closed autoclave and the water was injected as liquid. The carbon steel coupon had an even rusty brown surface (Figure 9-3A after the exposure. The reported water concentration was well below the solubility limit, so in principle no water precipitation should be expected. However, all the carbon steel coupons exposed to water concentrations from 240 ppmv to 3600 ppmv had similar attacks, which indicates that the results were affected by experimental artefacts. For example, there could have been more water present than the authors assumed, water may have precipitated during depressurization or possibly the coupons could have been subjected to corrosion in moist air (as indicated by the brown colour). Compared to the experiments of Hua et al. [14] (Figure 9-3B) and Morland et al. [1] (Figure 9-3C), the carbon steel coupons of Sim et al. had much more corrosion products even when the water content was reported to be lower. It might be due to liquid water hitting the coupons when the autoclave was loaded with CO_2, but it is more likely that water has precipitated onto the carbon steel surface during depressurization since the surface products was evenly distributed. Another possibility is water precipitation in the beginning of the experiment when the autoclave was heated up. During this period there is a temperature difference between the CO_2 phase and the carbon steel coupons hanging in the middle of the autoclave. This will be discussed further in chapter 9.1.2. Hua et al. (Figure 9-3B) found black spots on the coupons after 48 hours exposure to 80 bar CO_2 with 3400 ppmv water at 35 °C. They also used a closed autoclave with pre-injection of liquid water. The general corrosion rate was low, but underneath the black spots there were localized attacks. This occurred even when the water concentration was lower than the solubility limit at the test condition. There is no doubt that liquid water has been present on the steel surface, confirmed by black spots consisting of iron carbonate. The reason can be that the water was splattered on the coupons during loading of CO_2. The metal surface adjacent to the spots was unaffected and had

low/no corrosion. Most likely the splattered water was consumed by corrosion leaving behind localized attacks. For comparison, no attacks, general nor localized, were found on coupons exposed for 350 hours to 2500 ppmv water in 100 bar CO_2 at 35 °C (Figure 9-3C), using a flow loop with continuous injection of CO_2 with dissolved water.

9.1.3 Experiments in water-saturated CO_2 phase

Experiments with corrosion coupons exposed to water-saturated CO_2 are particularly vulnerable for temperature variations, since this may result in water precipitation on the corrosion coupons. The liquid water is quite often injected in excess of the solubility to ensure complete saturation. The amount of water that can precipitate depends on how much water that is available in the system. In Figure 9-4, a simplified mechanism of the water-saturation of CO_2 in a closed autoclave is shown, the principles of the autoclave are explained in Chapter 2.6.

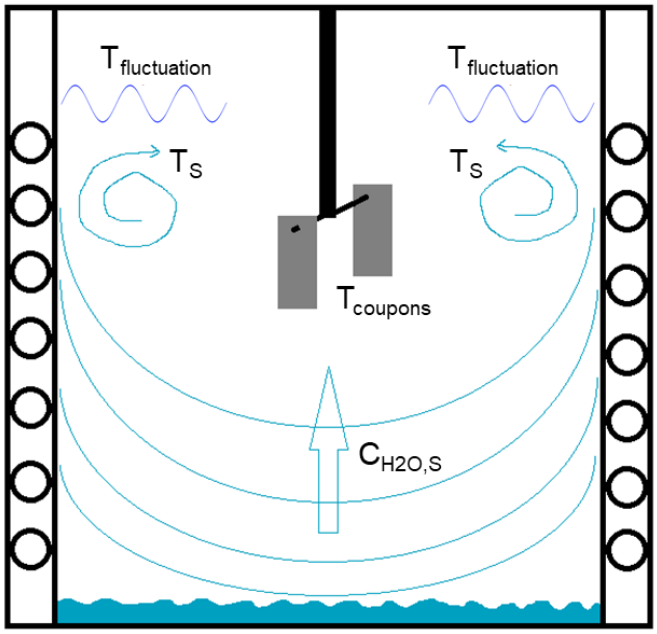

Figure 9-4: Simplified sketch of the water-saturation / water transportation process inside a closed autoclave that is subjected to external heating. $C_{H2O,S}$, is the water concentration at saturation, T_S is the saturation temperature, the temperature of the coupons is represented by $T_{coupons}$. $T_{fluctuation}$ indicates the influence from the temperature controller (heating jacket).

Although the experimental details often were poorly described, the following procedure was most likely used. The autoclave is loaded with water and CO_2 before the autoclave is heated to the designated temperature. When the temperature changes, there will be a water concentration/saturation-gradient that will be affected by water dissolution, diffusion and natural and thermal convection. Initially the CO_2 will be water-saturated ($C_{H2O,S}$) at the water-CO_2 interface, but it will take some time for the water-saturated CO_2 to distribute uniformly throughout the

autoclave, especially without mechanical convection. It is reasonable to assume that it will take many hours for the water content to reach saturation around the hanging coupons in the centre, since it took over 5 hours to fully dissolve a droplet of water, as discussed in chapter 9.1.1. This was actually reported by Tang et al. [9], who did in-situ electrochemical measurements in H_2O-saturated supercritical CO_2 environment, and they had to disregard the first 10 hours of measurements because the water film on the sample surface was not thick enough to run electrochemical measurements.

During the heat-up period there will be a temporary temperature gradient from the wall, which is the warmest point, to the centre of the autoclave, which would be the coldest place, until the whole system has reached equilibrium. The corrosion coupons in the centre of the autoclave will then constitute the coldest spot inside the autoclave and water condensation could therefore occur in the transient period until the system has reached even temperature. When water-saturated CO_2 arrives at this point, water will precipitate/condense at the coupons surface due to this temperature difference. The significance of this hypothesis has not been established experimentally but is believed to lead to high corrosion rates and localized attacks since a free water phase is formed on the steel surface. Even in the most advanced temperature-controlled systems there will be small temperature fluctuations. These small temperature fluctuations will for a system which is fully water saturated act as a "water pump" to the surface of the coupons. Since the system is balancing on the saturation limit, an increase in temperature will trigger precipitation/condensation since the temperature difference between the saturated CO_2 and the steel surface increases, while a decrease in temperature would stop the condensation on the coupons but would probably not dissolve/remove water from the coupons since the solubility limit has been shifted due to lower temperature. However, the temperature decrease could lead to some fogging in the rest of the autoclave. The excess water in the bottom of the autoclave (which has a large contact surface to the CO_2) would continuously replace the water that condensate on to surfaces. The corrosion products/salt would probably also contribute to keeping water at the steel surface due to the salting-out effect. The condensation of water would probably be more pronounce at the autoclave top, since the lid usually is subjected to cooling from the outside, droplets may form underneath the lid and potentially hit the coupons when falling. Thus, care should be taken when comparing the results from water-saturated experiments to experiment with under-saturated water unless they are kept under very strict temperature and pressure control to avoid these artefacts. However, the water-saturated experiments contribute to increase the understanding of the corrosion mechanisms that comes into play during condensing conditions, for example during operation upsets with

accidental water condensation. This should be avoided since the corrosion is high and quite similar to a large free water phase, which would threaten the pipeline integrity.

Chapter 4 discuss an experiment where the water addition exceeded the solubility limit. To do so, the loop was cooled while injection of CO_2 with 2200 ppmv of water was maintained. When the temperature reached about 14 °C the solubility limit was exceeded, but the cooling continued until the temperature was 6 °C.

9.1.4 Mechanism for CO_2 – H_2O corrosion

The corrosion mechanism for the different types of water condition (free, saturated, and under-saturated) was not studied in detail. SEM analyses showed that the composition and morphology of the corrosion products were apparently the same indicating that the same CO_2 corrosion mechanism is involved. SEM and EDS indicated that iron carbonate ($FeCO_3$) was formed in all experiments, consistent with the CO_2 corrosion mechanism for gaseous CO_2 and water[15,16] . The typically reaction route will be that CO_2 dissolves in the water phase, some of the CO_2 forms carbonic acid which dissociates and reacts with iron to form iron ion (Fe^{2+}), bicarbonate ($HCO3^-$), and H_2. When the concentration of these ions is high enough, iron carbonate will precipitate, and this might from a layer on the steel surface, as described in Chapter 2.1.1 and more thoroughly in the paper by Dugstad [16]. Very high corrosion rates have been reported with dense phase CO_2 when the water phase is large compared to the steel surface (5 to 50 mm/y is reported, Chapter 3). If the transport of species to and from the surface is high (high flow rates) and the water phase large enough to prevent super saturation of iron carbonate - no protective iron carbonate films can form and the corrosion will remain high. The situation will be different for experiments with water-saturated CO_2, since the amount of water is small and in many cases the availability of liquid water is limiting the corrosion process. However, there is still some water there and slight corrosion has been reported (>0.1 mm/y, Chapter 2). A limited water phase, which in this contest means very thin surface films, would be rapidly saturated by corrosion products, even with very low corrosion rates, which would create a partly protective layer of precipitated iron carbonate. The pH is a very important factor, even with very high CO_2 pressure, and as showed by Schmitt and Krieck-Defrain [17] the corrosion rate decreased with increasing pH in a water phase with 50 bar of CO_2. The experiment was carried out with injection of HCl to maintain a fixed pH during the whole experiment (i.e. counteract the effect of accumulated corrosion products). They also reported that the corrosion rate decreased when bicarbonate (Equation 2 and 4, Chapter 2.1.1) was allowed to accumulate in the water phase due to corrosion. For water completely dissolved in the CO_2 phase, the situation is different, the

water at the surface of the steel do not have the properties of bulk/free water phase until enough water molecules have adsorb to the surface. In atmospheric corrosion it is a rule of thumb that at least 60 to 80% relative humidity needs to be present before notable corrosion occurs [18,19]. If it is assumed that this principle also is valid for dense phase CO_2, then the water concentration should be about 60 to 80% of the solubility limits before corrosion is initiated. The reason for this limiting relative humidity is linked to monolayers of water adsorbed to the surface without actual having bulk water properties (less than three layers). A film thickness of 3 to 5 monolayers start to exhibit bulk water properties and species like CO_2 can absorb to form carbonic acid. The present work has shown that the water content could go up to the solubility limit and still the corrosion rate was very low, but traces of iron carbonate were found on the surface, which indicates that corrosion do occur but is slow. Even when the water monolayers transform to bulk/free water phase it would still be very little water available to corrode the steel surface, and amount of steel compared to water is enormous. So, it is reasonable to assume that the water phase would be quickly saturated with iron carbonate that may slow down the corrosion process further.

9.1.5 Exposure time and limiting corrosion rate

The duration of a corrosion experiments is an important parameter, particularly when corrosion rates are extrapolated, and extremely high corrosion rates could be reported especially if the exposure time is short. Normally, all experiment with liquid water injection and corrosion coupons in the CO_2 phase give an underestimation of the corrosion rate, since the water needs time to dissolve in the CO_2 Both literature [6,9] and unpublished work has shown that it may take 10 to 20 hours for one droplet to fully dissolve in the CO_2. If the experiment is performed in 24 hours, then the carbon steel coupons are only exposed for the correct conditions for a fraction of the exposure. Still many of these experiments reports relative high corrosion rates, if only the time when the experiment has correct water concentration is taken in account, the corrosion rates would be extremely high. The experiments performed in this thesis have the lowest corrosion reported of all, and all experiment was conducted with pre-dissolved water. The difference became even larger when other impurities were injected.

When a free water phase is present the corrosion rate will be between 5 to 50 mm/y, but this should not happen if the water concentration is below the solubility limit. However, when water is added by injection of liquid water (small amount to dissolve in the CO_2 phase), the coupons could be hit by droplets during loading of CO_2. As mention before, there might be a risk of condensation due to temperature difference inside the autoclave and during depressurization. It is also common practice

to cool the autoclave when the experiment is finalised for easy handling, and this will also change the solubility limit for water (see Figure 9-1). The only method to avoid condensation due to solubility changes is by removing the water before cooling and depressurization, as was routinely done in the present work. However, this is quite time consuming for water-saturated experiments which all has liquid water in excess. Experience from the laboratory work has shown that it may take about 4-5 days to remove 10 g of water from an autoclave if done gently, which is longer than the exposure time for most of the experiments in the literature. To theoretically investigate the impact of such an experimental artefact, it could be assumed that the coupon is exposed to a thin liquid water film in the end of an experiment during depressurizing and cooling. The corrosion rate in such a transient condition has not been studied in detail in the present work or by others, but if it is assumed "bulk water conditions" and at average 5 bar CO_2 and 25 °C, the NORSOK M-506 CO_2 corrosion model gives a corrosion rate of 15 mm/y for condensed water (pH 3.6) and 11 mm/y if the water is saturated with corrosion products (pH 4.8) and 2 mm/y for a pH of 6.5. Although the NORSOK model is not valid for thin water films; it indicates that the corrosion rate is significant, at least for a short period until the corrosion products builds up. If, for example, the whole process takes about 1 hour from onset of liquid precipitation until the autoclave is opened, the condensation artefact will then at maximum be 15 mm/y for 1 hour, which corresponds to about 2 µm corroded steel. If the experiment lasted for 24 hours this will contribute with an additional "corrosion rate" of 0.6 mm/y, while if the experiment lasted for 1 week it would correspond to 0.09 mm/y and for 1 year it would be 0.002 mm/y. The difference is huge if the 24 hours experiment is compared with a one-year experiment, and erroneous conclusions can be drawn due to this type of experimental artefacts. Since the difference between free water phase and under-saturated water corrosion is enormous it is strange that there has been so little focus on these experimental artefacts in the literature. Most likely these artefacts can explain a large fraction of the spread of the reported data for corrosion in CO_2 transport pipelines.

The over-estimation of corrosion rates in under-saturated water experiments can to a certain degree be estimated since water is the limiting factor for the corrosion rate. To corrode one mole of iron, one mole of water is needed (Equation (2-1) to (2-5), Chapter 2.1.1). If, for simplicity, it is assumed that all the dissolved water is converted to carbonic acid that corrodes the carbon steel coupons, the maximum possible corrosion can be calculated for a closed autoclave system. For example, a 1 L autoclave system with 1000 ppmv H_2O, 100 bar CO_2, 100 cm^2 carbon steel sample area, and 50 °C. The maximum achievable corrosion in this case is given by the following equations:

$$n_{H2O} = n_{Fe} \tag{9-1}$$

$$n_{H2O} = \frac{C_{H2O}}{1000000} \cdot n_{CO2} \quad (9\text{-}2)$$

$$CR = \frac{n_{H2O} \cdot MW_{Fe} \cdot 10}{\rho_{Fe} \cdot A_{Fe} \cdot \Delta t} \quad (9\text{-}3)$$

where n_{H2O} is mole water present, calculated by the concentration of water, C_{H2O}, in ppmv and the mole of CO_2 in the autoclave, n_{CO2}. MW_{Fe} is the molecular weight of iron (g/mol), ρ_{Fe} is the density of iron (g/cm^3), A_{Fe} is the total exposed area of the coupons (cm^2), and Δt is the exposure time in year.

At the case condition (100 bar and 50 °C), the density of CO_2 is 384 g/l, so the autoclave contains 8.7 moles CO_2, and the maximum achievable corrosion is 0.006 mm thickness loss (4.9 mg/cm^2) counted as average for the whole exposed surface. For an exposure time of one day this equals to 2.3 mm/y and for a week it equals 0.32 mm/y. A year of exposure gives a maximum corrosion rate of 0.006 mm/y. It is important to remember that for a closed autoclave this is the absolute maximum of corrosion possible when *all the water* is consumed, which of course is an overestimate since not all the water is likely to participate in the corrosion process. Still, this type of calculation will be a useful basis for evaluation of published results, which scatter a lot. Furthermore, this type of mass balance calculation also shows that if corrosion *do* occur, the initial water concentration will decrease, and gradually change from the target condition. In this case, if the measured corrosion rate from a one-day experiment is 1 mm/y then the final concentration of water would be 600 ppmv and not 1000 ppmv. So, if there is a water "threshold" where the corrosion sets on or starts to accelerate, the real corrosion rate at this point cannot be determined in a closed autoclave system since the water is consumed and the water concentration will decrease below the threshold value. One exception is for fully water-saturated conditions with a large liquid water reservoir in the autoclave, but this introduces other experimental challenges.

9.2 Impurity reactions and formation of liquid phases

The chemical reactions may occur in the dense phase CO_2 (homogeneous reactions) or on surfaces (heterogeneous reactions). Both reaction types can in principle produce species that results in corrosion of carbon steel, but homogeneous formation will involve a transportation step and could therefore be slower. Some reaction can produce species that is not necessary more corrosive and might be tolerated, while other reaction products could create an aqueous phase which would increase the corrosiveness of the transported CO_2.

9.2.1 Surface reactions

The literature on corrosion in CO_2 transport systems is mainly focused on steel, especially carbon steel. Since the material choice is a very important factor for the transportation system (pipelines or ships), it is natural that the focus is on the reactions and corrosion products that could be found on the surface of the steel. The corrosion mechanism (Chapter 2.1.1) involves typically a bulk water phase on the metal surface in which the impurities are absorbed which results in formation of species such as carbonic, nitric, and sulphurous/sulfuric acid. However, the water layer on the steel surface needs to be above a critical thickness to obtain the "bulk properties" of liquid water, which is the case for water-saturated and condensing water experiments. The mechanism when this occurs is well documented by others [20] and has not been in focus in the present work. The additional presence of 75 ppmv SO_2 and 220 ppmv O_2 changes the situation, and the water concentration needed to be 1900 ppmv (60% of saturation) before the first sign of corrosion was observed (Chapter 7). The corrosion rate increased just slightly when the water content was increased further to 2400 ppmv. It appeared, however, that the corrosion stopped after relatively short time, either due to formation of protective surface film or because the water was consumed. Nevertheless, this suggests that the mechanism for corrosion can be linked to an increasing thickness of surface water, analogue to findings in atmospheric corrosion [19]. An EDS-analysis of the carbon steel coupon exposed in the SO_2-O_2-H_2O experiment indicated that the corrosion product was $FeSO_4$, which is the expected corrosion product in the presence of sulfuric acid. There are also some reports of hydrated iron sulphite ($FeSO_3 \cdot xH_2O$) as corrosion product in some water-saturated/free water experiments [20-22].

$$\mathrm{Fe} + \mathrm{SO_2} + \mathrm{H_2O} \leftrightarrow \mathrm{FeSO_3} + \mathrm{H_2} \tag{9-4}$$

Iron sulphate is usually found when also O_2 is present and the reaction would be like this:

$$2\,\mathrm{Fe} + 2\mathrm{SO_2} + 2\mathrm{H_2O} + \mathrm{O_2} \leftrightarrow 2\mathrm{FeSO_4} + 2\mathrm{H_2} \tag{9-5}$$

The limiting amount of liquid water is therefore the most likely reason for the low corrosion rate and the small amount of corrosion products found on the carbon steel.

However, in experiments with NO_2 present, the first sign of corrosion was observed at a water content as low as 250 ppmv, and when the concentration was increased above 500 ppmv the corrosion rate became very high.

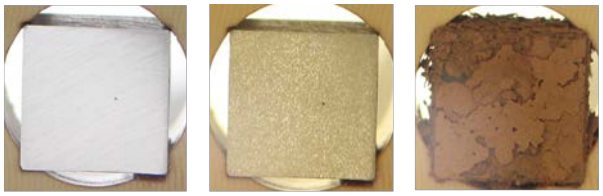

(a) 20 ppmv (b) 350 ppmv (c) 670 ppmv

Figure 9-5: Carbon steel exposed to CO_2 with NO_2 and H_2O (chapter 7).

This calls for another explanation than just the thickness of the water film. The mechanisms involved are not understood, but it could start with monolayers of adsorbed water and co-adsorption of NO_2 which triggers the first sign of corrosion. The products of these two might attract more water to the surface and at some point, even though the water concentration in the CO_2 bulk is very low compared to the solubility limit, the water film gets thick enough to withhold properties as liquid water. Then absorption of NO_2 into the water film is the driving force of the corrosion. It is also a point that HNO_3 is known to be an oxidation agent and possibly it could oxidise iron (steel) even with limited amount of water present. There is no direct evidence for the details in this process, but the indications are strong. Firstly, the low water content needed to start the attack with NO_2 present. Secondly, the published data on SO_2 solubility in water films is about 10 times higher than for NO_2 [23,24] meaning that, if the absorption of species in the water film is the *only* mechanism then corrosion in the SO_2 and O_2 experiment should have been observed at a lower water concentration. The rate of 3.6 µm/y with SO_2/O_2 versus 0.57 mm/y with NO_2 indicate that other factors, like reactivity and protective layer, also affect the corrosion rate. There was no indication that the solubility limit of water was significantly affected by the presence of NO_2 since there were no other phases observed e.g. nitric acids or other compounds. Low water content did not restrict the corrosion in the NO_2-H_2O experiment, the corrosion rate was high and large amount of corrosion products were formed. The products gave no protection as other corrosion film might do (e.g. $FeCO_3$ and FeS), the EDS-analysis of the coupons showed mainly the present of iron and oxygen, but due to technical issues it was not possible to say if nitrogen also was present (i.e. if the corrosion products also contained iron nitrate). Very few papers report iron nitrate when NO_2 is present [25], but it has been observed for atmospheric corrosion and may therefore not be directly comparable to CO_2 environment. The reaction could be:

$$\mathrm{Fe} + 3\mathrm{NO_2} + 3\mathrm{H_2O} \leftrightarrow \mathrm{Fe(NO_3)_3} + 3\mathrm{H_2} \qquad (9\text{-}6)$$

This could be a likely reaction when the amount of water was high as in water-saturated or free water experiments, but NO_2 is a strong oxidizer and the reaction route of NO_2 is complex so it cannot be ruled out that NO_2 just delivers oxygen for reaction with iron to form iron oxide in some form

(FeO, FeOOH, Fe_2O_3, or $FeO{\cdot}Fe_2O_3$) in under-saturated water system, especially at the low water content in ours experiment.

9.2.2 Homogenous reactions

Some of the reactions occur in the bulk CO_2 phase, while other reactions take place on (steel) surfaces. Chapter 5 [2] and Chapter 8 showed that H_2S and O_2 was consumed in reactions that produced SO_2 and H_2O (overall reactions). There was also measured an increase in NO when O_2 was low, and this observation led to the proposal of the following reactions:

$$H_2S + NO_2 + O_2 \rightarrow SO_2 + H_2O + NO \quad (9\text{-}7)$$

$$2NO + O_2 \rightarrow 2NO_2 \quad (9\text{-}8)$$

Since the NO/NO_2 concentrations were in inverse ratio, depended on the O_2 content, it was suggested that O_2 is not directly involved in reaction 9-7, and instead the reaction could be written:

$$H_2S + 3NO_2 \rightarrow SO_2 + H_2O + 3NO \quad (9\text{-}9)$$

In summary this means that NO_2 is acting as an oxidation agent for H_2S to form SO_2, H_2O, and NO, while the amount of available O_2 determine how much NO that is oxidized back to NO_2. This fits well with the observation and these reactions are not necessarily harmful (i.e. corrosive) if the concentrations are low enough. The reactions occurred in all tested concentration levels (5, 10, 30, and 35 ppmv). It has been shown that SO_2-O_2-H_2O system is depending on high water concentrations to start the corrosion. Indirectly, H_2S-SO_2-O_2-H_2O system has also proven to be none-corrosive in the initial part of the Chapter 5 experiment, where these impurities were present for 70 hours at a concentration of about 35 ppmv without harming the carbon steel coupons. In other words, no reactions were observed as long as NO_2 was absent and the concentration of SO_2 and H_2S was ≤ 35 ppmv. Therefore, the uncertainty is if the presence of NO_2 (or NO) will initiate corrosion also for the low impurity concentrations that did not result in a formation of a separate liquid phase (5 and 10 ppmv). Since the hub experiments in Chapter 8 were performed without steel coupons to avoid catalysing effects of corroding steel surfaces, it cannot be concluded that no corrosion will occur at these low concentrations where no liquid is formed.

9.2.3 Formation of liquid phase

In Chapter 8, series of experiments with mixing of multiple CO_2 streams were carried out to simulate a hub where CO_2 streams from different sources was mixed. From these experiments, it became clear that the concentration of NO_2, SO_2, and H_2S should be kept below 30 ppmv to avoid formation of a separate liquid phase. The limiting factor for formation of liquids seemed to be the total

concentration of H_2S and SO_2, since the experiments show that all H_2S is converted to SO_2 when NO_2 is present. Figure 9-6 shows two different scenarios with the same outcome. In the Hub03 experiment, where NO_2 already was present when the H_2S injection started, the SO_2 concentration increased gradually to about 60 ppmv (the sum of injected concentrations of SO_2 + H_2S was 80), after which the concentration started to decline with time. In the other experiment (Chapter 5), H_2S was present when the NO_2 injection started, and also here the SO_2 concentration increased gradually to about 75 ppmv before the decline of SO_2 started in the same manner as for Hub03. The latter case had already H_2S present in the autoclave and all of it was converted to SO_2, which is probably the reason why the concentration of SO_2 got somewhat higher (75 instead of 60 ppmv). However, the SO_2 curve in the right diagram in Figure 9-6 has a change in slope at 60 ppmv which may indicate that liquid started to form at this point, which is in accordance with the visual observation.

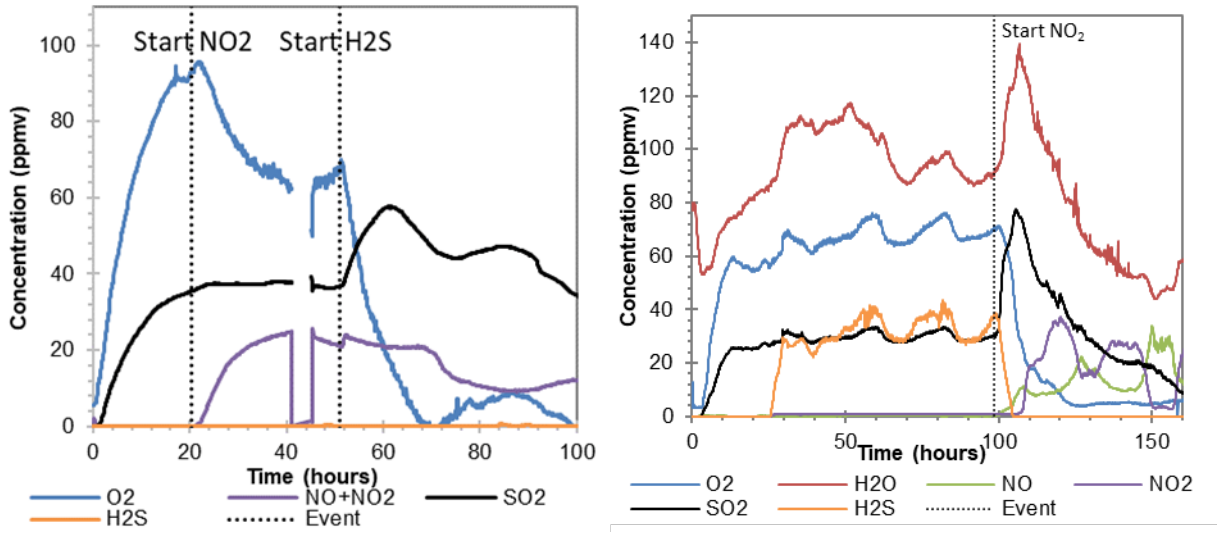

Figure 9-6: The diagram to the left (hub03) shows conversion of H_2S to SO_2 when NO_2 is present and H_2S injection starts, while the diagram to the right (Chapter 5) shows conversion of H_2S to SO_2 when H_2S is present and NO_2 injection starts.

The liquid that formed in these experiments was analysed with ion chromatography (IC), and both nitric and sulfuric acid were detected. This fits well with other findings in the literature [26-28]. It is not possible to determine whether H_2SO_4 or HNO_3 was produced first. But since the decrease in the SO_2 and H_2O concentrations was so clear at the same time as the first sign of liquid was observed inside the autoclave, it is suggested that H_2SO_4 was formed first according to this reaction:

$$SO_2 + H_2O + NO_2 \rightarrow NO + H_2SO_4 \qquad (9\text{-}10)$$

Thus, the results indicate that this can occur in the CO_2 bulk phase first, and afterwards precipitate on surfaces. However, occurrence of such reactions in a thin surface film cannot be fully ruled out. In Chapter 6, the acid solubility of both sulfuric and nitric acid was found in a series of experiments. The

solubility of H_2SO_4 was typically in the range of 0.1 – 8 ppmv, while the solubility of HNO_3 was three orders of magnitude higher, 500 – 2500 ppmv. The calculation based on the consumption of impurities preformed in Chapter 8 with the hub03 experiment (left diagram, Figure 9-6), shown in Figure 9-7, gave us an estimate of the amount of acid produced. The concentration of produced H_2SO_4, as it would have been without accumulation inside the test chamber, is higher than the solubility of this acid, and therefore a liquid phase will be formed.

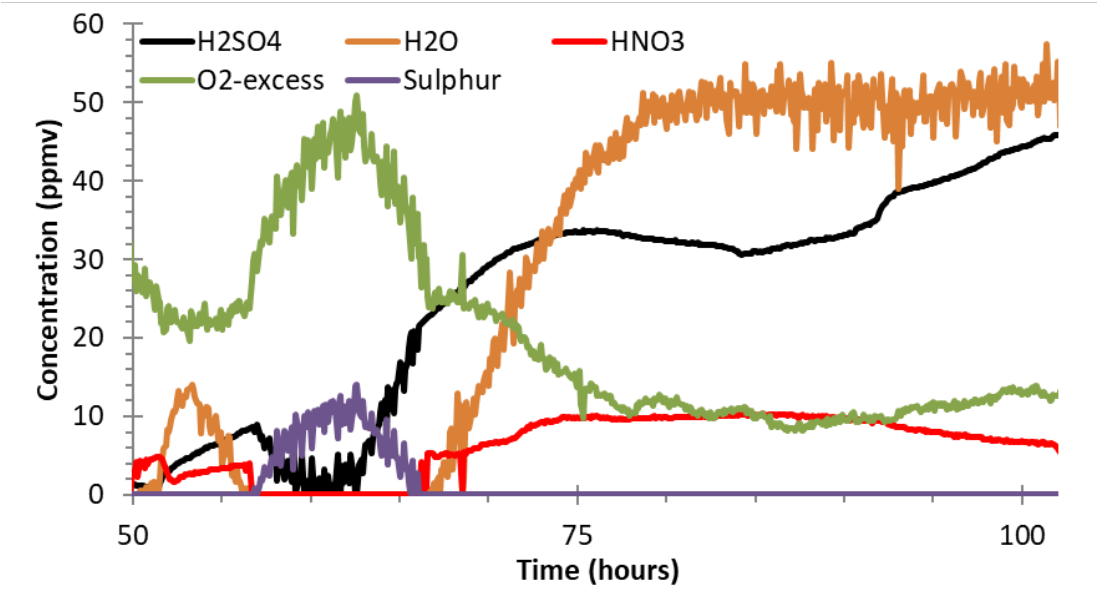

Figure 9-7: Estimate of the concentration produced species, Hub03 Chapter 8.

Sulfuric acid is known to be highly hygroscopic and could therefore absorb water from the CO_2 phase. This provides an aqueous solution for NO_2 to absorb into and form nitric acid. This reaction is more likely to happen in an aqueous solution, as described by [29]:

$$2NO_2 + H_2O \rightarrow HNO_3 + HONO \quad (9\text{-}11)$$

$$3HONO \rightarrow HNO_3 + 2NO + H_2O \quad (9\text{-}12)$$

If there is O_2 in excess, the NO will react to NO_2 (reaction 9-8). There are numerous reaction routes for NO_2, and it is outside the scope of the present work to study the details of these reactions. However, Finlayson-Pitts et al. [30] suggested that N_2O_4 (a dimer of NO_2), could be an important precursor for reaction 9-11. An interesting observation is the difference in corrosion between the carbon steel coupon exposed in a specification testing experiment (SPEC-1) with all impurities present and the coupons which was only exposed to NO_2 and H_2O in Ramp04 (Figure 9-8). The corrosion rate was higher and more severe in Ramp04 when only NO_2 and H_2O was present, than in SPEC-1 with SO_2, O_2, and water. The carbon steel coupon in SPEC-1 was clearly wetted by acids, but the water concentration was lower in addition to be consumed by reactions to form acid. Therefore,

little water was available to corrode the coupons and to dissolve the corrosion products. Panossian et al.[31] showed that the corrosion rate in concentrated (>90%, mass) H_2SO_4 was lower than in 50% H_2SO_4, since the solubility of $FeSO_4$ is much lower in concentrated H_2SO_4. Therefore, a surface layer of $FeSO_4$ will be formed faster in concentrated than in 50% H_2SO_4. A surface layer of $FeSO_4$ can act as a mechanical barrier that protects carbon steel and slow down the corrosion process [32]. Another observation in the SPEC-1 experiment (right picture, Figure 9-8), was that the attacks started from the contact points between the coupon and the PEEK-holder. Even after 170 hours in the "acid cloud", the carbon steel coupon had no significant corrosion attacks in the centre of the coupon. Apparently, the contact points acted as a flow path for either acid or water which enhanced the corrosion, possibly because liquid could form easier on the small contact point crevices. Note that liquid was observed at the centre of the coupon during the experiment.

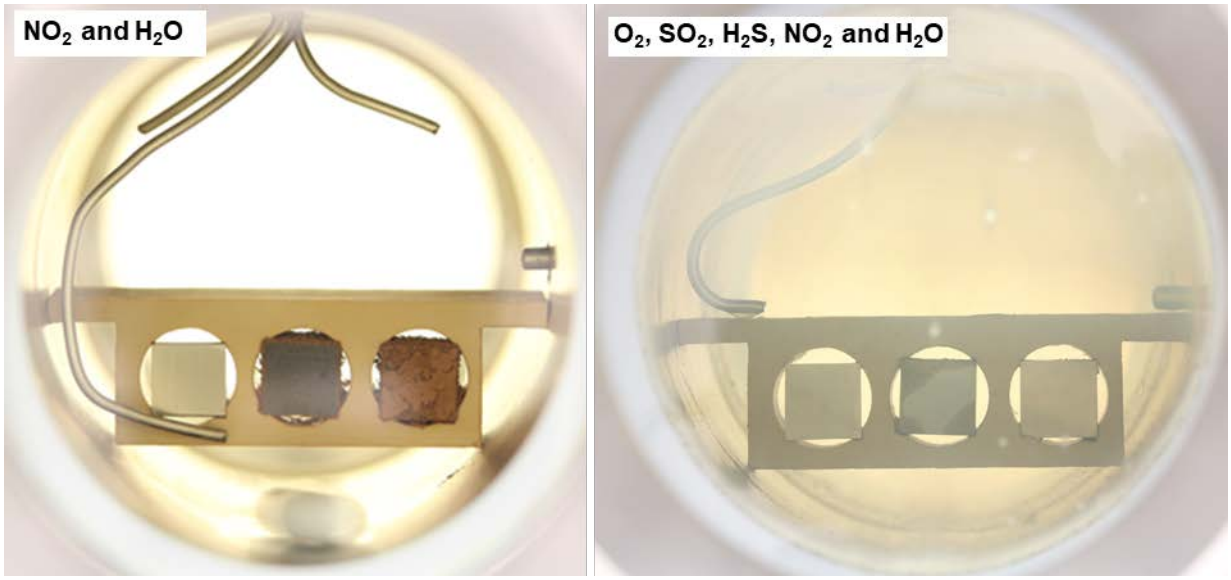

Figure 9-8: The coupons in the left picture were exposed to NO_2 and H_2O in Exp04, and the picture to the right was taken during SPEC-1 with O_2, SO_2, H_2S, NO_2, and H_2O present.

The ratio between sulfuric and nitric acid in the liquid phase analysed with IC was 10:1, nitric acid was a bit lower than compared with the ratio in Figure 9-7 which was 3:1. It is expected that more of the nitric acid is transported away with the CO_2 stream (exhaust CO_2) because of the higher solubility, but the consequence for the pipeline when running concentration levels shown in Hub03 and SPEC-1 with the products form as shown in Figure 9-7 would be severe. If the goal is to transport 1 Mt/y of CO_2 to storage, there could potentially precipitate about 30 tons of sulfuric acid and between 3 to 10 tons of nitric acid inside the pipeline every year when about 30 ppmv of NO_2, SO_2, and H_2S is present, according to Figure 9-7.

9.3 Limiting concentrations of impurities and making a CO_2 specification

The maximum allowed impurity concentration in a CO_2 specification should be set from one of two perspectives; either no chemical reactions should occur, or no corrosion of carbon steel should occur. In principle, some reactions could be allowed if the consequences are manageable from an operating perspective, meaning that no harmful reaction products should be formed, and that the corrosion rate should be very low. The latter would be a more realistic choice since cost is always in focus and unnecessary cleaning of the CO_2 will increase the overall price of the whole CCS chain. It is important to avoid precipitation of solid products since it may cause problems at the injection point and in the reservoir. The present work has clearly demonstrated that the number and types of impurities that are present is important for the maximum concentration for reactions and corrosion to occur. If the CO_2 contains fewer impurities, the acceptable maximum concentrations can be increased, sometimes significantly. Thus, it is clear that there must be a CO_2-specification for each combination of impurities, rather than one universal specification. This will be discussed further in the next sub-chapters.

9.3.1 CO_2 hub specification with H_2O, SO_2, H_2S, NO_2 and O_2 present

If the CO_2 specification should contain all impurities tested in this thesis, the impurity concentrations must be very low, including water, as summarised in Table 9-1. The CO_2 hub experiment showed that 5 and 10 ppmv of the SO_2, H_2S, and NO_2 (Hub01 and Hub02) did react but only to increase the SO_2 and H_2O concentration. While at an impurity content of 35 ppmv the acid precipitation started, and the liquid acid could be collected at the end of the experiment (Hub03 and SPEC-1).

Table 9-1. Proposed specification if all impurities are present at 25 °C and 100 bar.

Maximum impurity content (ppmv)					**Remark**
H_2O	**SO_2**	**H_2S**	**NO_2**	**O_2**	
200	20	20	10	20	Formation of H_2SO_4 and HNO_3 if (SO_2+H_2S) > 60 ppmv.

It should be noticed that the impurities in the proposed specification in Table 9-1 will react and therefore not be detected by analysis of the CO_2. Instead, the concentrations would be according to Equation 9-8 and 9-9, and the limiting reactant is oxygen. These reactions and products are perhaps most relevant when several individual CO_2 streams are mixed, for example in a CO_2 hub system. For a single CO_2 stream to the storage system, the reactions would have already occurred in the capturing plant or the compressor stage where it in principle could be removed.

The CO_2 specification (Table 9-1) is mainly based upon the Hub-experiments, where three individual CO_2 streams were mixed in a hub-system to follow the main flow out. Reactions did occur, and the critical point was when SO_2 and H_2S combined had a concentration above 60 ppmv, which led to formation of a liquid phase that contained acids. The presence of nitrogen dioxide acted as a catalyst that was back-produced as long as oxygen was in excess (Equation 9-8). Therefore, the sum of H_2S and SO_2 is set to maximum 40 ppmv in Table 9-1, to provide some safety margin. If nitrogen oxide is present, even at a concentration of a few ppm, it may catalyse the reaction with the help of oxygen. This was observed in the Hub-experiments, where NO_2 needed to be completely removed before the conversion of H_2S to SO_2 and H_2O stopped. The limit of 10 ppmv NO_2 in Table 9-1 was mostly set because of lack of experimental data, it might be that the concentration could have been higher based on the Ramp04-experiment as long as the water concentration is kept low (<250 ppmv). Water alone could threaten the pipeline integrity if precipitation is allowed and do accelerate surface reaction even below the solubility limit. This is the reason for the proposed low value of water in Table 9-1. For the Hub-experiments, water did not play an important role, except for when the acids already had precipitated. Then the water will absorb into the aqueous phase and increase the corrosion rate. The oxygen concentration was determined based on the restriction of NO_2, if oxygen is in excess there are no limits for which reactions NO_2 can “catalyse” since it is present in almost all proposed reactions (Equation 9-6, 9-7, 9-9, 9-10, and 9-11). By limiting oxygen, NO_2 will be limited to the conversion of H_2S to SO_2 and H_2O. It could be argued that the concentration of oxygen could have been set to 30 ppmv to achieve full conversion of H_2S, but instead a safe margin was used to ensure that no undesirable reaction occurs. It should be noted that much of the proposed specification in Table 9-1 is based on experiments carried out without carbon steel coupons.

9.3.2 Adapted CO_2 recommendation

There are several capture and purification methods for CO_2, and the impurities following the CO_2 stream will depend on the techniques used. Thus, using a CO2 specification with all the impurities in Table 9-1 will impose unnecessary restrictions if one or several of the impurities are not present. Therefore, an adapted CO_2 recommendation is proposed in Table 9-2.

Table 9-2. Recommended maximum concentration based on experimental data with several different impurity systems at 25 °C and 100 bar. No safety margins are included.

Maximum impurity content (ppmv)					**Remark**
H_2O	**SO_2**	**O_2**	**H_2S**	**NO_2**	
2500*					Negligible corrosion with under-saturated water. *
2500*	80**	240**			Slight corrosion for water > 1600 ppmv (about 4 µm/y). *
250				70**	Significant corrosion with 630 ppmv water.
100 (300)	35 (100)	60 (350)	35 (100)		Visual conformation and none reactive experiment. (None reactive experiment, but no visual conformation.)
50	35	80		30	Visual conformation and none reactive experiment.

** Precipitation of liquid water must be avoided. The water solubility varies with temperature and pressure. Check the temperature and pressure profile for the transportation system to identify the point with lowest solubility.*
*** These impurities might be increased, since it was the water concentration that controlled/ramped up until corrosion occurred.*

The three first recommendations in Table 9-2 are based on the findings in Chapter 3, Chapter 4, and Chapter 7. In the SO_2-O_2-H_2O recommendation, some corrosion would be expected at water concentration above 1600 ppmv but the corrosion rate found was low (4 µm/y). There should be done an assessment whether scale/products accumulating over several years of operation could detach from the steel surface and follow the CO_2 stream to the reservoir. As for the H_2S-SO_2-O_2-H_2O recommendation, no dedicated experiment was performed to confirm the safety in those values. However, several in-direct experiments have been performed. These in-direct experiments are the beginning of e.g. the acid formation experiment, SPEC-1, where the final goal of the experiment is to introduce NO_2 at the end. However, the injections in the beginning of the experiments were monitored with cameras and there were no visible attacks on the coupons even after 100 hours of stable impurity concentrations. No deviation between injection concentration and the concentration measured after the autoclave was detected. This was also the case for the numbers in the brackets in Table 9-2, but that experiment was not monitored by camera, so no visible conformation is available, and this should be confirmed in an additional experiment. The NO_2-SO_2-O_2-H_2O recommendation was confirmed in several in-direct experiments[33] with visual monitoring and impurity measurements, the longest exposure time was 330 hours without any sign of corrosion on the coupon surface [33]. There might be some reactions occurring which were not identified. In the Hub03 (Chapter 8), there was a sudden drop in the O_2 measurement in one of the laser-based analysers which measured in-situ, while another instrument using a different measuring technique did not detect this drop. This was thoroughly investigated and the drop in O_2 concentration was real but recovered when the vent-gas reach the second instrument. It was concluded that it might be intermediate/temporary species, the carbon steel coupon was not affected by the incident.

9.4 Implication of the proposed CO_2 specification

The proposed specification in Table 9-1 and Table 9-2 are solely made to identify maximum concentration of impurities in the transported CO_2 which do not harm carbon steel. It should be noted that there might be some type of carbon steel which reacts differently than the one used in this thesis (S355MC). The specifications/recommendations only apply for pipeline and ship and not for the injection point and the reservoir.

9.4.1 Oxy-fuel capturing vs. proposed specification

Three examples of the impurity content in the CO_2 from oxy-fuel capturing, are listed in Table 9-3.

Table 9-3. Expected impurities from oxy-fuel CO_2 capturing with combustion of pulverised coal.

Compound (ppmv)	**Example 1 [34]**	**Example 2 [35]**	**Example 3 [36]**	**Proposed specification (25 °C, 100 bar)**
H_2O	100	0	<20	200
SO_x	70	37	< 0.1	20
O_2	100	4000	<30	20
NO_x	100	33	<5	10
H_2S)	0	0	0	20
CO	50	-	<10	N/A
Ar, N_2	100	1500	Trace	N/A

Example 3 could most likely be transported without further cleaning, so might example 2 since there is not reported any water. But example 1 might be a problem because of the high SO_2 content. It was concluded that the total amount of SO_2 and H_2S should not be above 40 ppmv, and at 60 ppmv acid was produced in the experiment. The need for additional cleaning of the CO_2 depends on the oxy-fuel technique used.

9.4.2 Pre-combustion capturing vs proposed specification

In Pre-combustion, the CO_2 is captured before the combustion phase and solid fuel is converted to syngas. Some examples of the expected impurity concentrations are listed in Table 9-4.

Table 9-4. Expected impurities from pre-combustion CO_2 capturing with pulverised coal.

Compound (ppmv)	Example 1 [37]	Example 2 [38]	Example 3 [39]	Proposed specification (25 °C, 100 bar)
H_2O	600	378	10	200
SO_x	0	0	0	20
O_2	0	0	0	20
NO_x	0	0	0	10
H_2S/COS	<100	1700	20	20
CO	400	1300	400	N/A
Ar, N_2, H_2	10000	10000	10000	N/A

Pre-combustion might work without further cleaning of the CO_2, if adapted recommendation is used, but there are no data available for how COS and especially CO would affect the carbon steel pipeline, and this should be investigated before implementation. Blanco et al.[40] showed that CO had a negative effect on the storage process, but no corrosion related publications was found.

9.4.3 Post-combustion capturing vs proposed specification

Porter et al.[41] reviewed the range and concentration of impurities in the CO_2 stream from post-combustion capturing plants and they are listed in Table 9-5.

Table 9-5. Expected impurities from post-combustion CO_2 capturing with pulverised coal.

Compound (ppmv)	Amine PC plant [41]	MEA PC plant [41]	Proposed specification (25 °C, 100 bar)
H_2O	100	640	200
SO_x	10	1	20
O_2	150	61	20
NO_x	20	1.5	10
H_2S/COS	0	0	20
CO	10	0	N/A
Ar, N_2	450	1800	N/A

The expected concentration of impurities from post-combustion is low, especially for SO_2 and NO_2. Since H_2S is not present these CO_2 streams could very well be transported in carbon steel pipelines or ships without additional cleaning of the CO_2.

9.4.4 CO_2 hub system vs proposed specification

It has been suggested that multiple capturing sites can be connected to one storage site through a CO_2 transport network (pipelines). Such a network will result in mixing of CO_2 streams from different sources with different impurity species and concentrations. The present work has clearly

demonstrated that certain impurity combinations can result in corrosion and formation of solid. Thus, testing or prequalification of the CO_2 streams to be mixed is recommended. Neither oxy-fuel or post-combustion capturing streams could be mixed with pre-combustion capturing streams with high H_2S content. H_2S and NO_2 will react to form SO_2 and acid will form when the amount of SO_2 exceeds 60 ppmv. Oxy-fuel and post-combustion streams contain enough O_2 to keep the reactions going. With the high O_2 concentration only traces of NO_2 is needed to produce sulfuric acid. Therefore, to make the hub system work with all these capturing methods, all traces of NO_2 need to be removed from the CO_2 streams before they are mixed.

9.5 References

[1] B. H. Morland, A. Dugstad, G. Svenningsen, Corrosion of Carbon Steel in Dense Phase CO_2 with Water above and Below the Solubility Limit, *Energy Procedia*, 114, (2017) pp. 6752-6765.

[2] B. H. Morland, M. Tjelta, A. Dugstad, G. Svenningsen, "Formation of strong acids in dense phase CO_2", CORROSION/2018, paper no. 11429 (Houston, TX: NACE International, 2018).

[3] B. H. Morland, M. Tjelta, T. Norby, G. Svenningsen, Acid reactions in hub systems consisting of separate non-reactive CO_2 transport lines, *International Journal of Greenhouse Gas Control*, 87, (2019) pp. 246-255.

[4] B. H. Morland, M. Tjelta, A. Dugstad, G. Svenningsen, Formation of strong acids in dense phase CO_2, *CORROSION*, 0, 0 (2019) p. null.

[5] B. H. Morland, T. Norby, M. Tjelta, G. Svenningsen, Effect of SO_2, O_2, NO_2, and H_2O concentrations on chemical reactions and corrosion of carbon steel in dense phase CO_2, *CORROSION*, 0, 0 (2019) p. null.

[6] R. Thodla, A. Francois, N. Sridhar, "Materials Performance In Supercritical CO_2 Environments", CORROSION/2009, paper no. 09255 (Houston, TX: NACE International, 2009).

[7] F. Ayello, K. Evans, R. Thodla, N. Sridhar, "Effect of impurities on corrosion of steel in supercritical CO_2", CORROSION/2010, paper no. 10193 (Houston, TX: NACE International, 2010).

[8] F. Ayello, K. Evans, N. Sridhar, R. Thodla, Effect of liquid impurities on corrosion of carbon steel in supercritical CO_2, in: 8th International Pipeline Conference, (Calgary, Canada, 2010).

[9] Y. Tang, X. P. Guo, G. A. Zhang, Corrosion behaviour of X65 carbon steel in supercritical-CO_2 containing H_2O and O_2 in carbon capture and storage (CCS) technology, *Corrosion Science*, 118, Supplement C (2017) pp. 118-128.

[10] P. M. Wang, A. Anderko, R. D. Young, A speciation-based model for mixed-solvent electrolyte systems, *Fluid Phase Equilibria*, 203, 1-2 (2002) pp. 141-176.

[11] P. Wang, A. Anderko, R. Springer, R. Young, Modeling phase equilibria and speciation in mixed-solvent electrolyte systems: II. Liquid–liquid equilibria and properties of associating electrolyte solutions, *Journal of Molecular Liquids*, 125, 1 (2006) pp. 37-44.

[12] R. D. Springer, Z. Wang, A. Anderko, P. Wang, A. R. Felmy, A thermodynamic model for predicting mineral reactivity in supercritical carbon dioxide: I. Phase behavior of carbon dioxide–water–chloride salt systems across the H2O-rich to the CO2-rich regions, *Chemical Geology*, 322, (2012) pp. 151-171.

[13] S. Sim, F. Bocher, I. S. Cole, X. B. Chen, N. Birbilis, Investigating the Effect of Water Content in Supercritical CO_2 as Relevant to the Corrosion of Carbon Capture and Storage Pipelines, *CORROSION*, 70, 2 (2014) pp. 185-195.

[14] Y. Hua, R. Barker, A. Neville, Effect of temperature on the critical water content for general and localised corrosion of X65 carbon steel in the transport of supercritical CO_2, *International Journal of Greenhouse Gas Control*, 31, (2014) pp. 48-60.

[15] S. Nesic, "A Critical review of CO_2 corrosion modelling in the oil and gas industry", 10th Middle East Corrosion Conference 7-10 March 2004 (2004).

[16] A. Dugstad, "Fundamental aspects of CO_2 metal loss corrosion - Part 1: Mechanism", CORROSION/2006 (Houston, TX: NACE International, 2006).

[17] G. Schmitt, M. Krieck-Defrain, "pH-static experiments in high pressure CO_2 corrosion of steel. Effect on scale morphology and chemical composition, Corrosion rate, pitting susceptibility and inhibitor performance.", 11th International Corrosion Congress, paper no. 480 (1990).

[18] Y. Ben-Da, S. Meilink, G. W. Warren, P. Wynblatt, Water adsorption and surface conductivity measurements on alumina substrates, *Components, Hybrids, and Manufacturing Technology, IEEE Transactions on*, 10, 2 (1987) pp. 247-251.

[19] C. Leygraf, *P. Marcus, J. Oudar (Eds.), Corrosion Mechanisms in Theory and Practice*, (New York, 1995).

[20] Y. Xiang, M. Xu, Y.-S. Choi, State-of-the-art overview of pipeline steel corrosion in impure dense CO_2 for CCS transportation: mechanisms and models, *Corrosion Engineering, Science Technology*, 52, 7 (2017) pp. 485-509.

[21] Y. Hua, R. Barker, A. Neville, The influence of SO_2 on the tolerable water content to avoid pipeline corrosion during the transportation of supercritical CO_2, *International Journal of Greenhouse Gas Control*, 37, (2015) pp. 412-423.

[22] Y.-S. Choi, S. Nesic, "Effect of water content on the corrosion behavior of carbon steel in supercritical CO_2 phase with impurities", CORROSION/2011, paper no. 11377 (Houston, TX: NACE International, 2011).

[23] H. Takeuchi, M. Ando, N. Kizawa, Absorption of nitrogen oxides in aqueous sodium sulfite and bisulfite solutions, *Industrial Engineering Chemistry Process Design Development*, 16, 3 (1977) pp. 303-308.

[24] C. Arroyave, M. Morcillo, The effect of nitrogen oxides in atmospheric corrosion of metals, *Corrosion Science*, 37, 2 (1995) pp. 293-305.

[25] F. Samie, J. Tidblad, V. Kucera, C. Leygraf, Atmospheric corrosion effects of HNO_3—Comparison of laboratory-exposed copper, zinc and carbon steel, *Atmospheric Environment*, 41, 23 (2007) pp. 4888-4896.

[26] O. Yevtushenko, D. Bettge, R. Bäßler, S. Bohraus, Corrosion of CO_2 transport and injection pipeline steels due to the condensation effects caused by SO_2 and NO_2 impurities, *Materials and Corrosion*, 66, 4 (2015) pp. 334-341.

[27] B. Paschke, A. Kather, Corrosion of pipeline and compressor materials due to impurities in separated CO_2 from fossil-fuelled power plants, *Energy Procedia*, 23, (2012) pp. 207-215.

[28] A. Dugstad, M. Halseid, B. Morland, Testing of CO_2 specifications with respect to corrosion and bulk phase reactions, *Energy Procedia*, 63, (2014) pp. 2547-2556.

[29] D. Perner, U. Platt, Detection of nitrous acid in the atmosphere by differential optical absorption, *Geophysical Research Letters*, 6, 12 (1979) pp. 917-920.

[30] B. Finlayson-Pitts, L. Wingen, A. Sumner, D. Syomin, K. Ramazan, The heterogeneous hydrolysis of NO_2 in laboratory systems and in outdoor and indoor atmospheres: An integrated mechanism, *Physical Chemistry Chemical Physics*, 5, 2 (2003) pp. 223-242.

[31] Z. Panossian, N. L. d. Almeida, R. M. F. d. Sousa, G. d. S. Pimenta, L. B. S. Marques, Corrosion of carbon steel pipes and tanks by concentrated sulfuric acid: A review, *Corrosion Science*, 58, (2012) pp. 1-11.

[32] S. W. Dean, G. D. Grab, Corrosion of carbon steel by concentrated sulfuric acid, *Mater. Performance*, 24, 6 (1985).

[33] G. Svenningsen, A. Dugstad, M. Tjelta, A. Anderko, B. H. Morland, "CLIMIT Project 243624: Corrosion and cross chemical reactions in pipelines transporting CO_2 with impurities (KDC-II)", Institute for Energy Technology.

[34] A. Kather, S. Kownatzki, Assessment of the different parameters affecting the CO_2 purity from coal fired oxyfuel process, *International Journal of Greenhouse Gas Control*, 5, (2011) pp. S204-S209.

[35] G. Pipitone, O. Bolland, Power generation with CO_2 capture: Technology for CO_2 purification, *International Journal of Greenhouse Gas Control*, 3, 5 (2009) pp. 528-534.

[36] C. Spero, L. Chapman, F. Montagner, Callide oxyfuel project, in: CLET Seminar—Deployment of CCS in Queensland, July, (2007).

[37] A. Kather, B. Paschke, S. Kownatzki, "CO_2-Reinheit für Abscheidung und Lagerung", Report no. FKZ 0327790E, Hamburg University of Technology.

[38] DGCA, "Implementation of Directive 2009/31/EC on the Geological Storage of Carbon Dioxide", 2011, E. Communities.

[39] A. Prelipceanu, H. Kaballo, U. Keresteciogl u, Linde rectisol wash process, in: 2nd International Freiberg Conference on IGCC & XtL Technologies, (Freiberg, Germany, 2007).

[40] S. T. Blanco, C. Rivas, R. Bravo, J. Fernández, M. Artal, I. Velasco, Discussion of the Influence of CO and CH_4 in CO_2 Transport, Injection, and Storage for CCS Technology, *Environmental Science & Technology*, 48, 18 (2014) pp. 10984-10992.

[41] R. T. J. Porter, M. Fairweather, M. Pourkashanian, R. M. Woolley, The range and level of impurities in CO_2 streams from different carbon capture sources, *International Journal of Greenhouse Gas Control*, 36, (2015) pp. 161-174.

Chapter 10

Conclusions

Prior to this study, there was some discrepancy about the corrosion rates for carbon steel exposed to dense phase CO_2 with fully dissolved water. By using a controlled method to dissolve the water in CO_2, it was experimentally demonstrated that the presence of dissolved water in the CO_2 phase will not give significant corrosion (less than 2 µm/y) for carbon steel. However, if the water is present as a free water phase, it will result in 3 to 4 orders of magnitude higher corrosion rates, in the range from 5 to 50 mm/y. This shows that the form of the water (fully dissolved in the CO_2 phase, saturated or present as a liquid phase) is critical for the integrity of carbon steel components. It is more than likely that the discrepancy of the corrosion rates reported in the literature is caused by a combination of the experimental procedure and the handling of the water, as several possible artefacts could occur during loading and depressurisation of the autoclave.

The most referred (Dynamis, NETL, CarbonNet, etc.) recommendation of impurities (100 ppmv of SO_2, NO_2, and H_2S) was tested in a novel test system that mimic the CO_2 transport conditions in a realistic manner. The test showed that a separate aqueous phase containing nitric and sulfuric acid was formed, which is corrosive to carbon steel. Thus, such impurity levels cannot be accepted for CO_2 transportation in carbon steel pipelines. This raised many interesting questions, like impurity concentration limits, solubility limits, corrosion and chemical reactions, and which could be used to make a safe operation specification for CO_2 transport in carbon steel. Since acids were formed by reactions of impurities, solubility data was needed to predict when the acids could precipitate and form a separate phase.

The solubility of nitric acid and sulfuric acid in dense phase CO_2 was determined through organises experimental work. The results showed that the solubility of nitric acid (~1000 ppmv) was about 3 order higher than sulfuric acid (~1 ppmv). The solubility increases slightly with increasing temperature, while pressure has a much larger effect, especially between 1 and 100 bar. The pioneer results from the acid solubility in CO_2 was used as the foundation of the CO_2 - acid model that has been implemented in the OLI thermodynamic model.

The experimental testing showed that sulfuric acid was formed by reaction of water, sulfur dioxide and nitrogen oxide. Although the details around formation of these acids is not fully understood, it is

assumed that sulfuric acid forms in the bulk CO_2 phase and, due to its low solubility, it will precipitate. Sulfuric acid is hygroscopic and will most likely absorb water from the CO_2 phase, thus creating an acid-rich aqueous phase. The results further indicate that nitric acid formation take place in an aqueous phase, not in the bulk CO_2 phase. Thus, nitric acid may start to form once enough water has been absorbed in the sulfuric acid phase.

Systematic studies showed that formation of corrosive phases was strongly affected by which impurities that were present together. Certain impurity combinations were essentially inert, while other combinations resulted in chemical reactions and corrosion. The concentration of water was critical and ramping of water experiment was conducted to establish water limits for several of the impurities. The experiments showed that CO_2 streams containing SO_2 and O_2 are not corrosive if the water concentration is less than 1600 ppmv at 100 bar and 25 °C. However, the situation is quite different for the NO_2-H_2O system. A corrosion rate of 0.57 mm/y was measured with 70 ppmv of NO_2 and only 670 ppmv of H_2O at 100 bar and 25 °C. The first sign of corrosion started already at 250 ppmv of H_2O. This indicates that the corrosion mechanism for SO_2/O_2 and NO_2 is different. Presence of SO_2 and O_2 and high concentrations of water did only result in negligible corrosion, while presence of NO_2 results in significant corrosion even when a relatively small amount of water is present. The reason for this significant difference has not been fully understood. It could be related to different surface adsorption/absorption processes or differences in the protectiveness of the corrosion products that form.

A future CO_2 transport network will most likely include CO_2 from different sources that will be mixed at some point (hub). Even if the individual CO_2 streams are non-reactive on their own, mixing of the streams may give certain impurity combinations that trigger chemical reactions. In this study, three different non-reactive CO_2 streams were mixed, and the reaction was study through analysis of the exhaust gas and visual observation. The concentration level was set to approximately 5, 10 and 30 ppmv of SO_2, NO_2, and H_2S. Water and O_2 were also present, at a higher concentration. Acids were formed with 30 ppmv of impurities, while 5 and 10 ppmv of impurities gave reactions but no condensation of acids. These observations made it possible to identify two important reactions which produce reactants to the sulfuric acid reaction. The first was the reaction of H_2S and NO_2 to produce SO_2 and H_2O, and the second was the reaction between NO and O_2 to regain NO_2. Nitrogen dioxide acts like an oxidation agent and as long as O_2 is available, only trace amount of NO_2 is required to oxidise H_2S to SO_2. H_2S was always instantly fully consumed when NO_2 was injected to the autoclave.

The Hub-experiments gave also valuable inputs for cases with few impurities, since each impurity was introduced subsequently. Based on all the experimental testing, it was possible to establish limits for when corrosion and chemical reactions can be expected. Since the combination of impurities is so important, it was not possible to give a universal limit for each impurity, it had to be for a combination (Table 10-1). It should also be noted that the limits may change if other impurities (not yet tested) are present.

Table 10-1. Maximum level of impurity at 25 °C and 100 bar.

Maximum impurity content (ppmv/ppm mole)					**Remark**
H_2O	**SO_2**	**H_2S**	**NO_2**	**O_2**	
200	20	20	10	20	Formation of H_2SO_4 and HNO_3 if (SO_2+H_2S) > 60 ppmv.
2500*					Negligible corrosion with fully dissolved water. *
2500*	80**	240**			Slight corrosion for water > 1600 ppmv (about 4 µm/y). *
250				70**	Significant corrosion with 630 ppmv water.
100 (300)	35 (100)	60 (350)	35 (100)		Visual conformation and none reactive experiment. (None reactive experiment, but no visual conformation.)
50	35	80		30	Visual conformation and none reactive experiment.

** Precipitation of liquid water must be avoided. The water solubility varies with temperature and pressure. Check the temperature and pressure profile for the transportation system to identify the point with lowest solubility.*

*** These impurities might be increased, since it was the water concentration that controlled/ramped up until corrosion occurred.*

The recommendation in Table 10-1 was compared with published impurity concentrations from capturing of various combustion sources, and it suggests that CO_2 captured from oxy-fuel, pre-combustion, and post-combustion processes can be transported in carbon steel pipelines without further cleaning. However, the streams must be kept apart, acid will be produced if they are mixed, and the integrity of the pipeline or ship will be threatened.

Chapter 11

Further work

This thesis has covered many topics but also revealed some gaps in the knowledge for proposing a safe operation specification. In this work it was observed that the first condensation of acid occurred when SO_2 exceeded a threshold of about 60 ppmv. In the experiments, however, such high SO_2 contents were only reached because H_2S was converted to SO_2 by reaction with NO_2, and it is not really known if the presences of H_2S is needed or if SO_2 alone above 60 ppmv would result in formation of acids. This should be investigated further.

Some of the proposed impurity limits in Table 9-1 was based on the observation that no aggressive reaction products (acids) was produced, but some of these experiments were carried out in the absence of corrosion coupons. These limits should be confirmed in dedicated experiments with carbon steel coupons present. The concentration limits in the CO_2 recommendation in Table 9-2 is based on the available experimental data from this thesis, and the maximum allowed concentration may in some cases might be increased but this needs to be verified by experiments. Such experiments may for example be; fixed water concentration at the maximum identified value and increasing single or multiple impurity until corrosion occurs.

The time for liquid water to dissolve in dense phase CO_2 has so far not been quantified experimentally, as discussed in connection with experimental artefacts in this work it, is very relevant for corrosion testing. The kinetics for liquid water to dissolve in dense phase CO_2 is important in several other part of the CCS chain, such as after hydro testing of pipelines to be used for CO_2 transport, or in the case of accidental water ingress. The time for dissolving the water will, to some extent, determine the amount of corrosion to be expected during this dry-up phase of the pipeline.

Carbon monoxide as impurity was not tested in the present work but it is present in most of the previously proposed specifications from the capturing process. However, no experimental data is available with respect to corrosion or chemical reactions between impurities. This should be included in future experiments.

The ramping experiments in chapter 7 revealed that CO_2 mixtures with SO_2-H_2O or NO_2-H_2O as impurities behaved very different with respect to corrosion. This can be related to adsorption/absorption effects – or the protectiveness of the corrosion products, but the details are not yet understood. It is important to understand the mechanisms that are involved, in order to be in the forefront in predicting unacceptable corrosion of CCS installations.

The sulphur chemistry is very complex and further research is needed to fully understand when elemental sulphur is produced in the system as it can lead to production of large quantities of solid matter, which again can result in clogging of pipelines and injection reservoirs.

The CO_2 quality specification in this study is a good starting point for ensuring the integrity for the carbon steel components (pipes, tanks, …) involved in CCS, but it should be expanded to cover additional compounds like glycol and amines. Also, from a material aspect, the mechanism revolving phases, structures, and grain boundary in the metal could influence the initiation of corrosion and the amount of localised attacks.